Joint Scheduling and Duty Cycle Control Framework for Hierarchical Machine-to-Machine Communication Networks

by

Yun Li

A thesis submitted to the University of London for the degree of

Doctor of Philosophy

School of Electronic Engineering and Computer Science
Queen Mary University of London
United Kingdom

2015

TO MY FAMILY

Abstract

This thesis presents a novel distributed optimisation framework for machine-to-machine (M2M) communication networks with dynamic traffic generation, heterogeneous applications and different device capabilities. The aim of the framework is to effectively manage the massive access of energy constrained M2M devices while satisfying different application requirements. The proposed framework has three control blocks which run at cluster heads and M2M gateways:

i) The distributed duty cycle control that adapts to dynamic network traffics for IEEE 802.15.4 MAC layer protocol with stop-and-wait automatic repeat request (ARQ) and Go-Back-N ARQ schemes.

ii) The cluster head control that applies dynamic programming (DP) and approximate dynamic programming (ADP) techniques to maximise single cluster utility while balancing the tradeoff between system performance and algorithm complexity.

iii) The gateway control that applies network utility optimisation (NUM) and mixed integer programming (MIP) techniques to maximise the aggregated long-term network utility while satisfying different application requirements among clusters.

Both theoretical and practical concerns are addressed by the proposed control framework. Simulation results show that the proposed framework effectively improve the overall network performance in terms of network throughput, energy efficiency, end-to-end delay and packet drop ratio.

Acknowledgments

I would like to express my sincere gratitude to my supervisor, Dr. Michael Chai, for the continuous support during my Ph.D study and research. He guided me through my research and writing of this thesis with his patience, motivation, encouragement, enthusiasm, and immense knowledge.

I am also grateful to my independent accessor, Dr. Yue Chen, for her insightful suggestions and valuable discussions, and also for her consideration and sharing. I would also like to express my special thanks to Dr. Jonathan Loo, who has spent lots of time on discussing research ideas and writing skills with me.

I will also thank the Chinese Scholarship Council (CSC). Without the support of CSC, I could not have had this precious opportunity to study at this great university.

My gratitude goes to all the colleagues and friends, who have shared the time with me that made the past four years so memorable. Moreover, warm thanks are given to all the helpful staff at Queen Mary. It is you who make Queen Mary such a great place to do research.

At last, I would like to express my gratitude to my parents, in particular, for their love and support in all the important moments of my life. Without their love, I would not have made it through.

Declaration

I, Yun Li, confirm that the research included within this thesis is my own work or that where it has been carried out in collaboration with, or supported by others, that this is duly acknowledged below and my contribution indicated. Previously published material is also acknowledged below.

I attest that I have exercised reasonable care to ensure that the work is original, and does not to the best of my knowledge break any UK law, infringe any third partys copyright or other Intellectual Property Right, or contain any confidential material.

I accept that the College has the right to use plagiarism detection software to check the electronic version of the thesis. I confirm that this thesis has not been previously submitted for the award of a degree by this or any other university.

The copyright of this thesis rests with the author and no quotation from it or information derived from it may be published without the prior written consent of the author.

Signature: Yun Li

Date: January 27, 2016

Table of Contents

List of Figures

List of Tables

List of Abbreviations

ACK	Acknowledgement
AN	Access Network
ADP	Approximate Dynamic Programming
ARQ	Automatic Repeat Request
BE	Backoff Exponent
BI	Beacon Interval
BO	Beacon Order
BOAA	Beacon Order Adaptation Algorithm
BP	Backoff Period
BS	Base Station
CAP	Contention Access Period
CCA	Clear Channel Access
CFP	Contention-Free Period
CH	Cluster Head
CN	Core Network
CSMA/CA	Carrier Sense Multiple Access with Collision Avoidance
CTS	Clear-To-Send
CW	Contention Window

DCA	Duty Cycle Algorithm
DCLA	Duty Cycle Learning Algorithm
DM	Device Domain
DP	Dynamic Programming
DSMAC	Dynamic Sensor MAC
DW-MAC	Demand Wakeup MAC
EE	Energy Efficiency
ETSI	European Telecommunications Standards Institute
FFD	Full Functional Device
FPA	Fast Path Algorithm
GTS	Guaranteed Time Slot
IoT	Internet of Things
LOS	Line of Sight
LTE	Long-Term Evolution
LTE-A	Long-Term Evolution Advanced
LR-WPAN	Low-Rate Wireless Personal Area Network
M2M	Machine-to-Machine
MAC	Medium Access Control
MIP	Mixed Integer Programming
MDP	Markov Decision Process
ND	Network Domain
NLOS	None Line of Sight
NUM	Network Utility Maximisation
OSI	Open Systems Interconnection

PAN	Personal Area Network
PF	Proportional Fairness
PHY	Physical
PI	Policy Iteration
P-UPF	Proposed-Utility Proportional Fairness
QoS	Quality of Service
RA	Rollout Algorithm
RAN	radio access network
RACH	Random Access Channel
RL	Reinforcement Learning
RTS	Request-To-Send
SD	Superframe Duration
SO	Superframe Order
SMAC	Sensor MAC
SNR	Signal to Noise Ratio
TDDCA	Traffic-adaptive Distance-based Duty Cycle Assignment
TDMA	Time Division Multiple Access
TMAC	Timeout MAC
TLDTCA	Tree-Like Distributed Topology Control Algorithm
UFC	Utility Fairness Control
UPF	Utility Proportional Fairness
U-MAC	Utilisation based MAC
VI	Value Iteration
WSNs	Wireless Sensor Networks

Notations

n	M2M gateway in the network
$\mathcal{N}$	the set of M2m gateways in the network
N	the total number of M2M gateways in the network
$\mathcal{I}_n$	the set of child cluster heads of gateway $n \in [1, 2, \cdots, \mathcal{N}]$
i	the cluster head connected with the gateway n
I	the total number of cluster heads connected with gateway n
$\mathcal{L}_{i,n}$	the link set between cluster heads $i \in \mathcal{I}_n$ and gateway n
$l_{i,n}$	the link between cluster head i and gateway n
$\mathcal{C}_i$	the child nodes set of cluster head $i \in \mathcal{I}_n$
j	the child device of cluster head i, $j \in \mathcal{C}_i$
(i, n)	the device pair of cluster head i and gateway n
(i, j)	the device pair of cluster head i and its child devices j
$\mathcal{L}_{i,j}$	the link set between cluster head i and its child devices $j \in \mathcal{C}_i$
$l_{i,j}$	the link between cluster head i and its child device j
$g_{i,j}^t$	the traffic batch of cluster head i and its child device j at time period t
$\mathcal{H}$	the number of hops of a selected path
M	the total number of devices in the network

T	total control time periods
t	discrete time period of control system
S	the finite discrete states set of cluster heads
s_t	system state at time period t
A_i	the finite control decision set of cluster head i
a_t	decision action at time period t
w_t	disturbance random parameter at time period t
$P(s, s')$	probability that the system transit from state s to s'
$J(s, s')$	immediate cost of the system transit from state s to s'
γ	discount factor of the system
π	control policy of the system
μ_t	the control maps the state s_t into the decision action a_t at time period t
$Q(s_t, a_t)$	Q-factor at time period t with state s_t and action a_t
$L_{c,dB}$	channel propagation loss in dB
$L_{0,dB}$	reference base channel propagation loss in dB
$X_{s,dB}$	zero mean Gaussian random in dB
X_f	unit-mean gamma-distributed random in dB
d	distance between the sender and receiver
d_1	reference distance in propagation model
m	Nakagami fading parameter
$P^t_{rec,i}$	received power of cluster head i
$P^t_{tran,i}$	conducted power of cluster head i
$G^t_{tran,i}$	transmit antenna gain of cluster head i
$G^t_{rec,i}$	receive antenna gain of cluster head i

$\rho_{i,j}^t$	successful transmission probability between cluster head i and its child device j
$C_{i,n}^t$	Link capacity between cluster head i and gateway n at time period t
$C_{n,b}^t$	Link capacity between gateway n and the base station b at time period t
$H_{i,n}$	power gain between gateway n and cluster head i
B	bandwidth
N_0	noise spectral density
q_i^t	queue length of cluster head i at time period t
q_i^{max}	maximum queue length of cluster head i at time period t
r_i^t	number of packets received by cluster head i at time period t
f_i^t	number of packets transmitted by cluster head i at time period t
g_i^t	number of packets generated by cluster head i at time period t
c_f	cost function coefficients of transmitting
c_r	cost function coefficients of receiving
c_l	coefficients of idle listening
c_d	cost function coefficients of delay
θ_i^t	QoS indicator of cluster head i at time period t
α	weighting factor of energy efficiency in cost function
β	weightings factor of end-to-end delay in cost function
$E_t(f_i^t)$	transmitting energy consumption cost of cluster head i with f_i^t forwarded packets at time period t
$E_r(r_i^t)$	receiving energy consumption cost of cluster head i with r_i^t received packets at time period t

$E_l(r_i^t)$	idle listening energy consumption cost of cluster head i with r_i^t received packets at time period t
$D(r_i^t)$	end-to-end delay cost of cluster head i with r_i^t received packets at time period t
$J(r_i^t)$	joint-cost of cluster head i with r_i^t received packets at time period t
J_i^t	cost-to-go function of cluster i untill time period t
$U(f_i^t, r_i^t, \theta_i^t)$	system utility function in terms of number of forward packets f_i^t, received packets r_i^t and the QoS indicator θ_i^t
$\mathcal{U}(f_i^t, r_i^t, \theta_i^t)$	pseudo system utility function
$U_n(f_i^t, \theta_i^t)$	gateway utility function in terms of number of forward packets f_i^t and the QoS indicator θ_i^t
$U_i(r_i^t)$	cluster utility function in terms of received packets r_i^t
V_i^t	value function of cluster head i at time period t
R_i^t	economic return of cluster head i at time period t
p_i^t	bid price of cluster head i at time period t
$p_{i,n}^t$	charge price of gateway n to cluster head i at time period t
$SO(r_i^t)$	superframe order (SO) of cluster head i with r_i^t received packets at time period t
PD	total packet transmission duration
SD	superframe duration
D_{bcn}	beacon transmission duration
P_s	successful packet transmission duration with Stop-and-Wait ARQ
D_p	transmission duration per packet with Go-Back-N ARQ

δ	waiting time for ACK packet at IEEE 802.15.4 MAC layer
P_{CCA}	transmission time of two CCAs in IEEE 802.15.4 MAC layer
P_L	per packet transmission time
P_{ACK}	ACK packet transmission time

Chapter 1

Introduction

Machine to machine (M2M) communications refer to smart devices or machines automatically communicate with each other through a network with little or no human intervention. It contributes to the integration of advanced Internet of things (IoT) applications and services in various areas, such as smart cities, health care, transport systems, public safety, industrial and agricultural automations [CCC+10, ZYX+11, YZG+13, CCZS08, GC13, LLKC12, XYWV12]. To support IoT applications via wireless technologies, a hierarchical M2M communication architecture has been specified by European Telecommunication Standards Institute (ETSI) M2M Technical Committee [ETS].

1.1 Research Motivation

With the hierarchical M2M communication architecture proposed by ETSI in place, there are still numerous issues remaining for supporting M2M communications. As has been pointed by different standard bodies, channel access of massive amount devices has become one of the potential bottleneck of the M2M communications [3GP11c, 3GP11a, Soc12]. The channel access challenges of M2M

communication networks include:

i) **Capacity Limited Devices**: The devices involved in M2M networks have limited capacities in terms of computation and memory. These capacity limited devices are usually very cheap, so that they ensure the affordable deployment of M2M networks. However, with these computational and memory limited devices, the channel access algorithms for M2M communications need to have low computation and storage complexities.

ii) **Energy Efficiency**: Energy efficiency (EE) is one of the most of important design considerations due to the fact that most M2M devices are expected to be battery powered. EE is an important design criteria as it is also highly related with the operational costs and profit margins for network operators.

iii) **Network Throughput**: Maximising the network throughput is another essential design criteria. Wireless bandwidth is a scarce resource for M2M communications, due to massive amount of devices, limited spectrum resources, duty-cycled operation and the low data rate of low-power wireless radios. Additionally, serious degradation of throughput may occur due to the network congestion and packet drop when devices generate heavy traffics.

iv) **Adaptivity**: Flexible adaptation is required in many practical scenarios where both channel conditions and data arrival processes are changing over time. In addition, to increase the efficiency of data transmission, the adaptation should be achieved with little or no control information exchange.

v) **Feasibility**: The feasibility of channel access is another important issue that needs to be addressed in real-life scenarios. In practice, it is hard or impossible for devices to have reliable statistical network information, such

as real-time traffics, detailed device capabilities, various application requirements and instant channel conditions. Thus, the access control algorithm needs to work effectively with little or no priori network information.

vi) **Diverse Quality of Service (QoS)**: How to effectively multiplex the massive access with enormously diverse QoS requirements turns out to be one of the most challenging tasks. In [ITA14], the diverse QoS requirements of M2M applications are summarised as shown in Table 1-A.

In summary, the critical channel access challenges for M2M communications lies in facilitating channel access management to large number of capacity limited devices while supporting the diverse QoS requirements.

Table 1-A: Access Requirements of M2M Applications.

Applications	**Access requirements**
Real-time health services	Strict delay requirements
Non-real-time services	Periodic access, moderate delay requirements
Smart grid	Periodic access, moderate delay requirements
Security/surveillance	Periodic and/or event-driven access, moderate high delay requirements
Intelligent transport system	Periodic access, strict/moderate delay requirements
Industrial supply and provisioning	Periodic access, high delay requirements
Tracking inventory and security	Periodic and/or event-driven access, high delay requirements
Raw material supply and distribution supervision	Periodic access, high delay requirements

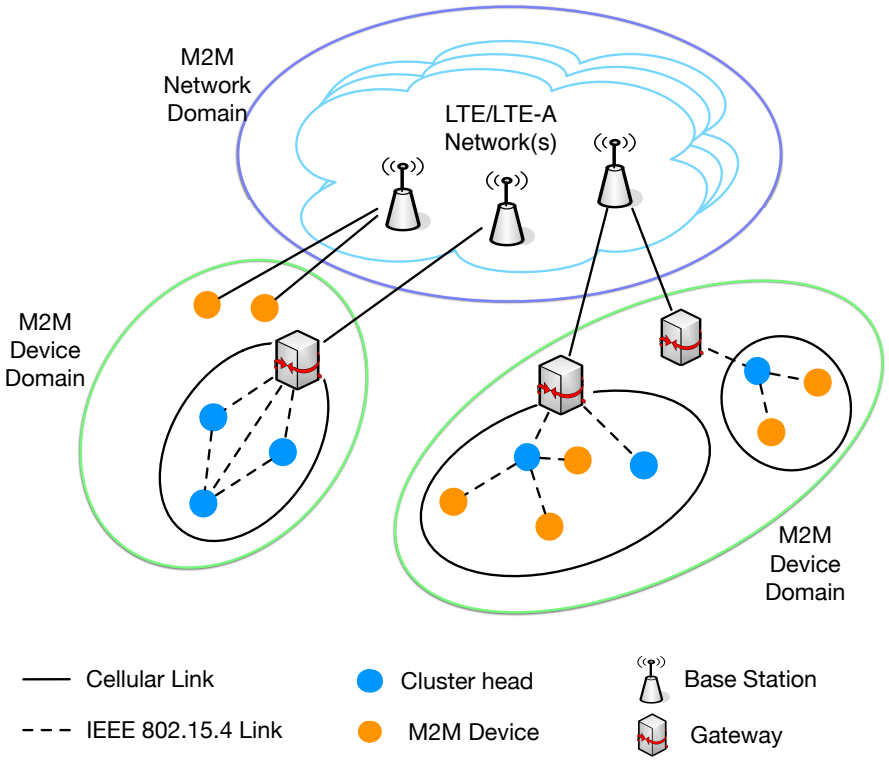

Figure 1.1: Hierarchical M2M networks.

1.2 Research Scope

This thesis focuses on access control management of ETSI compatible hierarchical M2M communication networks, as shown in Fig. 1.1. The aim of this thesis is to optimise the overall network performance, while satisfying different application requirements of hierarchical M2M communications, while exploiting the potential energy efficiency of duty cycle mechanism. Various network dynamics have been taken into consideration, such as network traffics, device capabilities, channel conditions and diverse application requirements.

To do so, a joint scheduling and duty cycle control framework for the ETSI compatible hierarchical M2M communication networks is proposed. The proposed

control framework consists of three control blocks, namely duty cycle control, cluster head control and gateway control.

i) The duty cycle control aims to address the trade-off between energy efficiency and delay for IEEE 802.15.4 based networks[1].

ii) The cluster head control aims to optimise the cluster empirical network performance and economic return while addressing the trade-off between optimality and algorithm complexity.

iii) The gateway control aims to conduct transmission schedule which optimises the long-term network utility while satisfying different QoS requirements among clusters.

To cope with the requirements of low computational complexity, non-prior network information and adjacent resource slots allocation for M2M communications, different control algorithms are developed for the proposed cluster head control and gateway control.

1.3 Contributions

- A practical and comprehensive Markov decision process (MDP) based network formulation is proposed for the ETSI compatible hierarchical M2M networks. The proposed network formulation takes various dynamics into account, such as time-varying link conditions, stochastic network traffics, various application requirements, and different device capabilities.

[1]The dominate short-range technology IEEE 802.15.4 is considered, as it has been widely adopted for various M2M applications, such as environment monitoring, scientific observation, emergency detection, field surveillance, and structure monitoring [TPS+05, WALJ+07, LL09, HVY+09, XRC+04]

- A joint scheduling and duty cycle control framework for M2M communications is proposed. The proposed framework consists of three control blocks: a duty cycle control for IEEE 802.15.4 based networks, a cluster head control and a gateway control. The proposed control framework aims at maximising the aggregated overall network utility and satisfying different application requirements, while exploiting the potential energy efficiency by applying duty cycle mechanism.

- The duty cycle controls for IEEE 802.15.4 based networks are designed based on local traffics. The duty cycle controls aim at jointly optimising the energy efficiency and end-to-end delay for IEEE 802.15.4 MAC protocol with both stop-and-wait automatic repeat request (ARQ) and Go-back-N ARQ schemes. The optimal duty cycle controls are derived by applying dynamic programming (DP). Simulation results shown that the proposed duty cycle controls achieve about 50% reduction in both energy consumption and end-to-end delay as compared to that of the current IEEE 802.15.4 standard.

- The cluster head control aims at optimising the single cluster utility. The optimal cluster head control is achieved by applying DP algorithm. A policy iteration (PI) based cluster control algorithm is proposed, taking into account the computational limitation of M2M devices. Simulation results shown that the proposed optimal cluster head control effectively improves energy efficiency, reduces end-to-end delay and packet drop ratio under various network traffics.

- A low complexity rollout algorithm (RA) based cluster head control is proposed to strike a reasonable balance between algorithm complexity and optimality. Simulation results shown that RA based cluster head control ef-

fectively improves the cluster head utility under various network traffics. In addition, RA based cluster head control achieves an exponential reduction of computational complexity compared with the DP optimal control.

- A reinforcement learning (RL) based cluster head control is proposed for practical M2M networks with non-priori network information, various network dynamics, and time-varying traffics. Simulation results shown that the proposed RL based cluster head control achieves the balance between optimality and stability, compared to the optimal solutions and the existing solutions.

- The gateway control optimises the long-term network utility, while satisfying different QoS requirements among clusters. The gateway control problem is formulated as a utility maximisation problem and the optimal Lagrangian solution is derived by using duality. Simulation results shown that the proposed Lagrangian based gateway control algorithm is capable of dealing with elastic applications and improves energy efficiency.

- A mixed integer programming (MIP) based gateway control is proposed to ensure the adjacent allocation of resource slots to each cluster. Simulation results shown that the MIP based control is capable of dealing with inelastic applications compare with the Lagrangian based control.

1.4 Thesis Structure

This thesis is organised as follow.

Chapter 2 provides a comprehensive introduction of current channel access

management approaches for M2M communication networks. Special attention is given for the IEEE 802.15.4 based hierarchical M2M networks. Then, the background of IEEE 802.15.4 MAC protocol is introduced, followed by the state-of-the-art of the duty cycle control for MAC protocols. In the end, the introduction of relevant methodologies used in this thesis are presented.

Chapter 3 presents the theoretical model of the ETSI compatible IEEE 802.15.4 based hierarchical M2M networks. The formulation of the system model, network model, traffic model and channel model are provided in detail.

Chapter 4 shows the designed joint scheduling and duty cycle control framework and simulation platform for the proposed hierarchical M2M networks. The theoretical analysis and derivation of the optimisation problem on maximise overall network utility are presented. In the end, the simulation platform validation is provided.

Chapter 5 solves the duty cycle control problem for IEEE 802.15.4 MAC protocol with Stop-and-Wait and Go-back-N ARQ schemes. The aim of the duty cycle control is to minimise a joint-cost of energy efficiency and end-to-end delay. The theoretical duty cycle control optimisation problem is derived through dynamic programming (DP). The performance of the proposed control algorithms are evaluated via simulations.

Chapter 6 focuses on the practical cluster head control for hierarchical M2M networks with the aim of maximising single cluster utility. Utility function is designed for each single cluster head. The utility function consists of both empirical network performance component and economic component. To meet different practical challenges, three control algorithms are proposed. Comprehensive discussion of each cluster head control algorithm are given based on both theoretical analysis

and simulation results.

Chapter 7 focuses on the gateway control with the aim of maximising network utility and satisfying different QoS requirements among clusters. Different utility functions are designed for different applications. The optimal gateway control is derived by applying network utility maximisation (NUM) and MIP approaches. In the end, the performance of the proposed gateway control algorithms are evaluated via simulations.

Chapter 8 presents the conclusions of this thesis. The ideas for future work based on the research carried out in this thesis are also presented.

1.5 Publications List

Journal Publications

1. **Y. Li**, K. K. Chai, Y. Chen and J. Loo,"Access Control Framework for IPv6-based Hierarchical Internet of Things Network", *Wireless Communication Magazine, IEEE*, accepted.

2. **Y. Li**, K. K. Chai, Y. Chen and J. Loo, "Joint Scheduling and Duty Cycle Control Framework for Hierarchical M2M Networks", *Mobile Computing, IEEE Transactions on.*, under revision.

3. **Y. Li**, K. K. Chai, Y. Chen and J. Loo, "Duty Cycle Control with Joint Optimisation of Delay and Energy Efficiency for Capillary Machine-to-Machine Networks in 5G Communication System", *Transactions on Emerging Telecommunications Technologies. Wiley*, vol.26, no.1, pp. 56 - 69, Jan. 2015.

Conference Publications

4. **Y. Li**, K. K. Chai, Y. Chen and J. Loo "QoS-Aware Joint Access Control and Duty Cycle Control for Machine-to-Machine Communications", in *Proc. of 2015 IEEE Global Communications Conference (Globecom)*, San Diego, CA, USA, Dec. 2015.

5. Y. Wang, **Y. Li**, K. K. Chai, Y. Chen and J. Schormans "Energy-aware Adaptive Restricted Access Window for IEEE 802.11ah Based Smart Grid Networks", in *Proc. of 6th IEEE International Conference on Smart Grid Communications (SmartGridComm 2015)*, Miami, FL, USA, Nov. 2015.

6. Y. Wang, **Y. Li**, K. K. Chai, Y. Chen and J. Schormans "Energy-aware Adaptive Restricted Access Window for IEEE 802.11ah Based Networks", in *Proc. of 26th Annual IEEE International Symposium on Personal, Indoor and Mobile Radio Communications (PIMRC)*, Hong Kong, China, Aug. 2015.

7. **Y. Li**, K. K. Chai, Y. Chen and J. Loo "Smart Duty Cycle Control with Reinforcement Learning for Machine to Machine Communications", in *Proc. of Communications Workshops (ICC), 2014 IEEE International Conference on*, London, UK, June 2015.

8. **Y. Li**, K. K. Chai, Y. Chen and J. Loo, "Optimised Delay-Energy Aware Duty Cycle Control for IEEE 802.15.4 with Cumulative Acknowledgement", in *Proc. of 25th Annual IEEE International Symposium on Personal, Indoor and Mobile Radio Communications (PIMRC)*, Washington, DC, USA, Sept. 2014.

9. **Y. Li**, K. K. Chai, Y. Chen and J. Loo, "Low Complexity Duty Cycle Control

with Joint Delay and Energy Efficiency for Beacon-enabled IEEE 802.15.4 Wireless Sensor Networks", in *Proc. of 11th International Symposium on Wireless Communication Systems (ISWCS)*, Barcelona, Spain, Aug. 2014.

10. **Y. Li**, K. K. Chai, Y. Chen and J. Loo, "Rollout Algorithm Based Duty Cycle Control with Joint Optimisation of Delay and Energy Efficiency for Beacon-enabled IEEE 802.15.4 Networks", in *Proc. of 20th European Wireless (EW)*, Barcelona, Spain, May. 2014.

11. **Y. Li**, K. K. Chai, Y. Chen, "Optimal Transmission Policy with Joint Minimization on Energy Consumption and Delay for Wireless Sensor Networks", in *Proc. of 15th IEEE International Conference on Communication Technology (ICCT)*, Guilin, China, Nov. 2013.

12. K. K. Chai, S. Jimaa, **Y. Li**, Y. Chen, "Multichannel MAC for Energy Efficient Home Area Networks", in *Proc. of 1st International Workshop on GReen Optimized Wireless Networks (GROWN'13)*, Lyon, France, Oct. 2013.

Chapter 2

Background and Methodology

This chapter presents the introduction of current research efforts on channel access management for hierarchical M2M networks. Taking the energy efficiency as key design criteria, special focus is given to the channel access management solutions for IEEE 802.15.4 based hierarchical M2M networks and different duty cycle control mechanisms. In the end, the basics of the relevant methodologies used in this thesis are provided.

2.1 Machine-to-Machine Communications

A machine-to-machine (M2M) communication system is a large-scale network with diverse applications and massive number of interconnected devices, such as sensors, actors, vending machines and vehicles. The devices are embedded in a remote asset and capture data such as temperature, location, consumption, heart rate, stress levels, light, movement, altitude and speed. These data will be transmitted wirelessly to central servers where the applications translate the data into meaningful information that can be analysed and acted upon.

M2M networks represent a future IoT which is expected to be widely utilised

in many fields, such as smart cities, health care, transport systems, public safety, industrial and agricultural automations [CCC+10, ZYX+11, YZG+13, CCZS08, GC13, LLKC12, XYWV12]. In addition, M2M communications have been listed as one of the horizontal topics of the Europe METIS 2020 project [MET]. More recently, following the study of M2M support in LTE-A networks [3GP11a, 3GP11b, 3GP11c, YZWG14, TLS+13], M2M communications have been identified as one of the key drivers to guide the design of 5G network [CFH14, BJL+14].

In the literature, two M2M communication architectures have been proposed [MMLN12]. One is the infrastructure-based approach which directly utilises cellular networks, such as LTE/LTE-A systems. The other is the infrastructure-less based approach, such as the ETSI proposed hierarchical M2M architecture [ETS].

Enabling M2M communications over LTE/LTE-A systems offers many benefits, due to its ubiquitous coverage, global connectivity with a number of providers, and well developed charging and security solutions [MMLN12]. A comprehensive survey of M2M communications with LTE/LTE-A systems is provided in [GC15], in terms of architectures, service requirements, challenges, and applications. There is a wide range of research for LTE/LTE-A based M2M communications [SJL+13, LC11, NK11, KKB+12, GLA12, WZJ+13, OHL15, WC15, PCLW14, SS14, THH11, HH12, LC11, LCL11, OKM12, ATN+14, DHVV14, LA11, LC11, LMWCFC12, SYCX15, LL15].

ETSI M2M technical committee has proposed an attempt to support M2M communications with a hierarchical architecture. The following part of this section will focus on the infrastructure-less based approach and give the state-of-the-art of channel access management for the ETSI compatible hierarchical M2M communications.

2.2 Hierarchical M2M Communication Networks

The hierarchical architecture consists of M2M Network Domain (ND) and M2M Device Domain (DD). Instead of direct cellular access, a large number of non-cellular M2M devices use short-range, low-cost, low-energy consumption radio interfaces, such as IEEE 802.15.4 or IEEE 802.11 to connect to the base station (BS) via M2M gateways. The networks with the non-cellular M2M devices are called capillary networks [ZHW+12]. The M2M gateways are acting as traffic aggregation and protocol translation points for the capillary networks to LTE/LTE-A networks [GLA12].

The M2M ND is the access and transport network that provides the interconnection of an M2M device or a gateway to application servers. The ND also includes the network management functions and the M2M device management functions. The ND is mainly composed of the core network (CN) and the access network (AN). The CN essentially provides: IP connectivity, interconnection with other networks, roaming with other CNs, service and network control functions. The AN represents the link, e.g. radio access network (RAN), to allow an M2M device or an M2M gateway to access CN services. Beside CN and AN, the ETSI proposed M2M architecture defines network management functions located in the CN or the AN, and M2M management functions located at M2M application level. The M2M DD involves the devices that support one or more M2M applications, by connecting them to application servers through the ND. The M2M DD, also referred as capillary networks in some literatures.

More specifically, the following devices are defined in the M2M DD (capillary networks):

i) **M2M Devices**: devices that can support one or more M2M applications. They are categorised into two classes: 1) LTE-A devices: they have LTE/LTE-A interface and can connect to the network domain by directly accessing the LTE-A network. 2) Non-LTE-A devices: they do not have LTE-A interface, but form capillary network(s) using short-range network access technologies, such as IEEE 802.15.4 or IEEE 802.11x. They can connect to the network domain through a M2M gateway, and run M2M applications locally.

ii) **Cluster Heads (CHs)**: They can be considered as more powerful M2M devices with some additional capabilities. Like regular M2M devices, they are also part of capillary networks and the communication from a regular M2M device may be directed through and managed by a CH. The functionalities of a CH may include data aggregation, and device management, etc.

iii) **M2M Gateway**: provides the inter connection between the core network, such as LTE-A network and the capillary networks. It provides various functionalities, such as protocol translation, resource management, device management and data aggregation, etc. In some cases, the gateway may also act as an application server which provides M2M services locally in the capillary network. It is expected that the M2M gateway will normally connect to the LTE/LTE-A network with a direct cellular link [GLA12].

The main advantages of hierarchical M2M approach over the LTE/LTE-A based approach lie on i) the low cost and low energy consumption M2M devices which do not require direct cellular interfaces; ii) its ability to aggregate, off-loading and shape M2M traffic for future transport to the LTE/LTE-A networks [Azi12].

With many solutions in place for M2M communications over LTE/LTE-A systems, however, these solutions cannot be applied to the hierarchical M2M networks

due to the different network architectures, operation radios and device limitations. On the other hand, there are only very limited work focus on the channel access management for hierarchical M2M communications.

A data compression strategy is proposed in [MAH13] with an attempt to reduce the traffic congestion. The proposed strategy operates at the gateways and aims at effectively exploiting the temporal and spatial correlation in sensors observations.

In [LCCZ13], topology control is discussed for M2M networks with two different types of devices. A tree-like distributed topology control algorithm (TLDTCA) is proposed taking the good characteristics of the hierarchical topology.

In [PKH14], a novel medium access control (MAC) protocol for hierarchical M2M networks, more specifically, the backoff time decision rule is proposed and evaluated by simulations. Analytical channel access success probability at cluster heads is derived and validated by simulations.

In [LYC+14], a scalable hybrid MAC protocol, which consists of a contention period and a transmission period, is designed for heterogeneous M2M networks. An optimisation problem is formulated to maximise the channel utility by finding the key MAC parameters.

Besides the aforementioned channel access management specially designed for hierarchical M2M communications, there is still a lack of systematic framework to optimise the overall network performance which fits the dynamic and practical M2M scenarios. With the aid of gateways, each M2M device is able to attach to the existing LTE/LTE-A cellular infrastructure. Thus, subsequent challenge lies in the massive access management for the capillary M2M network.

This thesis focuses on the M2M DD and aims to bridge the gap between theoret-

ical and practical work in hierarchical M2M networks. Both quantitative insights gained from mathematical theories and practical principles for real dynamic networks are taken into consideration.

2.3 IEEE 802.15.4 based M2M Device Domain

According to EXALTED [EXA], a hierarchical M2M communication project based on ETSI, the benefits of enabling capillary M2M communications over short-range communication technologies in M2M DD are:

i) The energy consumption of devices can be reduced. The devices lifetime is extended by transmitting at lower transmission power.

ii) The interference between devices can be reduced. This will enable the coexistence of a greater number of simultaneous operating networks.

iii) The cost of M2M devices can be reduced. The M2M devices are usually very cheap as they require less functionalities and capabilities.

iv) The traffic for the LTE-A system can be reduced. Thus, the load balance between wide-range communications (LTE-A networks) and short-range communications (capillary networks) is achieved.

IEEE 802.15.4 provides ultra low complexity, ultra low cost, ultra low power consumption, and low data rate wireless connectivity among inexpensive devices [Soc11]. IEEE 802.15.4 is regarded as the dominant short-range technology to implement in the hierarchical M2M networks. IEEE 802.15.4 has been widely adopted for various IoT applications, such as environment monitoring, scientific observation, emergency detection, field surveillance, and structure monitoring [TPS+05, WALJ+07,

LL09, HVY+09, XRC+04]. Thus, this thesis adopts the IEEE 802.15.4 as the short range wireless technology in the DD of the considered hierarchical M2M networks.

2.3.1 IEEE 802.15.4 Background

The IEEE 802.15.4 standard defines the physical layer (PHY) and MAC layer of the Open Systems Interconnection (OSI) model. The PHY defines frequency, power, modulation, and other wireless conditions of the link. The MAC defines the format of the data handling.

The IEEE 802.15.4 MAC protocol has two operation modes: beacon-enabled mode and non-beacon-enabled mode. The non-beacon-enabled mode uses unslotted carrier sense multiple access with collision avoidance (CSMA/CA) mechanism. The beacon-enabled mode uses a slotted CSMA/CA mechanism and it provides duty cycle based power management mechanism. This thesis focuses on the beacon-enabled mode.

2.3.1.1 Medium Access Control for beacon-enabled IEEE 802.15.4

For beacon-enable IEEE 802.15.4, each time period is composed of three parts: a beacon, a contention access period (CAP), and the optional contention-free period (CFP). Each CAP is divided into 16 equal slots. The slotted CSMA/CA algorithm in the CAP is illustrated in Fig. 2.1 and the relevant parameters are listed in Table. 2-A.

The IEEE 802.15.4 slotted CSMA/CA algorithm works as follows. All devices are synchronised via beacon transmission. Transmissions can begin only at the boundaries of time units, called backoff slots, which is denoted by *aUnitBackoff-*

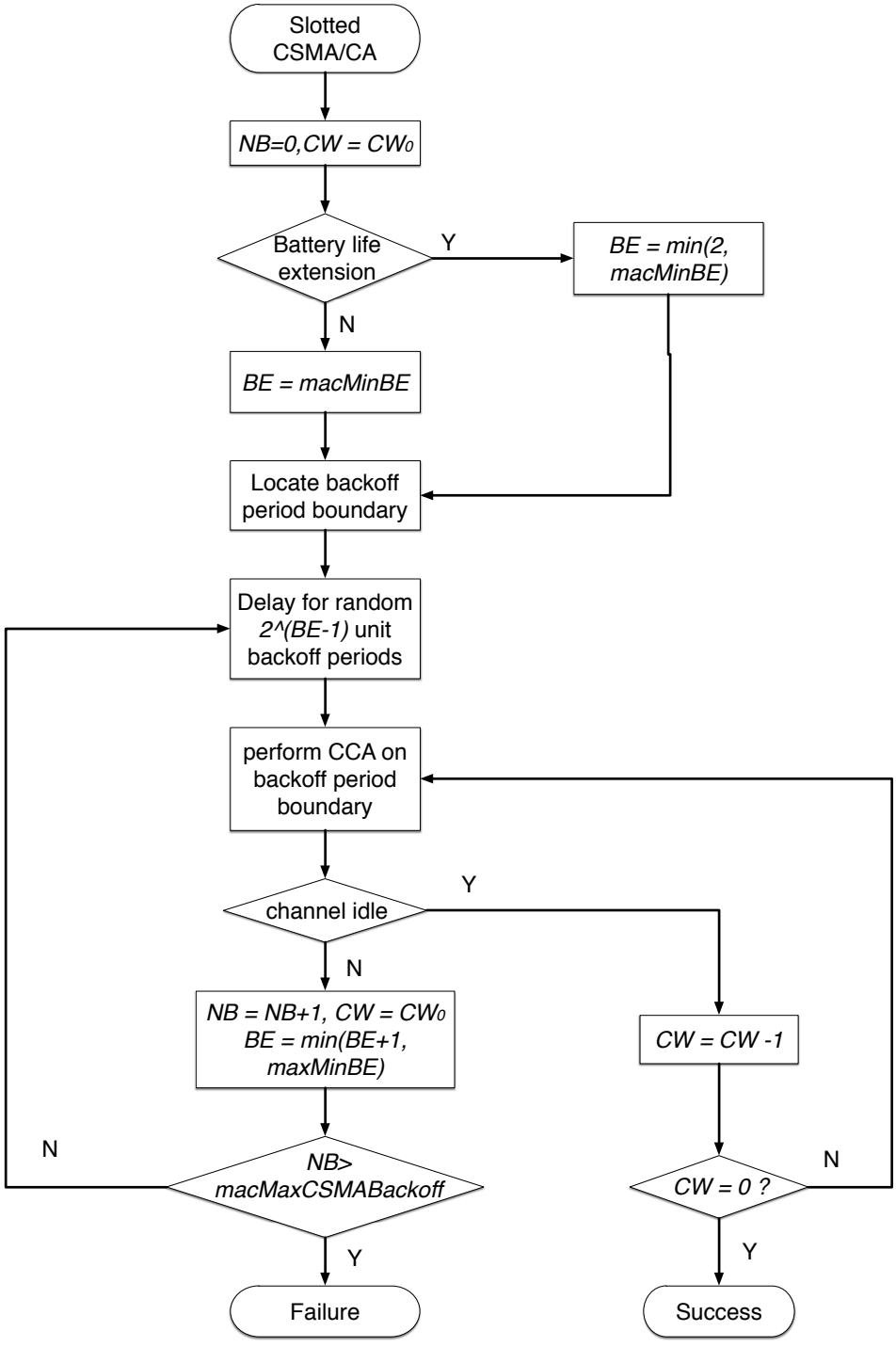

Figure 2.1: IEEE 802.15.4 CSMA-CA algorithm.

Table 2-A: Parameters in IEEE 802.15.4 CSMA/CA algorithm.

Attribute	**Description**	**Range**	**Default**
NB	the number of times required to back off while attempting the current transmission		0
CW	contention window length		initialise to CW_0
CW_0	initial value of CW		950 MHz band, 1; otherwise, 2.
$macMinBE$	minimum value of BE		3
$macMaxBE$	maximum value of BE	3 - 8	5
macMaxCSMABackoff	The maximum number of backoffs attempt before declaring a channel access failure	0 - 5	4

Period = 20 *symbols*. A device with a packet ready for transmission first back off for a random number of backoff slots before sensing the channel. The number of backoff slots is chosen uniformly between [0, *macMinBE*]. *macMinBE* is the minimum value of the backoff exponent (BE). The default value of BE is 3. The random backoff and the following channel sensing aim to reduce the probability of collisions among contending devices and ensure the channel is clear for a contention window (CW) duration. The CW duration is of two backoff slots in IEEE 802.15.4. This means that the device applies two channel clear assessments (CCAs) before transmitting. If the channel is found busy, BE is incremented by one, and a new backoff stage starts before channel sensing. This process is repeated until either BE equals *aMaxBE* (the maximum value of the BE whose default value is five) or until a certain maximum number of permitted random backoff stages is reached. In the former case, the value of BE is frozen at *aMaxBE* in the backoff periods. In the later case, an access failure is declared to the upper layer. The maximum number of permitted random backoff stages is determined by the parameter *macMaxCSMABackoff*, which has a default value of 4.

Furthermore, IEEE 802.15.4 supports optional retransmission scheme based on acknowledgements in beacon-enabled mode [ACF09]. When retransmissions are enabled, the receiver device must send a positive acknowledgement right after receiving a data frame. Acknowledgment and beacon frames are sent without using CSMA/CA mechanism.

2.3.1.2 Duty Cycle Control of IEEE 802.15.4

One of the most attractive features of IEEE 802.15.4 is that it utilises the duty cycle mechanism to save energy. A device can optionally bound its channel access time using a superframe structure. A superframe is bounded by the transmission of a beacon frame. A superframe has an active portion and an inactive portion. The devices enter sleep mode during the inactive portion to save energy. The duration between two consecutive beacons is called beacon interval (BI), while the duration of an active period is called superframe duration (SD), where

$$BI = aBaseSuperFrameDuration \times 2^{BO}, \tag{2.1}$$

$$SD = aBaseSuperFrameDuration \times 2^{SO}, \tag{2.2}$$

and beacon order (BO) and superframe order (SO) are two integers ranging from 0 to 14 ($0 \leq SO \leq BO \leq 14$), and $aBaseSuperFrameDuration = 15.36ms$ at 2.4 GHz with 250 kbps bandwidth. The duty cycle is defined as the ratio of the active portion over each BI, thus

$$Duty\ Cycle = SD/BI = 2^{SO-BO}. \tag{2.3}$$

The superframe structure in multi-hop scenarios is shown in Fig. 2.2. For each

cluster head, the BI is divided into two superframes, named incoming superframe and outgoing superframe. The cluster head receives the beacon from its parent gateway in the incoming superframe, and transmits its beacon in the outgoing superframe. As there are two SDs in each BI, according to (2.1) and (2.2), $SO \leq BO - 1$ for all cluster heads.

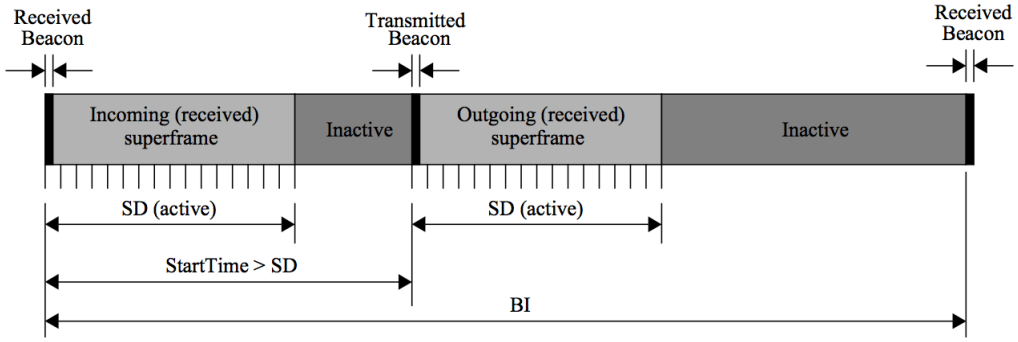

Figure 2.2: Superframe structure of IEEE 802.15.4.

Depending on the value of the parameter BO, the duration of each BI in 2.4 GHz varies from 15.36ms to 251.7s [CWGD10]. The duty cycle of different devices are equal in the current standard [Soc11]. Due to the fixed duty cycle, it is not possible for devices to dynamically change its own duty cycle to the time varying or spatially no-uniform traffic load among the network. In addition, the fixed duty cycle may result in high latency, especially for multi-hop networks, where devices on the routes may have different schedules [BDWL10] and the sleep delay will be accumulated hop by hop [SRS12].

2.3.1.3 Existing Adaptive Duty Cycle Control for IEEE 802.15.4

Determining the duty cycle is a crutial problem in beacon-enabled IEEE 802.15.4. However, such problem is complicated because simple and accurate models for

duty cycle control on reliability, delay and power consumption are not available. Moreover, it hard or impossible to compute the optimal duty cycle due to the scarce computational capacity of the devices and the lack of prior information of the network in real-life scenarios.

Some work have been done on duty cycle adaptation for IEEE 802.15.4 MAC protocol. A comprehensive survey of duty cycle control for beacon-enabled IEEE 802.15.4 MAC protocol can be found in [KGM14]. Some of the main duty cycle control approaches are listed below.

The earliest work on IEEE 802.15.4 duty cycle adaptation is known as the Beacon order adaptation algorithm (BOAA) [NPK]. In this work, the duty cycle adaptation is triggered by the change of traffic load in the network. The network traffic load is estimated from the number of packets received by the end devices. The proposed algorithm has the memory advantage as a buffer matrix is used to store the received packets. However, this buffer matrix made the algorithm unscalable for large networks which leads to the increase of end devices in the network.

Later, a duty cycle algorithm (DCA) is proposed in [JLHK07]. The duty cycle selection is based on additional information such as queue occupation and end-to-end delay. The reserved frame control field presented in the MAC frame header is modified, thus no extra overhead is incurred. The queue occupation is computed as the average of a queue indicator embedded in all frames during the active periods. However, this result is under the estimation that the number of transmission requested by devices decrease along with the decrease of active durations.

Authors in [LHJ+07] proposed the extension of the CAP based on a busy tone sent by devices. The busy tone is only sent if the device has failed to transmit all its

data frames. In [LJ08], the CAP extension is done based on the type of the traffic that is waiting in the queue. Specifically, the CAP is extended if there is some real-time data in the transmit queue at the end of the CAP. These extensions are however not compliant with the standard as they added the extension immediately after the CAP thus modifying the superframe structure. In addition, they are not proportional envisaged to the amount of traffic waiting to be transmitted. Finally, they are not as flexible as duty cycle adaptations because they still work on fixed active and beacon interval durations.

A duty cycle learning algorithm (DCLA) [AP12] adapts the duty cycle during run time without the need of human intervention. DCLA aims to minimise power consumption while balancing probability of successful data delivery and delay constraint of the applications. DCLA running on coordinator devices, it collects network statistics during each active duration to estimate the incoming traffic. Then, at each beacon interval the reinforcement learning (RL) is used to learn the optimal duty cycle. The algorithm is formulated as a multi-armed bandit problem where the agent's objective is to minimise idle listening and buffer overflows. DCLA adjusts its policy for selecting the duty cycle according to the feedback information provided by the network. Both the MAC parameters (BO, SO) are taken into consideration to find a compromise among beacon overhead and queuing delay. Basically, RL depends on repetitive interactions. The selected duty cycle is updated iteratively till the optimal one, which achieves the targeted performance.

In this way, DCLA achieves a fully adaptive system that can self-correct its parameters based on the traffic conditions, without the need for any manual configurations to specific requirements of different applications. This gives DCLA the credit of reducing time and cost of installation, operation and management. How-

ever, the learning processes presented slow convergence for non-stationary scenarios due to the selection of a large state-action space.

2.3.2 Delay Aware Duty Cycle Based MAC Protocols

Besides the duty cycle controls specifically designed for IEEE 802.15.4, there are some other duty cycle control mechanisms for general duty cycle based MAC protocols. In this part, the work with the aim of designing energy efficient and delay aware duty cycle based MAC protocols is given.

Sensor MAC (SMAC) [YHE02] is the fundamental work of energy efficient MAC protocol, which first introduces the periodic duty cycle concept to reduce idle listening power consumption. The key issue to improve the performance of SMAC lies on finding the adaptive optimal tradeoff between the sleep delay and energy efficiency [BDWL10].

The existing duty cycle controls based on SMAC are classified according to their specific approach and the aimed problem, as shown in Fig. 2.3. The detailed discussion on these controls are given in the following sessions.

2.3.2.1 Adaptive Active Periods

The motivation of solutions with this approach is to alleviate the high latency problem when the traffic load is high, while reducing the idle listening when the traffic load is low.

Timeout MAC (TMAC) [DL03] is the classic protocol to solve the fixed active

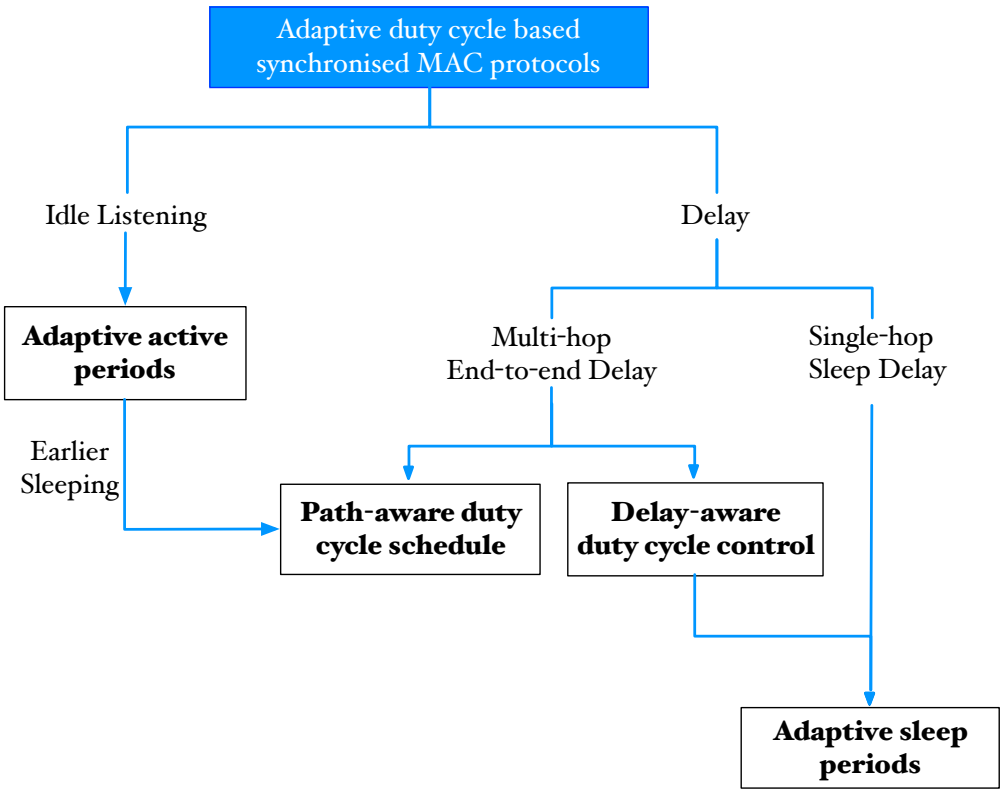

Figure 2.3: Classification of duty cycle based MAC protocols

period problem. With TMAC, the device can switch into sleep mode when it does not expect further transmission by predicting channel activity during an active period. A utilisation based MAC (U-MAC) [YTW+05] works similar with TMAC. UMAC controls the length of active periods based on a utilisation function, which is the ratio of the actual transmission and receptions performed by the device.

The main problems of this approach are: Firstly, by having device ending their active periods prematurely, TMAC and UMAC partially break the synchronisation among the devices, which leads to the *early sleep problem* [BDWL10]. The early sleep problem happens when a third-hop device, which supposes to be the next relay of an ongoing transmission, prematurely goes to sleep. Secondly, the

uniformed duty cycle for all devices is not flexible when each device generates different amount of traffic with different quality of service (QoS) requirements.

2.3.2.2 Adaptive Sleep Periods

Sleep delay is the delay caused by waiting to be transmitted when devices are in sleep mode. Sleep delay is the main cause of delay due to the long sleeping periods in low duty cycle MAC protocols. To reduce the sleep delay, some of the research try to adapt the length of sleep periods according to the traffic conditions in the network.

The idea of achieving a good trade-off between energy efficiency and end-to-end delay through adaptive sleep intervals was first explored by dynamic sensor MAC protocol (DSMAC) [LQW04]. DSMAC is able to dynamically change the sleeping intervals. The key idea of DSMAC is to maintain the synchronisation, thus the initial active periods never get changed. Devices reduce the length of sleep periods by inserting extra active periods in the middle of the sleep periods when less latency is required or when it observes an increasing traffic load. Thus the duty cycle adaptation of DSMAC can only be double or half of the initial setting.

Similar with DSMAC, the fast path algorithm (FPA) proposed in [LYH05] provides fast data forwarding paths by adding additional active periods along the paths from the sender to the destination. A device uses its hop distance from the sender to estimate when its upstream neighbour will send a packet to it. Then, the device wakes up at the estimated time to receive and potentially forward the packet to its next-hop neighbour, so that devices along the path can wake up at the right time to avoid schedule misses.

The concern with this approach is its implementation issue. To establish the schedule the device must have some additional information, such as the average latency and the transmission path information, which increases the overhead of the transmission.

2.3.2.3 Path-aware Duty Cycle Schedule

The key idea of this approach is to sequentially schedule the active periods for the devices along the transmission path. Thus, with a properly schedule, the packets can be sent out immediately hop by hop once received without queuing.

RMAC [DSJ07] is a novel scheme to cope with the end-to-end delay accumulation. Each operation cycle contains a Synch, Data, and a Sleep period. To reduce end-to-end latency, RMAC forwards a control frame called PION over multi-hops during a Data period, and schedules the upcoming data packet delivery along that route. Each intermediate device along the data packet delivery route sleeps and wakes up at the scheduled time to forward data (only devices involved in the communication will wake-up, while others keep in sleep mode). However, RMAC has a long latency when packet transmission errors occur, and two hidden sources that have succeeded in scheduling through PIONs will cause collisions at the beginning of the next sleep period. In this case, RMAC simply resumes the packet transmission in the next time period without any immediate packet retransmission.

Demand-wakeup MAC (DW-MAC) [SDGJ08] relies on RMAC's approach and tries to reduce the delay caused by collisions and transmission errors. DW-MAC assumes that a separate protocol is used to synchronise the clocks in sensor devices during the Sync period, which ensures the required precision. The DW-MAC's scheduling mechanism ensures that data transmissions do not collide at

their intended receivers. The proposed protocol works under random topology and supports both unicast and broadcast traffics. DW-MAC sets up a one-to-one mapping between a Data period $TData$ and the following Sleep period $TSleep$. In such a way that the time, when the scheduling frame is transmitted, determines the corresponding offset of the DATA packet exchange.

2.3.2.4 Delay-aware Duty Cycle Control

With this approach, the end-to-end delay requirement of the whole transmission is broken down into several single-hop delay requirements.

In [WWXY10], DutyCon is proposed to guarantee end-to-end delay by assigning a local delay requirement to each single hop along the transmission path. However, as a feedback controller is designed, this approach requires significant amount of signalling from the neighbour devices to compute the delay. To reduce the signalling among neighbour devices, a distributed duty cycle controller is proposed in [BY13] aiming at controlling the local queue length of the device to be the same as the predetermined threshold. The distributed duty cycle control is achieved by adjusting the sleep duration of each device based on its local queue length independently. However, this approach needs specific syntonisation scheme, and the evolution of the proposed control requires carefully setting of the initial duty cycle and control parameters.

2.4 Relevant Control and Scheduling Methodologies

In this section, the introduction of relevant methodologies used to solve the massive access and various QoS requirements problem for IEEE 802.15.4 based hierarchical M2M networks are given. The mentioned methodoligies are stochastic control, dynamic control and approximate dynamic control.

Stochastic control is a subfield of control theory that deals with the existence of uncertainty that drives the evolution of the system. Optimal control is one of the most useful systematic methods to provide solutions to control problems.

Stochastic optimal control aims to design the desired control variables over time so that the controlled task is accomplished with minimum cost or maximum reward under the existence of uncertainty. The stochastic optimal control has found its applications in areas such as industrial control systems, inventory management, dynamic resource allocation, production planning, queuing networks, finance and so on [Ast70, Aok76, BSLG74, KS98, SZ94, YZ99].

In M2M communication networks, a massive amount of M2M devices are random distributed in large areas. These M2M devices generate different traffics and communicate with each other through stochastic wireless channels, and the transmitted signals are subjected to random fading. Thus, modelling and optimisation of the emerging M2M communication networks are naturally resort to stochastic optimal control.

The general form of the discrete-time stochastic system is described as,

$$s_{t+1} = f_t(s_t, a_t, w_t), \quad t = 0, 1, , \cdots, T-1 \tag{2.4}$$

where

- t is the discrete time periods of the control;
- s is the state of the system, which summarises past information that is relevant for future optimisation;
- a is the control, which is the decision to be selected at time t from a given valid control set;
- w is the random parameter, which is also called "disturbance" or "noise".

Dynamic programming (DP) offers a unified approach to deal with complex multistage stochastic problems by breaking them down into simpler subproblems [Ber05].

Principle of optimality and *Bellman equation* are two conditions for problems can be solved by DP. The *principle of optimality* means that the tail policy is the optimal solution to the tail subproblem, in other words, the optimisation of the future does not depend on what we did in the past.

The DP optimal algorithm works as follows: first, the cost-to-go function $J_t(s)$ is computed from time period t back to time period 0; Then, the policy from time period 0 to time period t is selected with the minimum $J_t(s)$ and the control is decided based on the selected policy.

Approximate dynamic programming (ADP) is a method for modelling and solving DP problems that are large, complex, and stochastic. ADP often presents as a

method for overcoming the classic *curse of dimensionality* of DP by finding good suboptimal solutions [Pow11].

The basic idea of ADP is on replacing the cost-to-go function $J(s)$ by an approximation $\tilde{J}(s)$. Thus, this method applies at time period t and state s_t a control $\mu_t\hat{(}s_t)$ that minimise the cost-to-go function over $u_t \in U_t(s_t)$,

$$\mathbb{E}\Big\{ g_t(s_t, u_t, w_t) + \tilde{J}_{t+1}(f_t(s_t, u_t, w_t)) \Big\}. \tag{2.5}$$

The corresponding suboptimal policy $\bar{\pi} = \{\bar{\mu}_1, \bar{\mu}_2, \cdots, \bar{\mu}_T\}$ is determined by the approximate cost-to-go functions $\tilde{J}_1, \tilde{J}_2, \cdots, \tilde{J}_T$. The approximation of the cost-to-go function is calculated either by functional form or by an algorithm to calculate their values at each state.

There are several alternative approaches for selecting or calculating the approximate cost-to-go function $\tilde{J}(s)$, rollout algorithm and reinforcement learning (RL) are two widely used online approximation methods [Pow11].

2.5 Summary

This chapter provides the introduction of current research efforts on massive access control for hierarchical M2M networks. With the focus on IEEE 802.15.4 based capillary M2M DD networks, the state-of-the-art review on duty cycle controls with the aim of joint improving energy efficiency and delay are presented. In the end, the relevant methodologies applied in this thesis are provided.

Chapter 3

Hierarchical Machine-to-Machine Communication Networks

In this chapter, the mathematical formulation of an IEEE 802.15.4 based capillary M2M system is presented. Then, the network model, traffic model and channel model of the formulated capillary M2M system are given.

3.1 System Model

The LTE/LTE-A base station (BS), M2M gateways, cluster heads and M2M devices are four types of devices in an ETSI compatible M2M network [ETS, EXA]. A set of statically-deployed devices with uplink transmission to BS is considered in this thesis.

The network operates at discrete time domain where time is divided into time periods $t = 0, 1, \ldots, T$. Each device is equipped with a single omnidirectional antenna. As shown in Fig. 3.1, the set of M2M gateways is denoted as $\mathcal{N}$. The child cluster heads of gateway n forms the cluster head set $\mathcal{I}_n$ and the link set between gateway n and cluster head i is denoted as $\mathcal{L}_{i,n}$. The immediate child

devices of cluster head $i \in \mathcal{I}_n$ form the child devices set $\mathcal{C}_i$ and the link set between cluster head i and its child device $j \in \mathcal{C}_i$ is denoted as $\mathcal{L}_{i,j}$. The link $l \in \mathcal{L}_{i,j}$ or $l \in \mathcal{L}_{i,n}$ can also be represented by device pair (i, j) and device pair (i, n), respectively.

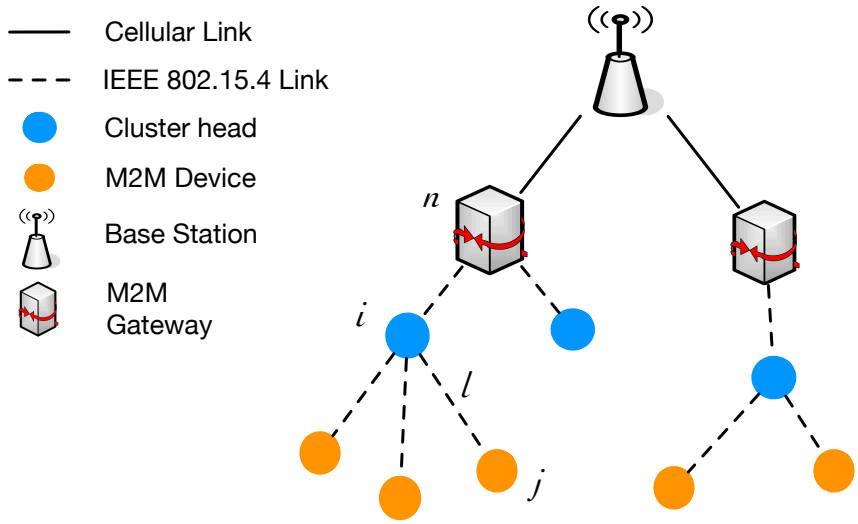

Figure 3.1: ETSI compatible hierarchical M2M system model.

For a given capillary M2M network, different clusters may run different applications. According to [ZHW+12], four classes of applications are considered in this thesis,

i) Elastic applications: these applications are rather tolerant of delays, the environment monitoring is a typical example of such application.

ii) Hard real-time applications: these applications need their data to be served within a given delay constraint. Vehicle and asset tracking are typical M2M service application fall into this class.

iii) Delay adaptive applications: these applications are delay sensitive but can be made rather tolerant of occasional delay bound violation and dropped

packets. A typical example is remote monitoring in e-Health services.

iv) Rate-adaptive applications: these applications adjust their transmission rates according to available radio resources while maintaing moderate delays. Video transmission is one example application in this class.

3.2 Network Model

3.2.1 Markov Decision Process

Markov decision process (MDP) is a discrete time stochastic control process. MDP provides a mathematical approach for modelling decision making in situations where outcomes are partly random and partly under the control of a decision maker or controller.

A controller interacts with the system by taking actions based on its observations at each discrete decision period. Associated with each action in each state, there is a cost to the controller. Typically, an action will lead the system from the current state to some other states with certain probabilities. The goal of the controller is to minimise the total cost over finite or infinite time horizon by making sequential decisions based on its current observations.

An general MDP based system is described by a tuple $< S, A, P, J, \gamma >$, where

- S is a finite set of states;

- A is a finite set of actions (alternatively, A_s^t is the finite set of actions available at state s_t);

- $P_a(s, s')$ is the probability that action a in state s_t at time t will lead to state s' at time $t+1$, thus $P_a(s, s') = \Pr(s_{t+1} = s' \mid s_t = s, a_t = a)$;

- $J_a(s, s')$ is the immediate cost (or expected immediate cost) of transition to state s' from state s;

- $\gamma \in [0, 1]$ is the discount factor, which represents the importance between future costs and the present cost.

The core problem of a MDP system is to find a policy π for the controller. A policy π specifies the action rules μ_t the controller will follow at state s_t,

$$\pi = \mu_1, \mu_2, \cdots, \mu_T, \tag{3.1}$$

where μ_t maps states s_t into control $a_t = \mu_t(s_t)$, such that $\mu_t(s_t) \in a(s_t)$ for all $s_t \in S$.

Note that MDP is an extension of Markov chains. Once a MDP is combined with a particular policy, which fixes the action for each state, the resulting combination of the MDP and the policy behaves as a Markov chain.

MDPs are useful for studying a wide range of optimisation problems which can be solved by applying DP and RL.

3.2.2 Markov Decision Process based Network Formulation

The access control of the formulated hierarchical capillary M2M network is formulated as a finite-state MDP. For each cluster head $i \in \mathcal{I}_n$, the cluster is described

as a tuple $< I, S, A, P, U, \gamma >$ where

- I is the total number of cluster heads connected to gateway n;
- S is a finite set of discrete states of cluster heads. For the cluster head i at time period t, its state $s_i^t \in S$ is represented by its queue length q_i^t;
- A_i is the finite set of control decision available to the cluster head i, and $A = A_1 \times A_2 \times \cdots A_I$;
- U is the utility function of cluster heads. Thus, for the cluster head i,$s_i^t \times a_i^t \mapsto U_i^t$.
- P is the transition function. $S \times A \times S \mapsto [0, 1]$, and $P(s_i^t, a_i^t, s_i^{t+1}) = 1$ represents the transmission link between the M2M device and its cluster head meets the sensitivity requirements of the cluster head i. Note that $\forall s_i^t \in S$, $\forall a_i^t \in A$, $\sum_{s_i^{t+1} \in S} P(s_i^t, a_i^t, s_i^{t+1}) = 1$.
- $\gamma \in [0, 1]$ is the discount factor, which represents the difference between future utility and current utility.

For each cluster head, the MDP is repeated over T time periods, as shown in Fig. 3.2. More specifically, at each time period t, each cluster head $i(0 \leq i \leq I)$ will senses its own queue length $q_i^t \to s \in S$, then the cluster head i decides the number of packets it will receive $r_i^t \to a \in A_i$. As a result, the queue length of cluster head i transits to $q_i^{t+1} \to s' \in S$ according to transition probability $P_{ss'}(a) \in P$ and thereby generates a utility $U_i^t = U(s, a)$ passing to the cluster head i.

As shown in Fig. 3.2, the access control between each cluster head i and its child M2M devices follows the formulated MDP $< I, S, A, P, U, \gamma >$, where S is the queue length of the cluster, A is the cluster head control decision and U is the

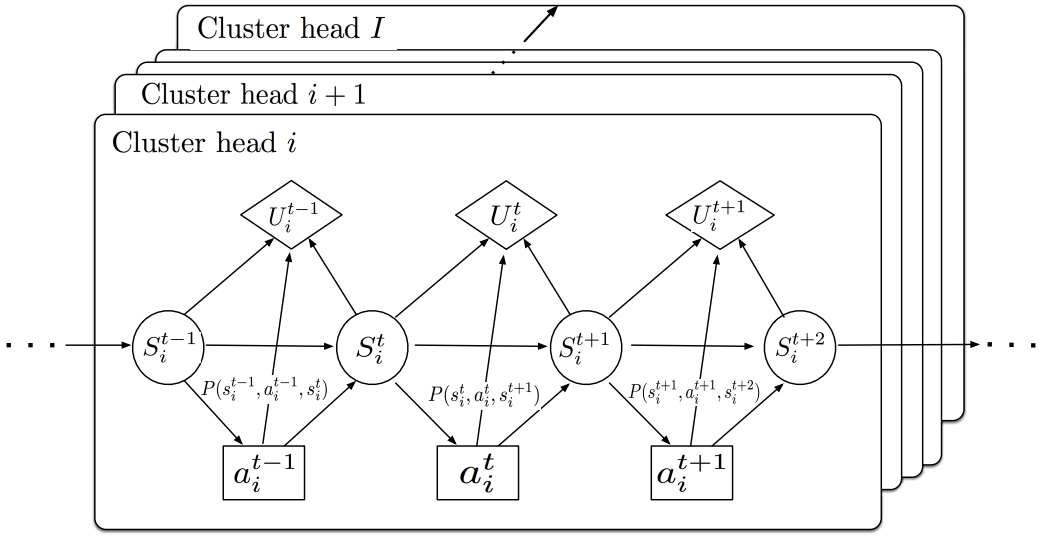

Figure 3.2: MDP model of gateway.

cluster utility.

3.3 Traffic Model

The queue length of a device is defined as the number of packets in the transmission queue. Assume all generated and received packets are available at the beginning of each time period t. Let q_i^t denote the queue length of the cluster head i at the beginning of superframe at time period t. The change of queue length of cluster head i is given as

$$q_i^{t+1} = \min\left([q_i^t + r_i^t - f_i^t + g_i^t]^+, q_i^{max}\right), \tag{3.2}$$

where $0 \leq t \leq T-1$, $[\cdot]^+ = \max(0, \cdot)$, g_i^t is the number of packets being generated by device i at time period t; f_i^t is the number of packets transmitted by cluster head i at time period t; and r_i^t is the number of packets received by cluster head i

at time period t, as shown in Fig. 3.3. In addition, let q_i^{max} denote the maximum queue length of cluster head i, which is also the buffer size of cluster head i. The new arrived packets will be dropped if the queue length reaches its maximum q_i^{max}, as shown in Fig. 3.4.

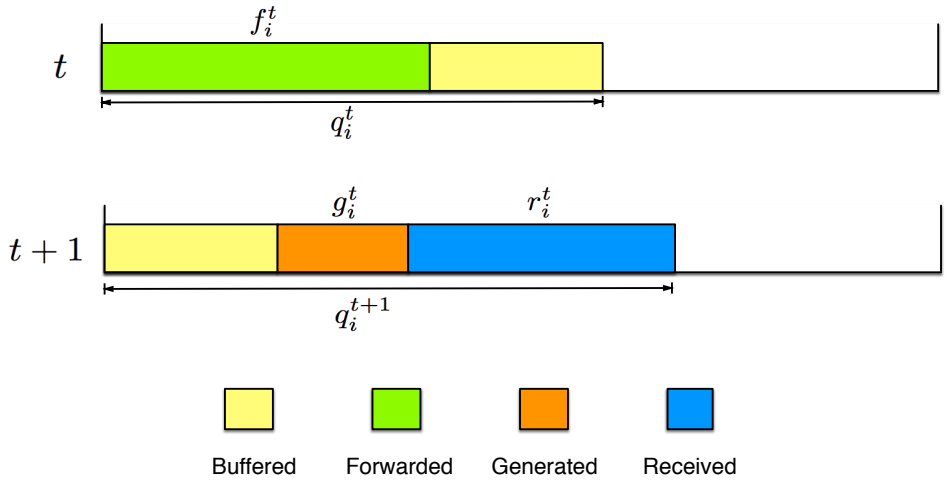

Figure 3.3: Change of queue length of devices.

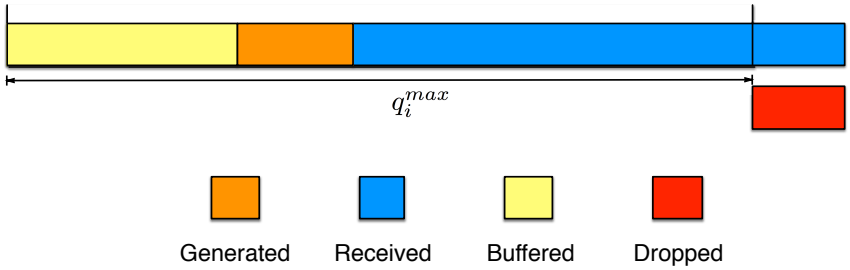

Figure 3.4: Packet drop due to reach the buffer size.

The batch Poisson process is applied as the traffic arrival model for all devices. This is different from the assumption in most of the existing work that there is only one packet being transmitted in each time period. In this batch Poisson process model, the number of arrived packets, a batch, follows the Poisson process. The number of packets of the link $l_{i,j}$ batch is denoted by $g_{i,j}^t$. $g_{i,j}^t$, is identically and independently Poisson distributed.

Since the traffic arrival of each M2M device follows a batch Poisson process, the traffic arrival of each cluster follows a compound Poisson distribution. Thus, the arrived traffic of each cluster $g_i^t = \sum_{j \in \mathcal{C}_i} g_{i,j}^t$.

This traffic model is adopted in the utility optimisation problem formulation and access management control in the following chapters. In addition, it is also implemented in the simulations to evaluate the performance of all proposed controls.

3.4 Channel Model

To fit the practical scenarios, this thesis adopts an empirical dual-slope propagation model of path loss with distance, Nakagami frequency-flat small-scale fading, and lognormal shadowing [NIS11]. Based on this dual-slope propagation model, the overall channel propagation loss is expressed as

$$\begin{aligned} L_{c,dB} =& L_{0,dB} + X_{s,dB} + X_{f,dB} \\ &+ \begin{cases} 10n_0 \log(d) & d \leq d_1 \\ 10n_0 \log(d_1) + 10n_1 \log(\frac{d}{d_1}) & d > d_1 \end{cases}. \end{aligned} \tag{3.3}$$

where $L_{0,dB}$ is the reference path loss where the distance between the sender and receiver is 1m; $X_{s,dB}$ is a zero mean Gaussian random variable with standard deviation σ_s. d is the distance between the sender and receiver and d_1 is the reference distance; $X_{f,dB} = 10\log(X_f)$ and X_f is a unit-mean gamma-distributed random variable with variance $1/m$ (m is the Nakagami fading parameter), and all logarithms are base 10.

As 2.4GHz is globally available for the IEEE 802.15.4, Table. 3-A, Table. 3-B and Table. 3-C list the channel model parameters at 2.4GHz for the modelled capillary M2M network. These parameters are set based on the data provided in [NIS11].

Table. 3-A shows the parameters of the channel model for indoor-indoor environments. Each environment is further differentiated into line-of-sight (LOS) and non-line-of-sight (NLOS) conditions. Note that in some environments the applied dual-slop model simply collapses to the single-slope model by setting $n_1 = n_0$ and choosing $d = d_1$. And the path loss exponents are stated relative to the free space path loss. Table. 3-B shows the channel model parameters for outdoor-outdoor urban-canyon environments. Table. 3-C shows the channel model parameters for outdoor-indoor environments. Because of the nature of the outdoor-indoor environment, all parameters are for NLOS conditions.

Table 3-A: Channel Model Parameters of Indoor-indoor Environments

	Environment	L_0	n_0	n_1	d_1	σ
LOS	residential	16.3	2.2	2.2	1	2.4
	office	22.8	1.2	1.2	1	1.7
	industrial	22.4	1.1	1.1	1	2.1
	cinder block	24.2	1.5	1.5	1	2.8
NLOS	residential	12.5	2.2	5.6	11	3.0
	office	26.8	2.2	6.7	10	3.7
	industrial	29.4	1.4	1.4	1	6.3
	cinder block	9.1	4.9	4.9	1	6.7

The received power $P^t_{rec,i}$ of cluster head i is a function of the transmitted power, antenna gains, and channel attenuation. It is modelled (in decibels referenced to

Table 3-B: Channel Model Parameters of Outdoor-outdoor Environments

	Environment	L_0	n_0	n_1	d_1	σ
LOS	urban-canyon	6.9	1.7	1.7	1	2.4
NLOS	urban-canyon	21.3	1.6	1.6	1	7.4

Table 3-C: Channel Model Parameters of Outdoor-indoor Environments

Environment (NLOS)	L_0	n_0	n_1	d_1	σ
office	0.2	2.0	4.2	70	3.3
high-rise	8.8	2.2	2.2	1	5.6
convention center	4.2	0.6	3.7	100	4.6
mine tunnel	5.7	0.7	18.3	70	5.8

1mw) as

$$P^t_{rec,i} = P^t_{tran,i} + G^t_{tran,i} + G^t_{rec,i} - L^t_{c,i}, \tag{3.4}$$

where $P^t_{tran,i}(dBm)$ is the conducted power to the transmit antenna (dBm), $G^t_{tran,i}(dBi)$ and $G^t_{rec,i}(dBi)$ are the transmit and receive antenna gains (dBi), respectively, $L^t_{c,i}$ is the loss due to channel propagation.

It is assumed that the fading and shadowing are constant during each time period. The condition for the successful transmission is that the received signal power $P^t_{rec,i}$ is above the sensitivity threshold $P^t_{sens,i}(dBm)$ of the device. The

successful transmission probability $\rho_{i,j}^t$ is denoted as,

$$\rho_{i,j}^t = \begin{cases} 1 & P_{rec,i}^t \geq P_{sens,i}^t, \\ 0 & P_{rec,i}^t < P_{sens,i}^t. \end{cases} \tag{3.5}$$

The transition function $P_{i,j}$ gives the successful transmission probability that action a in states s at time period t will lead to state s' at next time period $t+1$:

$$P_{i,j}(s, a, s') = P_{ss'}(s^{t+1} = s' | a^t = a, s^t = s, \rho_{i,j}^t = 1). \tag{3.6}$$

As defined in the standard, the transmission rate of IEEE 802.15.4 is 250kbps at 2.4GHz. Due to the duty cycle mechanism, the amount of data could be transmitted within each BI should be the transmission rate times the active period length. Thus, we denote the equivalent actual link capacity as

$$C_{i,n}^t = 250kbps \times \textit{duty cycle}. \tag{3.7}$$

3.5 Summary

In this chapter, the system model, network model, traffic model and channel model of IEEE 802.15.4 based hierarchical capillary M2M network are presented. The system of the capillary M2M communication takes elastic applications, hard real-time applications, delay adaptive applications and rate-adaptive applications into consideration. The network formulation is based on discrete time MDP. The traffic model of the M2M network is formulated into a batch Poisson process and an empirical dual-slope propagation model is adopted as the channel model.

Chapter 4

Joint Scheduling and Duty Cycle Control Framework

In this chapter, the utility maximisation problem of the modelled IEEE 802.15.4 based hierarchical capillary M2M networks is formulated. The formulated network utility optimisation problem takes link constraints, application types and device capacities into consideration. Then, a joint scheduling and duty cycle control framework for M2M communication networks is presented. The design of simulation platform and validation are presented at the end of this chapter.

4.1 Network Utility Optimisation for Hierarchical M2M Communications

For the modelled hierarchical M2M communication networks with multi-class applications in Chapter 3, the network utility optimisation problem aims not only to maximise the overall network utility, but also meet different QoS requirements among clusters.

In order to optimise the network utility, the utility function for each applica-

tion needs to be designed carefully. The widely adopted utility function design approach uses a logarithmic function for the elastic source (elastic applications), and a sigmoid function for the inelastic source (hard-real time applications, delay adaptive applications and rate adaptive applications) [She95, JSKP10, ZHW+12]. Fig. 4.1 illustrates the utility function of each application class considered in this thesis.

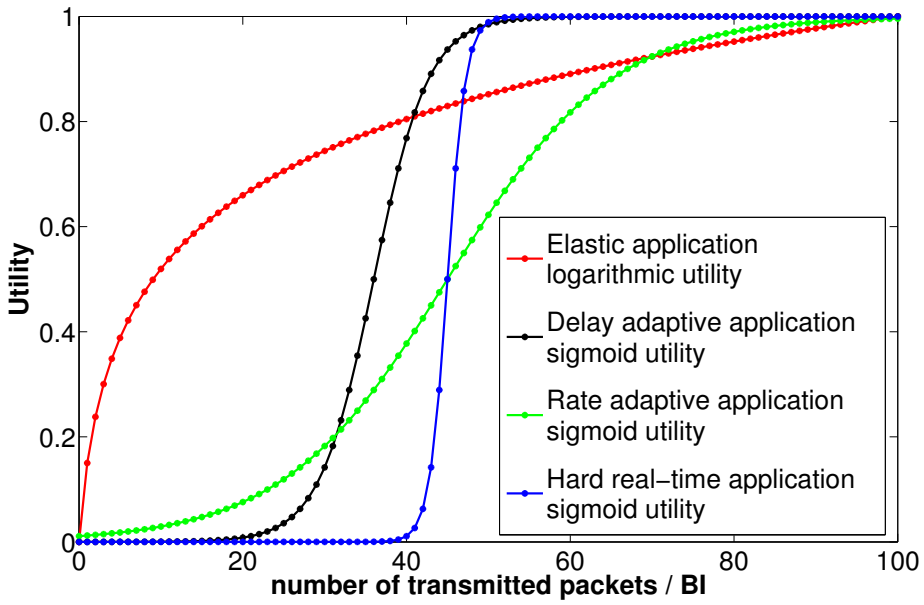

Figure 4.1: Utility illustration for different applications.

Different from the formulation in the existing work, the problem formulation of the network utility optimisation in this thesis takes multi-class applications into consideration by introducing the application factor θ_i^t of each cluster head i. The application factor θ_i^t indicates, i)the application class of each cluster, and ii) the priority of clusters within the same application class.

Application factor θ_i^t is considered as one of the parameters in the proposed network optimisation problem. Then, the joint scheduling and duty cycle control

optimisation problem for the modelled hierarchical M2M networks with multi-class applications is formulated as,

$$\mathcal{P}1: \quad \min \sum_{t=0}^{T} \sum_{i \in \mathcal{I}_n} U_i(f_i^t, r_i^t, \theta_i^t) \tag{4.1a}$$

$$s.t. \qquad \sum_{i \in \mathcal{I}_n} f_i^t \leq C_{n,b}^t, \tag{4.1b}$$

$$0 \leq f_i^t \leq C_{i,n}^t, \qquad i \in \mathcal{I}_n \tag{4.1c}$$

$$r_i^t \leq \min(C_{i,n}^t, q_i^{max}), \quad i \in \mathcal{I}_n. \tag{4.1d}$$

The objective of $\mathcal{P}1$ (4.1a) is to maximise the network long-term aggregated utility, taking into account the application indicator θ_i^t, number of packets each cluster head received r_i^t, and number of packets each cluster head forward f_i^t of cluster i at time period t. The constraints (4.1b) to (4.1d) are the link capacity constraints stating that the total transmitted packets of each link should be no more than its link capacity or its maximum queue length.

It is worth noting that the utility functions for the inelastic applications (hard-real time applications, delay adaptive applications and rate adaptive applications) are not concave functions. This makes the problem $\mathcal{P}1$ hard to be solved by classic network utility maximisation (NUM) directly.

The NUM problem was firstly formulated as an optimisation problem in [KMT98]. The objective of NUM in [KMT98, LL99] was to maximise the aggregate utility in wired networks with delay-tolerant applications for all users under the link capacity constraints. In [LMS05, Kur12], the NUM framework was extended to wireless networks with real-time applications. Using duality, the distributed iterative algorithm for the optimal rate allocation was achieved.

The overall objective of NUM is to maximise the utility $U(s)$. The problem can be achieved by solving the following primal optimisation problem,

$$\begin{aligned} \mathcal{P}: \quad & \max \sum_{s=1}^{\mathcal{S}} U(s) \\ s.t. \quad & \sum_{s \in \mathcal{S}_l} s \leq c_l, l = 1, \cdots, L. \end{aligned} \tag{4.2}$$

At convergence, the bandwidth proportional fairness is achieved for a logarithmic utility function. The rate allocation is fair with respect to utility percentage. A resource allocation $x^* = [x_1^*, x_2^*, \cdots, x_S^*]^T$ is proportionally fair, if it is feasible for any other feasible allocation x,

$$\sum_{x \in S} \frac{x_s - x_s^*}{x_s^*} \leq 0. \tag{4.3}$$

A common theme underlying NUM protocols is that they are targeted managing the elastic traffics. This means that the traffic will present a non-zero utility as long as non-zero bandwidth is allocated to it.

4.2 Problem Analysis on Network Utility Optimisation for Hierarchical M2M Communications

As has pointed out by [JSKP10], the NUM has made great advances in dealing with resource allocation. However, serious limitations still exist as shown below,

i) NUM aims at managing elastics traffics, the utility of which can be modelled

by strictly concave functions.

ii) For the scenario where applications have different QoS requirements, a serious conflict exists between the utility maximisation and the utility fairness. In particular, the elastic traffics will always get allocated due to the rapid increase of utility with little resource allocated to them, while the inelastic traffics might receive less resource than its minimum requirement.

Thus the conventional criteria proportional fairness may not be suitable to address the resource allocation for networks with different QoS requirements [JSKP10]. In [CZ99], the concept of *utility max-min fair* is suggested to support resource allocation for networks with different applications.

An allocation $x^* = [x_1^*, x_2^*, \cdots, x_I^*]^T$ is *utility max-min fair*, if it is feasible for each user i, the utility $U_i(x_i^*)$ cannot be increased while still maintaining feasibility, without decreasing the utility $U_{i'}(x_i'^*)$ for some other user i' with a lower utility $U_{i'}(x_i'^*) \leq U(x_i^*)$. Max-min fair allocation is recovered with

$$U_i(x_i) = x_i, i = 1, \ldots, I. \tag{4.4}$$

More recently, the *utility-fair* based resource allocation strategy is proposed for networks with both elastic and inelastic traffics [WPL06]. The proposed strategy also guarantees the utility fairness among different traffics.

A bandwidth allocation $x^* = [x_1^*, x_2^*, \cdots, x_I^*]^T$ is *utility proportionally fair*, if it is feasible and for any other feasible allocation x,

$$\sum_{x \in I} \frac{x_i - x_i^*}{U_i(x_i^*)} \leq 0. \tag{4.5}$$

To achieve the *utility-fair* resource allocation, each source device i with utility function $U_i(x_i)$ has a pseudo utility" $\mathcal{U}_i(x_i)$ associated with it. $\mathcal{U}_i(x_i)$ is defined as

$$\mathcal{U}_i(x) = \int_{c_s}^{C_s} \frac{1}{U_i(x)} dx, \quad c_i \leq s \leq C_i. \tag{4.6}$$

where (c_i, C_i) is the capacity region of $x_i \in \mathcal{I}$.

Due to the non-negative and strictly increasing properties of U_i, it is clear that $\mathcal{U}_i$ is a strictly increasing concave function regardless the concavity of the original utility function U_i. Thus, with this "pseudo utility", the original optimisation problem with both elastic and inelastic traffics is mapped into a convex NUM optimisation problem. And the solution of the "pseudo utility" problem achieves *utility proportionally fair* [JSKP10].

The "pseudo utility" is adopted in this thesis to solve the original joint scheduling and duty cycle control problem $\mathcal{P}1$. Replacing the utility function of $\mathcal{P}1$ with "pseudo utility" leads to a convex optimisation problem $\mathcal{P}2$,

$$\mathcal{P}2: \quad \min \sum_{t=0}^{T} \sum_{i \in \mathcal{I}_n} \mathcal{U}(f_i^t, r_i^t, \theta_i^t) \tag{4.7a}$$

$$s.t. \quad \sum_{i \in \mathcal{I}_n} f_i^t \leq C_{n,b}^t, \tag{4.7b}$$

$$0 \leq f_i^t \leq C_{i,n}^t, \qquad i \in \mathcal{I}_n \tag{4.7c}$$

$$r_i^t \leq \min(C_{i,j}^t, q_i^{max}), \quad i \in \mathcal{I}_n, j \in \mathcal{C}_i. \tag{4.7d}$$

Furthermore, $\mathcal{P}2$ can be decomposed into the following cluster head optimisation problem $\mathcal{P}3$ and gateway optimisation problem $\mathcal{P}4$:

$$\mathcal{P}3 : \max \sum_{t=0}^{T} \sum_{i \in \mathcal{I}_n} \mathcal{U}_i(r_i^t) - p_{i,n}^t \tag{4.8a}$$

$$s.t. \qquad p_{i,n}^t \geq 0, \tag{4.8b}$$

$$r_i^t \leq \min(C_{i,j}^t, q_i^{max}) j \in \mathcal{C}_i, \tag{4.8c}$$

where $p_{i,n}^t = p_i^t f_i^t$ is the charged price by gateway n for cluster head i with the forwarded flow f_i^t. The constraint (4.8c) is the link capacity constraint. And

$$\mathcal{P}4 : \max \sum_{t=0}^{T} \sum_{i \in \mathcal{I}_n} p_{i,n}^t \mathcal{U}_n(f_i^t, p_i^t, \theta_i^t) \tag{4.9a}$$

$$s.t. \qquad \sum_{i \in \mathcal{I}_n} f_i^t \leq C_{n,b}^t \tag{4.9b}$$

$$0 \leq f_i^t \leq C_{i,n}^t, \tag{4.9c}$$

where p_i^t is the bid price per unit/packet of cluster head i for the transmission at time period t. The constraints (4.9b) and (4.9c) are link capacity constraints.

Based on the problem formulation in [KMT98], an example bid price p_i^t updating algorithm proposed in [LL99] is,

$$p_i^{t+1} = \left[p_i^t + \gamma (\sum_{i \in \mathcal{I}_n} f_i^t - C_{n,b}^t) \right]^+. \tag{4.10}$$

This equation indicates that if the aggregated number of packets exceeds the maximum queue length q_i^{max}, the bid price will be increased; otherwise it will be

decreased.

After the transmission, cluster head i is charged $p_{i,n}^t = p_i^t f_i^t$ by gateway n for the forwarded flow f_i^t. Suppose the gateway n knows its revenue vector $P_n = (p_{i,n}^t, i \in \mathcal{I}_n)$ and the application indicator θ_i^t. To guarantee the gateway is able to gain some profit, in this thesis $p_{i,n}$ is calculated as

$$p_{i,n}^t = p_i^t + 1. \tag{4.11}$$

Due to the structures of the decomposed $\mathcal{P}3$ and $\mathcal{P}4$, it is possible to design the cluster head utility function and gateway utility function separately, so that the cluster head and gateway can address their application requirements and device capabilities, separately.

As the utility function $\mathcal{U}_i$ of cluster head is not required by the gateway, and it only appears in the optimisation problem $\mathcal{P}3$ faced by cluster head i, that the joint scheduling and duty cycle control problem is solvable in a distributed way.

Compared with the centralised approach where the central controller needs to assign the scheduling for the whole network, the distributed approach described above has the following advantages:

i) Scalability. For distributed controls, devices make decisions based on their local information rather than global information covering the whole network. As a result, the control overheads, energy and memory of distributed controls can be much less than those of centralised controls, especially in large-scale network.

ii) Adaptability to network dynamics. In M2M communications, the changes

in network conditions at some individual devices would only affect local network conditions rather than the whole network. As a result, distributed controls can address the dynamic network changes locally without expensive communications across the whole network.

iii) Faster response. To save energy, M2M networks normally operate at a low duty cycle mode. Compared to centralised low duty cycle networks, distributed controls significantly reduce the response time by reducing the time for transmitting the local information from each device to the central controller and the time for disseminating information from the central controller to each device.

4.3 Control Framework Design

Based on the aforementioned analysis, the network utility optimisation problem $\mathcal{P}1$ is solved by two distributed problems $\mathcal{P}3$ and $\mathcal{P}4$. A joint scheduling and duty cycle control framework is proposed with three controls, named as duty cycle control, gateway control and cluster head control. The detailed solution for each control will be presented in the following Chapter 5, Chapter 6 and Chapter 7, respectively.

The overall control process of the proposed framework for hierarchical M2M networks is shown in Fig. 4.2. The proposed framework incorporates with the current IEEE 802.15.4 standard.

IEEE 802.15.4 beacon transmission

For beacon-enabled IEEE 802.15.4, a beacon is transmitted from the parent

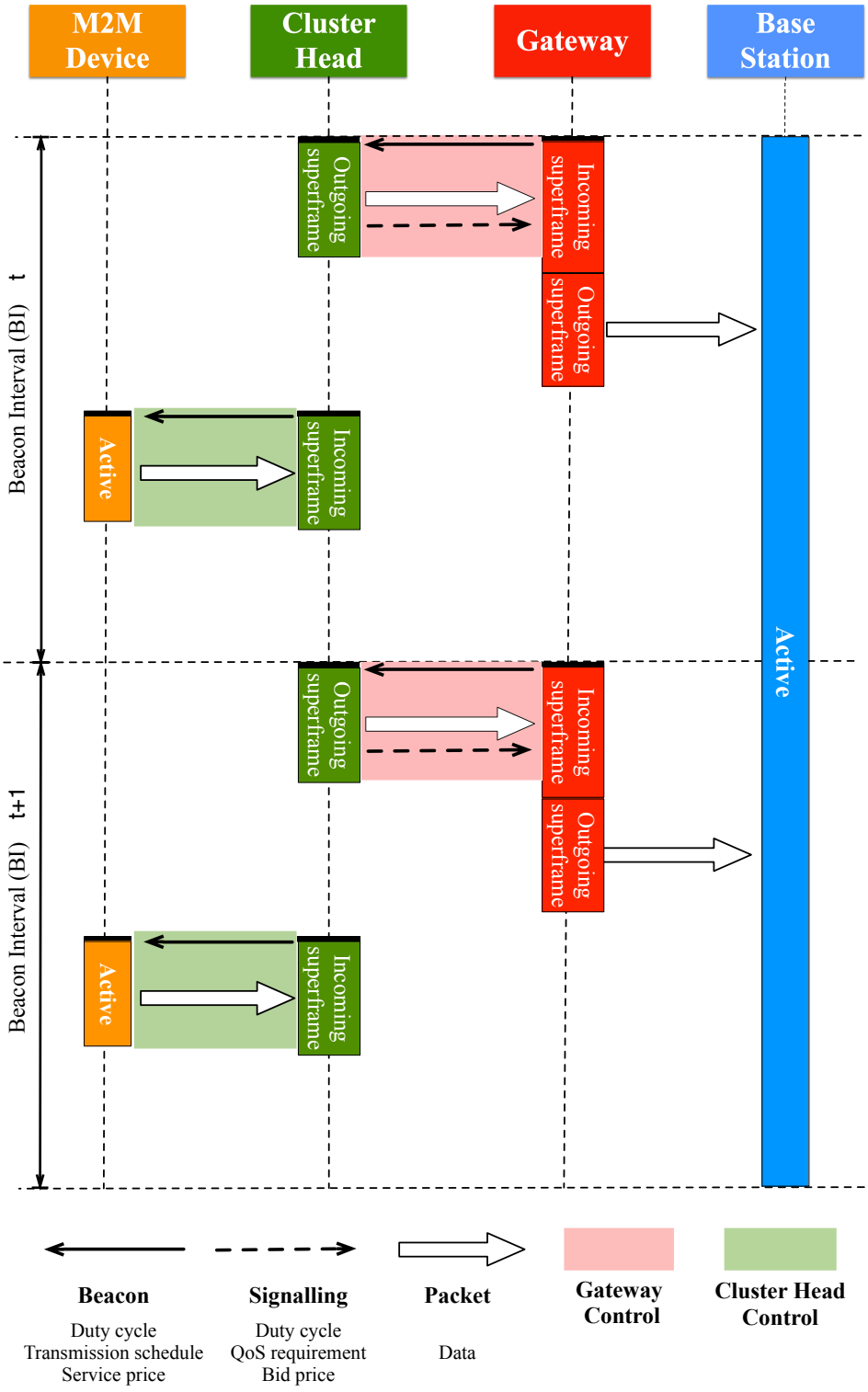

Figure 4.2: Transmission process of designed control framework.

device to its child devices at the beginning of each superframe. A device needs to listen for the beacon from its parent device before transmiting data to the parent device. When the beacon is found, the device synchronises to the superframe structure based on the information within the beacon.

For the proposed control framework, the beacon from the parent device will provide duty cycle, transmission schedule and the charged price for each child device. More specifically, for each time period t, the beacon from the cluster head i to its child M2M devices $j \in \mathcal{C}_i$ will contains the duty cycle parameters $SO(r_i^t)$ and $BO(r_i^t)$, transmission schedule r_i^t, and the charged price $p_{i,j}^t$ for each M2M device j.

Cluster head signalling transmission

At the end of the packet transmission duration from cluster heads to their parent gateway, each cluster head will send a signalling to its parent gateway. The information enclosed is its current duty cycle, the QoS requirement of its application and its bid price p_i^t for the transmission in next time period.

Cluster head control

The cluster head control is operated at each cluster head to decide its local transmission schedule, control the duty cycle and operate the bid price to the gateway depending on the local traffics. The cluster head control is based on the optimisation problem $\mathcal{P}3$ with the aim of maximising the single cluster utility.

For cluster head i, the output of the cluster head control are the cluster duty cycle parameters $SO(r_i^t)$, the transmission schedule r_i^t, and the bid price p_i^t offered to its parent gateway n. The information about bid price p_i^t is enclosed in the signalling to the gateway at the end of time period $t-1$.

Gateway control

The gateway control is implemented at each gateway to adapt the amount of traffic each child cluster head will forward to it. The gateway control is based on the optimisation problem $\mathcal{P}4$, and the aim is to maximise the aggregated network utility with the consideration of different application requirements of clusters.

After the gateway n receives the signalling from all its child cluster head $i \in \mathcal{I}_n$ and the bid price p_i^t. The gateway control will conduct the transmission schedule f_i^t for all cluster head $i \in \mathcal{I}_n$ and set the outgoing surperframe paramters. The gateway will also calculate the charged price $p_{i,n}^t$ for each cluster head $i \in \mathcal{I}_n$ according to the amount of traffic cluster head i has forwarded. The charged price is enclosed in the beacon of the gateway at the beginning of time period $t+1$.

4.4 Simulation Platform Design

The main modules of the simulation platform in this thesis are summarised in this section.

4.4.1 Simulation Flow Design

The simulation process is composed of a number of simulation iterations, and each simulation iteration consists of T time periods. In each time period, the joint scheduling and duty cycle control for the hierarchical M2M network is processed. The simulation flow chart is given in Fig. 4.3.

Network Initialisation: Firstly, this module initialises the devices deployment, including the number and position for the base station, M2M gateways,

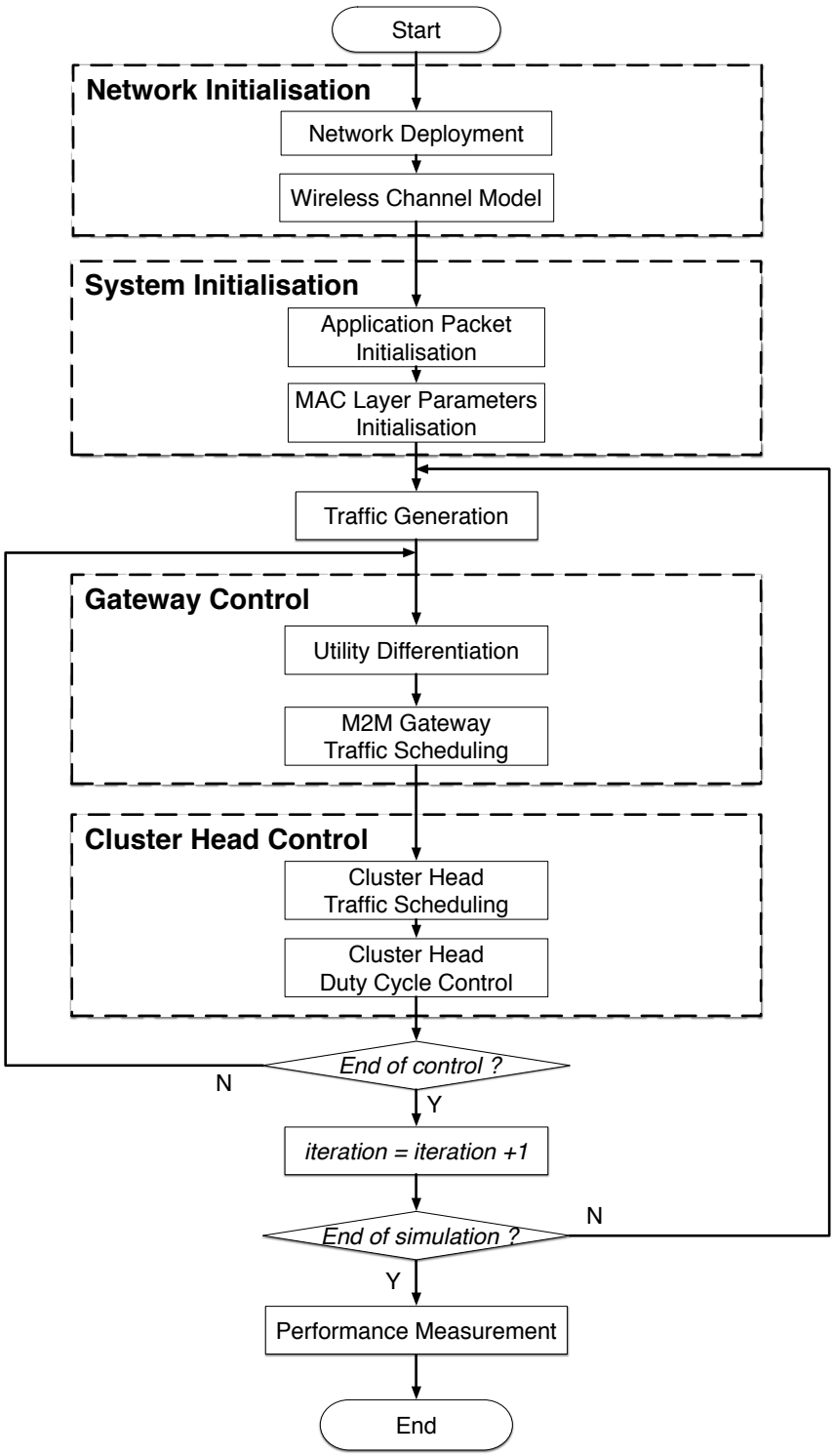

Figure 4.3: Flow chart of designed simulation platform

cluster heads and M2M devices. Then, it calculates the path loss, adds shadow fading and calculates the received energy level of each device. The output of this module is one network deployment with all successful links.

System Initialisation: This module initialises the application related parameters θ_i, U_i, and the simulated MAC layer parameters. It also initialises the buffer capacity of each M2M device, cluster head and M2M gateway.

Traffic Generation: This module generates traffic of each cluster head and M2M device. It also initialised the packet transmission table, which helps to keep a record of the time periods at which the packets have been generated, transmitted, received or dropped.

Gateway Control: This module assigns the utility functions to clusters according to its application class. Then, it conduces the transmission schedule between cluster heads and the parent M2M gateway. The aim of the scheduling is to maximise the network throughput whiling satisfying different QoS requirements among clusters.

Cluster Head Control: This module conduces the transmission schedule within each cluster. Then, the duty cycle for IEEE 802.15.4 is adapted based on the cluster head transmission scheduling results. The aim of the cluster head scheduling is to achieve the joint optimisation of energy efficiency and delay.

4.4.2 Performance Metrics

During the simulation, each packet has a packet transmission table. The table keeps all the information about this packet, including the packet generation time, the packet forwarded time to cluster head, gateway and base station, and the packet

drop time. With this table, given the device energy consumption parameters, the performance metrics including energy efficiency, end-to-end delay, packet drop ratio and throughput can be obtained.

The following parts give the definitions and calculation methods of the performance metrics for the modelled hierarchical M2M networks.

4.4.2.1 Energy Efficiency

For energy-efficient communications, it is desirable to maximise the amount of data been sent with a given amount of energy. Thus, energy efficiency is defined as the ratio of transmission rate to energy consumption. The unit of energy efficiency is bits per Joule, which has been frequently used in literature for energy-efficient communications [MPSM05] [GM00] [FMM04].

The duty cycle determines transmission energy consumption as it defines the medium access and active/sleep operation of devices. The overall transmission energy consumption contains:

$$\begin{aligned} \textit{transmission energy} &= \textit{sending energy} + \textit{receiving energy} \\ &\quad + \textit{idle listening energy} + \textit{sleeping energy}. \end{aligned} \tag{4.12}$$

Thus, energy efficiency of duty cycle based MAC protocols is calculated as:

$$\textit{energy efficiency} = \frac{\textit{total amount of data been transmitted}}{\textit{transmission energy consumption}}.$$

4.4.2.2 End-to-end Delay

Delay is a very important QoS measurement since it influences the performance and stability of some applications, such as industrial control system. In this thesis, the end-to-end delay is measured as an average over a certain period of time.

The end-to-end delay is defined as the time consumed for a packet from the arrival at the source to the reception at the destination. The one-hop delay at MAC layer is defined as:

$$\begin{aligned} \textit{one-hop delay} = &\textit{processing delay} + \textit{queuing delay} + \textit{channel access delay} \\ &+ \textit{transmission delay} + \textit{propagation delay} + \textit{reception delay}. \end{aligned}$$

The end-to-end delay, which is the accumulation of the one-hop delay from sender to receiver, is expressed as:

$$\textit{end-to-end delay} = \sum_{h}^{H} \textit{one-hop delay},$$

where $h = 1, \cdots, \mathcal{H}$ is the number of hops of a selected path.

4.4.2.3 Network Throughput

Network throughput is measured as the average number of packets successfully transmitted over the whole network per unit time. For the modelled cluster-based hierarchical M2M network, the network throughput is the sum of the throughput

of all clusters.

$$\textit{per cluster throughput} = \textit{transmitted data to the cluster head per unit time},$$
$$\textit{network throughput} = \sum_{i=1}^{I} \textit{throughput of cluster } i.$$

where I is the number of clusters of the gateway.

4.4.2.4 Packet Drop Ratio

Due to the limited buffer size, the packets are dropped when the queue length exceeds the buffer limitation of the device. For each device the packet drop ratio is defined as the ratio between the number of packets been dropped and the total number of packets been generated by the device. The averaged packet drop ratio in the network is given as,

$$\textit{device packet drop ratio} = \frac{\textit{data dropped due to buffer limitation}}{\textit{data generated by the device}}, \tag{4.13}$$
$$\textit{averaged packet drop ratio} = \frac{1}{M} \sum_{j=1}^{M} \textit{packets drop ratio of device } j,$$

where M is the total number of devices in the network.

4.4.3 Platform Validation

In this part, the validation of the designed simulation platform is presented. The validated modules in this section are channel module and network initialisation module.

4.4.3.1 Channel Model

The validation of the channel model is done by comparing the results with that in [NIS11]. Fig. 4.4 shows the modelled dual-slop path loss model for indoor-indoor residential environment at $f_c = 5GHz$. As shown in Fig. 4.4, the trend and value in the simulated scenario align with the ones presented in [NIS11] with the same environmental settings.

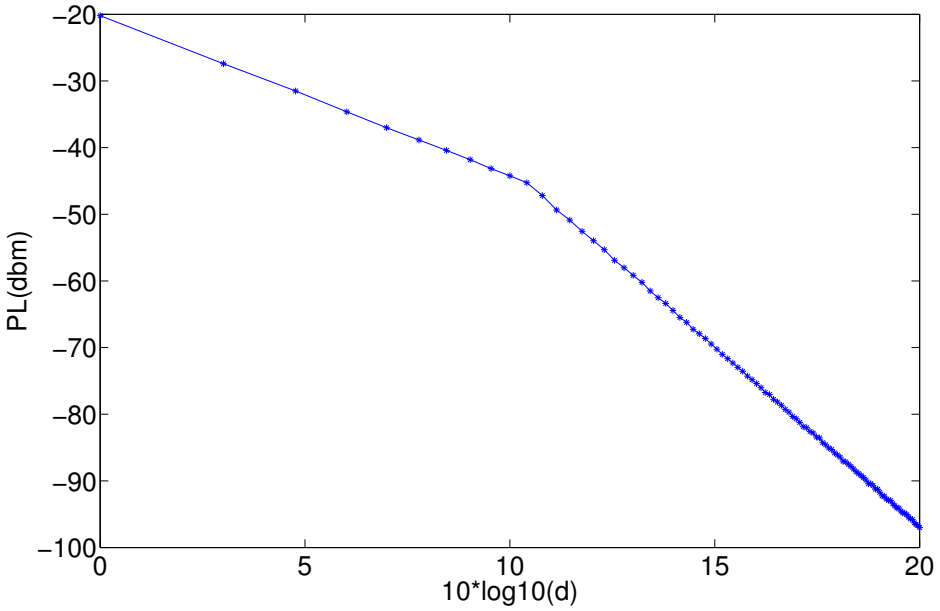

Figure 4.4: Dual-slope path loss model.

4.4.3.2 Network Initialisation

The flow chart of the network initialisation module is shown in Fig. 4.5. The network initialisation module has four steps:

i) Randomly deployed M2M gateway n within the simulated area;

ii) Randomly deployed cluster head $i \in \mathcal{I}_n$;

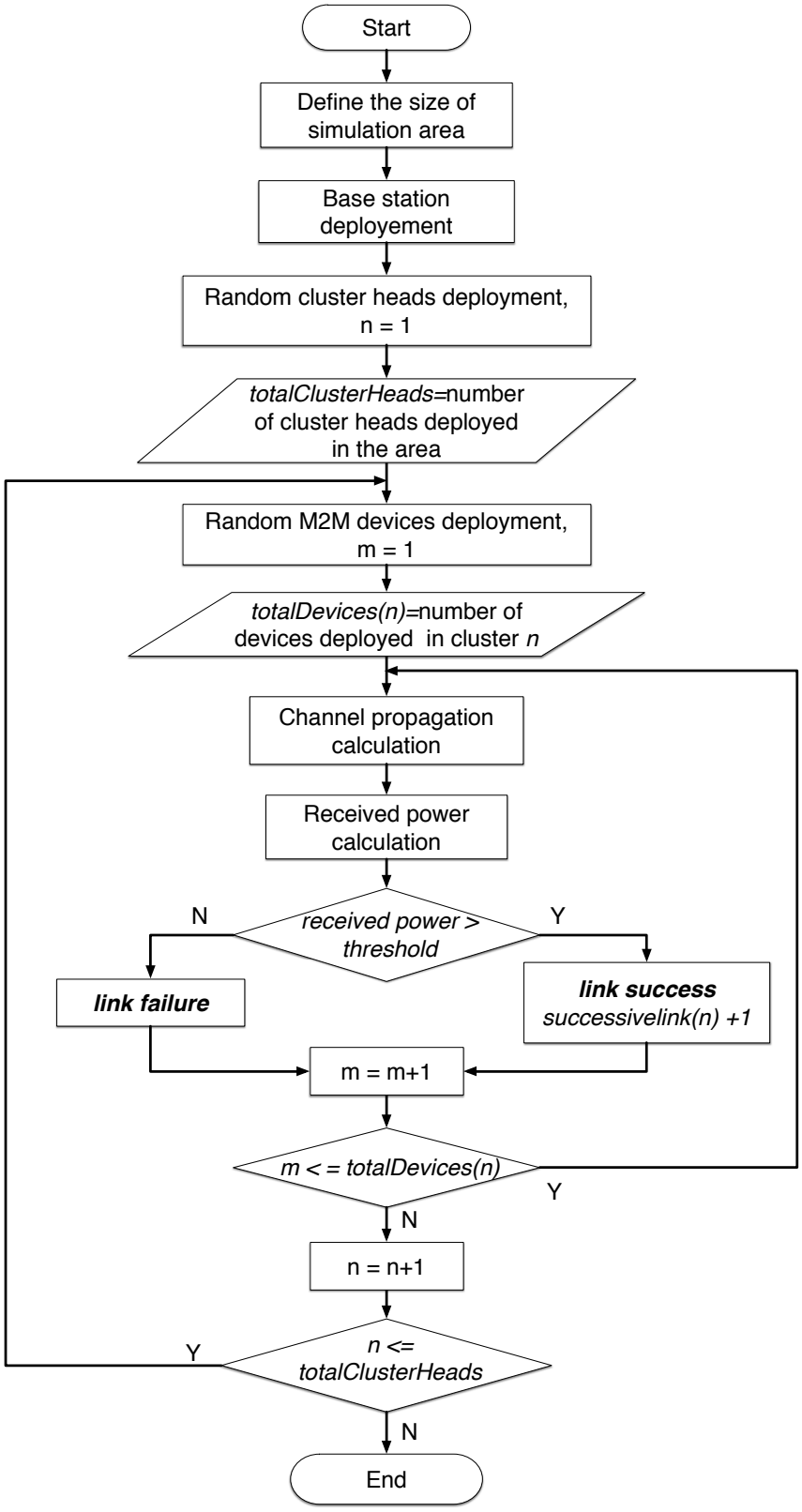

Figure 4.5: Flow chart of network initialisation module

iii) Randomly deployed M2M device $j \in \mathcal{C}_i$ of each cluster head i;

iv) Check link quality for $\mathcal{L}_{i,n}$ and $\mathcal{L}_{i,j}$.

To validate the network initialisation module, one realisation of modelled hierarchical M2M network is carried out. The device energy consumption parameters are based on XBee®/RF data sheet [Int]. The XBee® 802.15.4 devices are used as M2M devices and XBee-PRO® 802.15.4 devices are used as cluster heads.

The setting of device parameters are given in Table. 4-A. The MAC layer parameters for the validated scenario are given in Table. 4-B.

Table 4-A: Device Parameters of Example Hierarchical M2M Network

	XBee® 802.15.4	**XBee-PRO® 802.15.4**
Transmit Power	0 dBm	10 dBm
RF Line of Sight Range	300ft / 90m	3200ft / 1 km
Receiver Sensitivity (1%PER)	-92 dBm	-100 dBm
RF Data Rate	250 Kbps	250 Kbps

Table 4-B: IEEE 802.15.4 MAC Layer Parameters

Parameter	**Value**
frequency	2.4 GHz
CCA size	8 symbols
unit backoff period	20 symbols
data rate	250kbps
packet size	100 bytes
ACK packet size	10 symbols

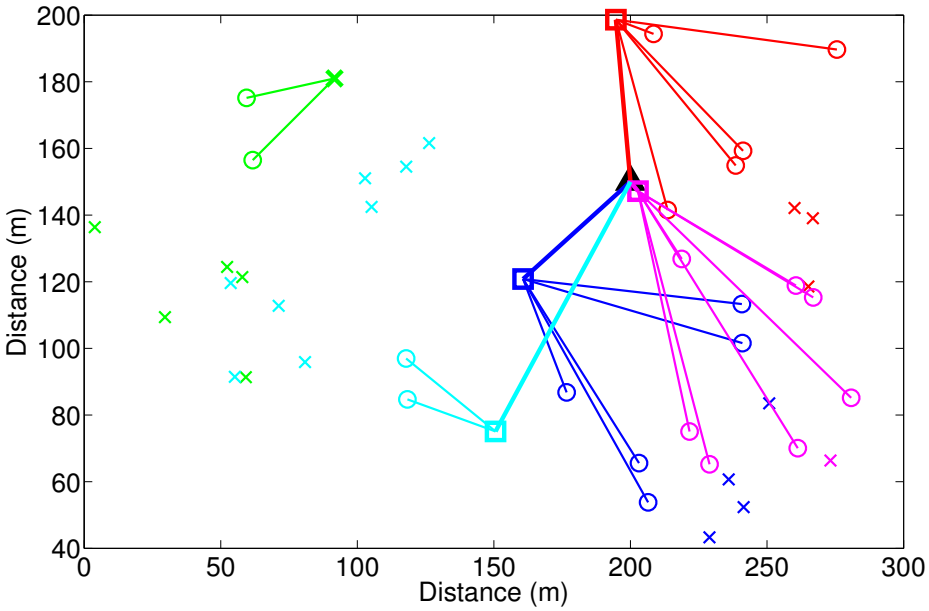

Figure 4.6: One realisation of network deployment.

Fig. 4.6 shows the deployed network, where the M2M gateway is represented by black triangle, cluster head is represented by square and M2M devices are represented by circle. The cross dots represent the failure devices (cluster head and M2M devices). The different colours represents different clusters of the gateway. The device sensitivity requirement, which gives the minimum receive power, determines whether the link is successful or not.

Fig.4.7 shows the averaged received power of cluster heads and M2M devices in the deployed M2M network. Comparing Fig.4.7 and Table. 4-A, it can be seen that the successful transmission range of the simulated network over the formulated channel aligns with that of the presented device sensitivity requirements and RF transmission range according to the device data sheet [Int]. This also validates the accurate of the built channel module.

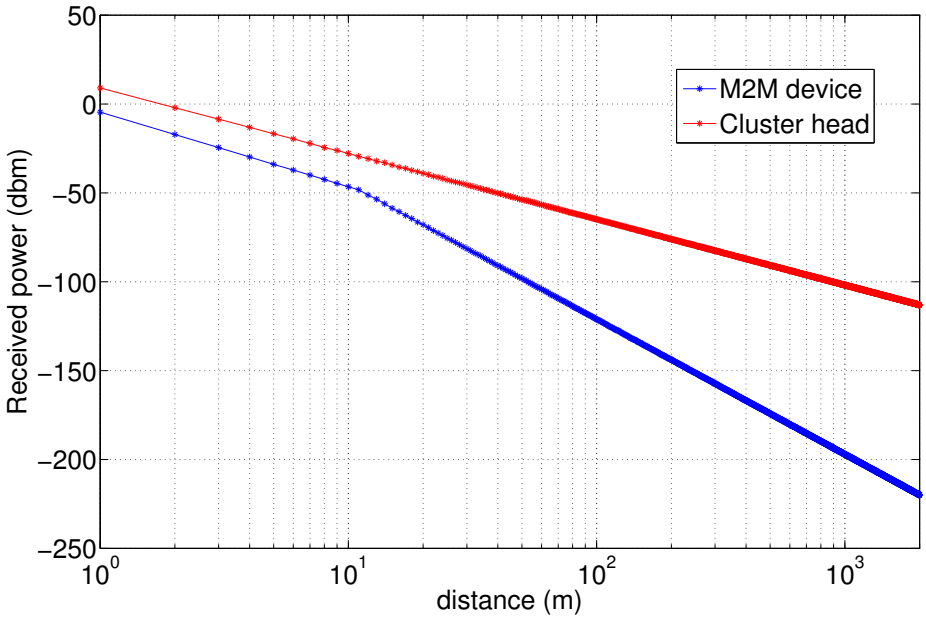

Figure 4.7: Received power of devices.

4.5 Summary

In this chapter, the joint scheduling and duty cycle control optimisation problem for the modelled hierarchical M2M networks with multi-class applications is formulated as $\mathcal{P}1$. However, the utility functions for inelastic applications (hard-real time applications, delay adaptive applications and rate adaptive applications) are not concave functions. This makes the problem $\mathcal{P}1$ hard to be solved by applying classic NUM directly.

Next, the $\mathcal{P}1$ has been transferred into the convex optimisation problem $\mathcal{P}2$ by replacing the utility function of $\mathcal{P}1$ with "pseudo utility". Then, the $\mathcal{P}2$ has been decomposed into distributed optimisation problems $\mathcal{P}3$ and $\mathcal{P}4$, which are named as cluster head control and gateway control, respectively.

Then, a joint scheduling and duty cycle control framework for M2M communi-

cation networks is proposed. The outcome of the control framework is a distributed optimal solution for the modelled hierarchical M2M networks with three controls: i) the duty cycle control with the aim of joint optimisation on energy efficiency and delay, ii) the cluster head control with the aim of maximising the single cluster utility, and iii) the gateway control with the aim of maximising network utility while satisfying different QoS requirements among clusters.

In the end, the design of simulation platform for the formulated hierarchical M2M networks is provided. The channel model and network deployment module of the platform are validated.

Chapter 5

Duty Cycle Control with Joint Optimisation of Energy Efficiency and Delay

This chapter focuses on the duty cycle control of the proposed control framework in Chapter 4. The theoretical optimal duty cycle control for IEEE 802.15.4 with both Stop-and-Wait and Go-Back-N ARQ are derived by applying dynamic programming (DP). The aim of the duty cycle control is to minimise the joint cost of energy consumption and end-to-end delay. Simulation results and discussion are presented at the end of this chapter.

5.1 Duty Cycle Control for IEEE 802.15.4 with Stop-and-Wait ARQ

The background of duty cycle control for IEEE 802.15.4 has been presented in the Section 2.3. Recall the duty cycle is defined as the ratio of the active portion over each time period. The duty cycle of IEEE 802.15.4 is controlled by the parameter

pair (SO, BO),

$$Duty\ Cycle = SD/BI = 2^{SO-BO}. \tag{5.1}$$

The duty cycle control designed for IEEE 802.15.4 works in a distributed manner. Each cluster head and gateway decides its own incoming duty cycle based on its local traffic. The outgoing superframe duty cycle of the cluster head is controlled by its parent gateway and enclosed in the received beacon. In this thesis, same BO is set to all devices to simplify the synchronisation. Thus, the duty cycle control of each device is achieved by setting the incoming duty cycle control parameter $SO(r_i^t)$.

The device can only transmit packets when it is in active mode. Thus, there is an direct link between the length of SD and the total number of transmitted packets r_i^t. Due to the collision of CSMA/CA, the actual transmission throughput has a co-relation with the number of contending devices. The throughput limitation coefficient b is adopted for IEEE 802.15.4 CSMA/CA according to [PKC+05].

Thus, within each SD, if the beacon transmission duration is denoted as D_{bcn}, the total packet transmission duration PD is given as,

$$PD = SD - D_{bcn} = b \times (r_i \times P_s), \tag{5.2}$$

where P_s is the the successful single packet transmission time.

In each contention access period (CAP), IEEE 802.15.4 adopts CSMA/CA for packet transmission. Before the packet transmission, devices need to perform two clear channel accesses (CCAs). If Stop-and-Wait ARQ is applied, an acknowledgement (ACK) is required for each successful received packet. Thus, the successful

single packet transmission time P_s is

$$P_s = \lceil P_{CCA} + P_L + \delta + P_{ACK} \rceil, \tag{5.3}$$

where P_{CCA} is the transmission time for two CCAs, P_L is the transmission time for each packet, δ and P_{ACK} are waiting and transmission time of the ACK packet, respectively. Thus,

$$r_i = \lfloor \frac{SD - D_{bcn}}{b \times P_s} \rfloor. \tag{5.4}$$

Based on (5.2) - (5.4), the relationship between the incoming $SO(r_i^t)$ of the cluster head i and the amount of packets the device could receive from its child devices r_i^t at time period t is given as,

$$SO(r_i^t) = \left\lceil \log_2(\frac{r_i^t \times P_s}{b} + D_{bcn}) \right\rceil. \tag{5.5}$$

5.2 Cluster Head Control with Stop-and-Wait ARQ

In this part, the cluster head control with the aim of joint-optimisation of energy efficiency and delay is formulated and solved by applying DP.

The cluster head control is formulated based on the classic inventory control problem, due to the good match between these two problems. The inventory control problem is a classical DP problem with the aim of minimising the overall cost by properly deciding the inventory level at each time period while meeting the

customer demand. This is similar to the cluster head control problem, which is to control the duty cycle with the aim of minimising energy consumption while reducing delay. The trade-off between energy consumption and delay of the duty cycle control lies: the reduced number of transmitted packets will reduce the transmission energy consumption, however this is at the cost of increasing the end-to-end delay and idle listening energy consumption.

Taking inventory control problem as the fundamental approach, the following four costs are defined for each cluster head i,

- $E_t(f_i^t)$ is the transmitting energy cost;
- $E_r(r_i^t)$ is the receiving energy cost;
- $E_l(r_i^t)$ is the idle listening energy cost;
- $D(r_i^t)$ is the end-to-end delay cost.

To ensure the costs of energy consumption and end-to-end delay are additive, the above costs are all defined with the unit "number of packets". The energy consumption of ACK packet transmission exists only when the cluster head receives packets. With the Stop-and-Wait ARQ scheme, an ACK packet is required by each packet successfully received by the receiver. The definitions of the costs are given

as:

$$E_r(r_i^t) = \begin{cases} c_r \cdot \frac{r_i^t}{q_i^{max}} & \text{if} \quad r_i^t > 0, \\ 0 & \text{if} \quad r_i^t = 0. \end{cases} \tag{5.6}$$

$$E_f(f_i^t) = c_f \cdot \frac{f_i^t}{q_i^{max}}, \tag{5.7}$$

$$E_l(r_i^t) = c_l \cdot \frac{[f_i^t - g_i^t - q_i^t - r_i^t]^+}{q_i^{max}}, \tag{5.8}$$

$$D(r_i^t) = c_d \cdot \frac{[q_i^t + r_i^t + g_i^t - f_i^t]^+}{q_i^{max}}, \tag{5.9}$$

where c_f, c_r, c_l and c_d are the cost coefficients of transmitting, receiving, idle listening and delay, respectively. Note that $c_r < c_l$, as if c_r were greater than c_l, it would never be optimal to receive packets at the last period and possibly in earlier periods.

Coefficients α and β are further introduced to assign the weightings of energy efficiency and end-to-end delay for different application requirements. Then, the expected weighted-sum joint-cost function for cluster head i at time period t is

$$J(r_i^t) = \mathbb{E}\Big\{\alpha\Big(E_f(f_i^t) + E_r(r_i^t) + E_l(r_i^t)\Big) + \beta D(r_i^t)\Big\}. \tag{5.10}$$

The objective is to find the optimal cluster head control policy π_i^* for each cluster head i over T time periods, which minimises the overall expected joint-cost. Hence, the joint optimisation problem is:

$$\begin{aligned} \mathcal{P}_i: \quad & \min_{\pi_i \in \mathfrak{D}} \quad \mathbb{E}\left\{\sum_{t=0}^{T-1} J(r_i^t)\right\} \\ & \text{s.t.} \quad q_i^T = 0, \\ & \qquad r_i^t \leq r_i^{max}, \end{aligned} \tag{5.11}$$

where $\mathfrak{D}$ is valid policy sets of cluster head i, r_i^{max} is the maximum number of packets cluster head i could receive. r_i^t subjected to the active duration and maximum queue length q_i^{max} of cluster head i at time period t.

5.3 Optimal Distributed Cluster Head Control with Stop-and-Wait ARQ

By applying the principle of DP, the problem $\mathcal{P}_i$ can be decomposed into a sequence of subproblems $\mathcal{S}(r_i^t)$, where $0 \leq t \leq T$. The objective of each subproblem $\mathcal{S}(r_i^t)$ is to minimise the sum of joint-cost functions from time period t to T. Thus, the total cost of $\mathcal{P}_i$ is equal to that of $\mathcal{S}(r_i^0)$, which means the optimal solution of $\mathcal{S}(r_i^0)$ is the optimal solution of $\mathcal{P}_i$. Based on (5.10), the cost-to-go function J_i^t, which is the sum of joint-cost functions from time period t to T is given as

$$J_i^t = \min_{\pi_i \in \mathfrak{D}} \mathbb{E}\Bigg\{ \alpha\Big(E_r(r_i^t) + E_t(f_i^t) \Big) + H(r_i^t) + \mathbb{E}\{J_i^{t+1}\} \Bigg\}, \tag{5.12}$$

where

$$\begin{aligned} H(r_i^t) = &\quad \mathbb{E}\Big\{ \alpha E_l(r_i^t) + \beta D(r_i^t) \Big\} \\ = &\quad \mathbb{E}\{ \alpha \cdot c_l \cdot \frac{[f_i^t - q_i^t - r_i^t - g_i^t]^+}{q_i^{max}} + \beta \cdot c_d \cdot \frac{[q_i^t + r_i^t + g_i^t - f_i^t]^+}{q_i^{max}} \}. \end{aligned} \tag{5.13}$$

shows the tradeoff between the energy consumption cost due to idle listening and the end-to-end delay cost.

The objective of each subproblem $\mathcal{S}(r_i^t)$ for cluster head i is to minimise the

cost-to-go function J_i^t

$$\begin{aligned} \mathcal{S}(r_i^t): \quad & \min_{\pi_i \in \mathfrak{D}} \quad \mathbb{E}\left\{\sum_{k=0}^{t-1} J_i^t\right\} \\ & \text{s.t.} \quad q_i^t = 0, \\ & \qquad r_i^t \leq r_i^{max}. \end{aligned} \tag{5.14}$$

To solve the subproblem $S(r_i^t)$, $m_i^t = q_i^t + r_i^t$ and $n_i^t = f_i^t - g_i^t$ are introduced for notation clarity. Then, combined with (5.10) and (5.11), $H(r_i^t)$ in (5.13) can be rewritten as

$$H(m_i^t) = \mathbb{E}\left\{\alpha c_l \times \frac{\max(q_i^{max}, [n_i^t - m_i^t]^+)}{q_{max} \times l_i} + \beta c_d \times \frac{\max(q_i^{max}, [m_i^t - n_i^t]^+)}{q_{max} \times l_i}\right\}. \tag{5.15}$$

As the convexity preserved by taking expectation over n_i^t, with each fixed n_i^t, $H(m_i^t)$ is convex. Due to the convexity of $H(m_i^t)$, the cost-to-go function J_i^t is rewritten as

$$J_i^t(m_i^t) = \min_{\pi_i \in \mathfrak{D}} \mathbb{E}\left\{W(m_i^t) - \alpha c_r \times \frac{q_i^t}{q_i^{max} \times l_i}\right\}, \tag{5.16}$$

where

$$W(m_i^t) = \alpha c_r \times m_i^t + \alpha \times E_f(f_i^t) + H_i(m_i^t) + \mathbb{E}\{J_i^t(m_i^{t+1})\}. \tag{5.17}$$

Then the objective of each subproblem $\mathcal{S}(r_i^t)$ is to find the minimum value of (5.17).

Before giving the solution to each subproblem $\mathcal{S}(r_i^t)$, the following **Lemma 5.1** gives the sufficient condition for the convexity of functions $W(m_i^t)$.

Lemma 5.1. *If $H(m_i^t)$ and $U(m_i^t)$ are convex functions, so is $W(m_i^t)$.*

Proof. Based on the definition of convex function, $W(m_i^t)$ is convex if,

$$W(\frac{m_i^t + \bar{m}_i^t}{2}) \leq \frac{W(m_i^t) + W(\bar{m}_i^t)}{2}. \tag{5.18}$$

After eliminating, it is clear that (5.18) is satisfied if

$$H(\frac{m_i^{t_1} + m_i^{t_2}}{2}) + \mathbb{E}\{U(\frac{(m_i^{t_1}+1) + (m_i^{t_2}+1)}{2})\} \leq \frac{H(m_i^{t_1}) + H(m_i^{t_2})}{2} + \frac{\mathbb{E}\{U(m_i^{t_1}+1) + U(m_i^{t_2}+1)\}}{2}. \tag{5.19}$$

Since $H(m_i^t)$ and $U(m_i^t)$ are convex functions, we have

$$H(\frac{m_i^t + \bar{m}_i^t}{2}) \leq \frac{H(m_i^t) + H(\bar{m}_i^t)}{2}. \tag{5.20}$$

and

$$U\left(\frac{(m_i^t+1) + (\bar{m}_i^t+1)}{2}\right) \leq \frac{U(m_i^t+1) + U(\bar{m}_i^t+1)}{2}. \tag{5.21}$$

Adding (5.21) and (5.22), the inequality (5.19) is satisfied. Thus, $W(m_i^t)$ is also a convex function. □

Based on **Lemma 5.1**, the following Theorem gives the optimal transmission policy of problem $\mathcal{P}_i$.

Theorem 5.1. *If $W(m_i^t)$ is convex, and the minimising scalars of $W(m_i^t)$ denoted as*

$$m_i^{t*} = T_i = \arg\min_{m_i^t \in \Re} W(m_i^t). \tag{5.22}$$

where $\Re$ is the set of all valid values of m_i^t.

Based on (5.22) and $r_i^t = m_i - q_i^t$, the minimum cost-to-go function value is attained at $r_i^t = T_i - q_i^t$ if $q_i^t < T_i$, and at $r_i^t = 0$ otherwise. Thus, the optimal transition policy of $\mathcal{P}_i$ is

$$r_i^{t*} = \begin{cases} T_i - q_i^t & \text{if} \quad q_i^t < T_i, \\ 0 & \text{if} \quad q_i^t \geq T_i. \end{cases} \tag{5.23}$$

Proof. Based on the above **Lemma 5.1**, (5.12) to (5.18), the convexity of $W(m_i^t)$ can be proved if function $U(m_i^t)$ is a convex function, and $\lim_{|m_i^t|} W(m_i^t) = \infty$.

For $t = T$, function $U(m_i^t)$ is a zero function, so it is convex.

As $c_r < c_l$, and the derivative of $H(m_i^t)$ tends to $-c_l$ as $m_i^t \to -\infty$. Thus, $H(m_i^t)$ is convex. Based on *Lemma 1*, given the convexity of $U(m_i^t)$, $W(m_i^t)$ is also convex. In addition, $W(m_i^t)$ has a derivative that becomes negative as $m_i^t \to -\infty$ and becomes positive as $m_i^t \to \infty$, thus

$$\lim_{|m_i^t| \to \infty} W(m_i^t) = \infty.$$

Since $W(m_i^{t-1})$ is minimised by T_i, the convexity of $U(m_i^{t-1})$ is obvious. Furthermore, we have

$$\lim_{|m_i^{t-1}| \to \infty} U(m_i^{t-1}) = \infty.$$

As shown above, the optimal policy at time $T-1$ is given by

$$r_i^{T-1} = \begin{cases} T_i - q_i^{T-1} & \text{if} \quad q_i^t < T_i, \\ 0 & \text{if} \quad q_i^t \geq T_i. \end{cases} \tag{5.24}$$

Then the cost-to-go function at the time period $T-1$, is derived as

$$U(r_i^{T-1}) = \begin{cases} \alpha \cdot c_r(T_i - q_i^{T-1}) + \alpha \cdot E_f(f_i^{T-1}) + H(r_i^{T-1}) & \text{if} \quad q_i^t < T_i, \\ \alpha \cdot E_f(f_i^{T-1}) + H(r_i^{T-1}) & \text{if} \quad q_i^t \geq T_i. \end{cases} \tag{5.25}$$

For $t = T-1, \cdots, 0$, the above arguments can be repeated: if

i) $U(m_i^{t+1})$ is convex;

ii) $\lim_{|m_i| \to \infty} U(m_i^t) = \infty$; and

iii) $\lim_{|m_i| \to \infty} W(m_i^t) = \infty$.

Recursively, the cost-to-go functions can be derived as

$$U(r_i^t) = \begin{cases} \alpha \cdot c_r(T_i - q_i^t) + \alpha \cdot E_f(f_i^{t-1}) + H(r_i^t) + \mathbb{E}\{U(r_i^{t+1})\} & \text{if} \quad q_i^t < T_i, \\ \alpha \cdot E_f(f_i^{t-1}) + H(r_i^t) + \mathbb{E}\{U(k+1)\} & \text{if} \quad q_i^t \geq T_i. \end{cases} \tag{5.26}$$

and

i) $U(m_i^t)$ is convex;

ii) $\lim_{|m_i^{t-1}| \to \infty} U(m_i^{t-1}) = \infty$; and

iii) $\lim_{|m_i^{t-1}| \to \infty} W(m_i^{t-1}) = \infty$.

Thus, $W(m_i^t)$ is convex over t time periods, which means the minimal scalars T_i exist. Thus, the proof of **Theorem 5.1** is completed. □

According to the optimal transmission policy π^*, by substituting the optimal value of r_i^t into (5.5), the optimal duty cycle control for IEEE 802.15.4 with Stop-

and-Wait ARQ is derived as

$$SO(r_i^t)^* = \begin{cases} \left\lceil \log_2(\frac{r_i^{t^*} \times P_s}{b} + D_{bcn}) \right\rceil & \text{if } q_i(k) < T_i, \\ \lceil \log_2(D_{bcn}) \rceil & \text{if } q_i(k) \geq T_i. \end{cases} \tag{5.27}$$

Thus, the optimal duty cycle control is a *multi-period policy*: for each time period t, before the cluster head i makes the decision on the duty cycle, it will check the current queue length q_i^t. If the queue length q_i^t is smaller than the threshold T_i^t of the optimal transmission policy, the SO of current time period is set based on the optimal number of packets it should receive $r_i^{t^*}$; otherwise, SO is set to its minimum value $\lceil \log_2(D_{bcn}) \rceil$.

5.4 Duty Cycle Control for IEEE 802.15.4 with Go-back-N ARQ

The energy consumption and end-to-end delay can be further reduced by applying Go-Back-N ARQ transmission scheme. Go-Back-N ARQ uses cumulative ACK scheme, where the receiver only sends one ACK signifying that the receiver has received all the transmitted packets in a certain time period. By doing so, the energy consumption of ACK transmission is reduced, and the end-to-end delay caused by waiting for ACK transmission is also reduced.

The formulation of the packet transmission duration in each BI is similar to that of the duty cycle control with stop-and-wait ARQ. However, with Go-back-N ARQ, only one ACK packet is required for each successful transmission (may include multiple packets). Thus, for each cluster head, the total packet transmission

duration is given as

$$PD = SD - D_{bcn} = \sum_{j=1}^{J} \lceil D_j \rceil + \lceil \delta + D_{ACK} \rceil \,, \tag{5.28}$$

where D_j is the packet transmission duration of child device $j \in \mathcal{C}_i$, δ and D_{ACK} are waiting time and transmission duration of the ACK packet, respectively. Then the number of packets that can be received by i is

$$r_i^t = \sum_{j=1}^{J} b \cdot \lfloor D_j / D_p \rfloor \,, \tag{5.29}$$

where D_p is transmission duration per packet and b is the throughput limitation coefficient, which shows impact of the backoff and contention during CSMA/CA transmission. Then, the $SO(r_i^t)$ is presented as

$$SO(r_i^t) = \left\lceil \log_2 (\left\lceil \frac{r_i^t D_p}{b} \right\rceil + \lceil \delta + D_{ACK} \rceil + \lceil D_{bcn} \rceil) \right\rceil . \tag{5.30}$$

5.5 Cluster Head Control with Go-back-N ARQ

As the energy consumption of ACK packets transmission exists only when the cluster head receives packets. For Go-back-N ARQ, one ACK is required for each successful transmission between the sender and receiver. Thus a fixed ACK transmission energy cost A is introduced as part of the energy consumption. A has a linear correlation with the number of the child devices of the cluster head i. Similar to the costs definition for the stop-and-wait ARQ scheme, for Go-back-N ARQ

scheme, the definition of each cost is given as:

$$E_r(r_i^t) = \begin{cases} A + c_r \cdot \frac{r_i^t}{q_i^{max}} & \text{if} \quad r_i^t > 0, \\ 0 & \text{if} \quad r_i^t = 0. \end{cases} \tag{5.31}$$

$$E_f(f_i^t) = c_f \cdot \frac{f_i^t}{q_i^{max}}, \tag{5.32}$$

$$E_l(r_i^t) = c_l \cdot \frac{[f_i^t - g_i^t - q_i^t - r_i^t]^+}{q_i^{max}}, \tag{5.33}$$

$$D(r_i^t) = c_d \cdot \frac{[q_i^t + r_i^t + g_i^t - f_i^t]^+}{q_i^{max}}, \tag{5.34}$$

where $A = c_f \cdot M_i, M_i$ is the total number of child devices of cluster head i; c_f, c_r, c_l and c_d are the cost coefficients of transmitting, receiving, idle listening and delay, respectively. Note that $c_r < c_l$, as if c_r were greater than c_l, it would never be optimal to receive new packet at the last period and possibly in earlier periods.

The expected weighted-sum form of the joint-cost function for cluster head i at time period t is

$$J(r_i^t) = \mathbb{E}\Big\{\alpha\Big(E_f(f_i^t) + E_r(r_i^t) + E_l(r_i^t)\Big) + \beta D(r_i^t)\Big\}, \tag{5.35}$$

where α and β are the weighting factors for energy efficiency and delay.

The objective is to find the optimal cluster head control policy π_i^* for each cluster head i over T time periods, which minimises the overall expected joint-cost. Hence,

the joint optimisation problem for the duty cycle control with Go-back-N ARQ is:

$$\begin{aligned} \mathcal{P}_i: \quad & \min_{\pi_i \in \mathfrak{D}} \quad \mathbb{E}\left\{\sum_{t=0}^{T-1} J(r_i^k)\right\} \\ & \text{s.t.} \quad q_i^T = 0, \\ & \qquad r_i^t \leq r_i^{max}, \end{aligned} \tag{5.36}$$

where $\mathfrak{D}$ is valid policy sets of device i, r_i^{max} is the maximum number of packets cluster head i could receive which is subjected to the active duration at time period t and maximum queue length q_i^{max}.

5.6 Optimal Distributed Cluster Head Control with Go-back-N ARQ

Similar to the duty cycle control problem with Stop-and-Wait ARQ, the cost-to-go function J_i^t, which is the added sum of joint-cost functions from time period t to T is given as

$$J_i^t = \min_{\pi_i \in \mathfrak{D}} \mathbb{E}\Bigg\{\alpha\Big(E_r(r_i^t) + E_t(f_i^t)\Big) + H(r_i^t) + \mathbb{E}\{J_i^{t+1}\}\Bigg\}, \tag{5.37}$$

where

$$\begin{aligned} H(r_i^t) = & \quad \mathbb{E}\Big\{\alpha E_l(r_i^t) + \beta D(r_i^t)\Big\} \\ = & \quad \mathbb{E}\{\alpha \cdot c_l \cdot \frac{[f_i^t - q_i^t - r_i^t - g_i^t]^+}{q_i^{max}} + \beta \cdot c_d \cdot \frac{[q_i^t + r_i^t + g_i^t - f_i^t]^+}{q_i^{max}}\}. \end{aligned} \tag{5.38}$$

shows the tradeoff between idle listening energy consumption cost and the end-to-end delay cost.

Different from the case with stop-and-wait ARQ, it is not trivial to find the optimal solution of the problem with Go-Back-N scheme, as function j_i^t is not a convex function due to the $[\cdot]^+$ operation of limited buffer size. However, it has been proved by Scarf that an optimal $multi-period$ (s,S) solution exists, if j_i^t is $A-convex$ function [Sca60].

Definition 1. *The real-valued function f is an $A-$convex function, if $A \geq 0$, for all $z \geq 0, b > 0$, f satisfies the $A-$convexity property*

$$A + f(z+y) \geq f(y) + z\left(\frac{f(y) - f(y-b)}{b}\right). \tag{5.39}$$

Next step is to find out the sufficient condition to the $A-convexity$ of the cost-to-go function J_i^t. To reduce the number of notations in the equations, denote $m_i^t = q_i^t + r_i^t$ and $n_i^t = f_i^t - g_i^t$. If $\delta(0) = 0$, $\delta(r_i^t) = 1$ for $r_i^t > 0$, based on (5.33) - (5.36), we have

$$J_i^t = \min_{\pi_i \in \mathfrak{D}} \mathbb{E}\left\{ A\delta(r_i^t) + W(m_i^t) \right\} - \frac{\alpha c_r \cdot q_i^t}{q_i^{max}}, \tag{5.40}$$

where

$$W(m_i^t) = \alpha E_f(f_i^t) + \alpha E_r(r_i^t) + \alpha c_l \cdot \frac{[n_i^t - m_i^t]^+}{q_i^{max}} + \beta c_d \cdot \frac{[m_i^t - n_i^t]^+}{q_i^{max}} + J([m_i^t - n_i^t]^+). \tag{5.41}$$

Lemma 5.2. *According to (5.40), if $W(m_i^t)$ is an $A-$convex function, so is J_i^t.*

Proof. Based on the definition of $A-convex$, it is necessary to show the following

equation holds for all $z \geq 0, b > 0$,

$$A + J_i^t(r_i^t + z) \geq J_i^t(r_i^t) + z\left(\frac{J_i^t(r_i^t) - J_i^t(r_i^t - b)}{b}\right). \tag{5.42}$$

As $A > 0$ and $W(m_i^t)$ is $A - convex$, denote

$$T_i^t = m_i^{t*} = \arg\min_{m_i^t \in \Re} W(m_i^t). \tag{5.43}$$

Based on (5.40), the cost-to-go at time period t is

$$J_i^t = \begin{cases} A + W(T_i^t) - \frac{\alpha \cdot c_r \cdot q_i^t}{q_i^{max}} & q_i^t < t_i^t, \\ W(m_i^t) - \frac{\alpha \cdot c_r \cdot q_i^t}{q_i^{max}} & q_i^t \geq t_i^t. \end{cases} \tag{5.44}$$

Three cases are discussed to distinguish the $A - convexity$ of$J_i^t(q_i^t)$:

Case 1: $q_i^t \geq t_i^t$. If $q_i^t - b \geq t_i^t$, then function J_i^t is the sum of a $A - convex$ function and it is also a linear function. Hence, J_i^t is $A - convex$ and (5.42) holds. If $q_i^t - b < q_i^t$,, (5.42) can be written as

$$A + W(m_i^t + z) \geq W(m_i^t) + z\left(\frac{W(m_i^t) - W(t_i^t)}{b}\right). \tag{5.45}$$

i) If $J_i^t(q_i^t) \geq J_i^t(t_i^t)$, then by $A - convexity$ of $W(m_i^t)$,

$$\begin{aligned} A + W(q_i^t + z) &\geq W(m_i^t) + z\left(\frac{W(m_i^t) - W(t_i^t)}{q_i^t - t_i^t}\right) \\ &\geq W(m_i^t) + z\left(\frac{W(m_i^t) - W(t_i^t)}{b}\right). \end{aligned} \tag{5.46}$$

ii) If $J_i^t(q_i^t) < J_i^t(t_i^t)$, then

$$\begin{aligned} A + W(q_i^t + z) &\geq A + W(T_i^t) = W(t_i^t) > W(m_i^t) \\ &\geq W(m_i^t) + z\left(\frac{W(m_i^t) - W(t_i^t)}{b}\right). \end{aligned} \tag{5.47}$$

So for this case, (5.45) and hence (5.42) hold.

Case 2: $m_i^t \leq m_i^t + z \leq t_i^t$. In this region, the function J_i^t is linear hence (5.42) holds.

Case 3: $m_i^t \leq t_i^t \leq m_i^t + z$. For this case, write (5.42) as $A + J_i^t(q_i^t + z) \geq J_i^t(t_i^t)$ which holds by the definition of t_i^t. Thus the $A - convexity$ of J_i^t is proved given the $A - convexity$ of $W(m_i^t)$. □

To show the property between $J_i^t([m_i^t - n_i^t]^+)$ and $W(m_i^t)$, rewrite (5.41) as

$$W(m_i^t) = \alpha\left(E_f(f_i^t) + E_r(r_i^t)\right) + \frac{\beta c_d \cdot [m_i^t - n_i^t]^+}{q_i^{max} p[} + R(m_i^t), \tag{5.48}$$

where

$$R(m_i^t) = \alpha c_l \cdot \frac{[n_i^t - m_i^t]^+}{q_i^{max}} + J_i^t([m_i^t - n_i^t]^+). \tag{5.49}$$

The $A - convexity$ of $W(m_i^t)$ holds if the $A - convexity$ of $W(m_i^{t+1})$ implies $A - convexity$ of $R(m_i^t)$.

Lemma 5.3. *According to (5.48), if $W(m_i^{t+1})$ is an $A - convex$ function, so is $R(m_i^t)$.*

Proof. Four cases are discussed to show the $A - convexity$ of $R(m_i^t)$:

Case 1: $0 \leq m_i^{t+1} - b < m_i^{t+1} \leq m_i^{t+1} + z, A - convexity$ of $R(m_i^t)$ follows that of $W(m_i^{t+1})$.

Case 2: $m_i^{t+1} - b < m_i^{t+1} \leq m_i^{t+1} + z \leq 0$: in this region, $R(m_i^t)$ is linear and hence $A - convex$.

Case 3: $m_i^{t+1} - b < m_i^{t+1} \leq 0 \leq m_i^{t+1} + z$: for simplicity, denote $x = m_i^{t+1} + z$ in this region.

i) $0 < t_i^{t+1} \leq x$:

$$\begin{aligned} A + J_i^t(x) &\geq A - x \cdot \frac{\alpha c_l \cdot q_i^{t+1}}{q_i^{max}} + J_i^t(T_i^{t+1}) \\ &= J_i^t(0) - x \cdot \frac{\alpha c_l \cdot q_i^{t+1}}{q_i^{max}}. \end{aligned} \tag{5.50}$$

ii) $t_i^{t+1} \leq 0 \leq x$ and $0 \leq x \leq t_i^{t+1}$:

$$\begin{aligned} A + J_i^t(x) &= 2A - x \cdot \frac{\alpha c_r \cdot q_i^{t+1}}{q_i^{max}} + J_i^t(T_i^{t+1}) \\ &\geq J_i^t(0) - x \cdot \frac{\alpha c_l \cdot q_i^{t+1}}{q_i^{max}}. \end{aligned} \tag{5.51}$$

Thus $A + J_i^t(x) \geq J_i^t(0) - x \cdot \frac{\alpha c_l \cdot q_i^{t+1}}{q_i^{max} \cdot l_i}$ in this case. According to the definition of $R(m_i^t)$, the $A - convexity$ of $R(m_i^t)$ holds.

Case 4: $m_i^{t+1} - b < 0 < m_i^{t+1} \leq m_i^{t+1} + z$. Then, $0 < m_i^{t+1} < b$.

i) If $\frac{R(m_i^{t+1}) - R(0)}{m_i^{t+1}} \geq \frac{R(m_i^{t+1}) - R(m_i^{t+1} - b)}{b}$, thus

$$\begin{aligned} A + R(m_i^{t+1} + z) &\geq R(m_i^{t+1}) + z\frac{R(m_i^{t+1}) - R(0)}{m_i^{t+1}} \\ &\geq R(m_i^{t+1}) + z\frac{R(m_i^{t+1}) - R(m_i^{t+1} - b)}{b}, \end{aligned}$$

ii) If $\frac{R(m_i^{t+1})-R(0)}{m_i^{t+1}} < \frac{R(m_i^{t+1})-R(m_i^{t+1}-b)}{b}$, then we have

$$\begin{aligned} R(m_i^{t+1}) - R(0) &< \frac{m_i^{t+1}}{b}\Big(R(m_i^{t+1}) - R(m_i^{t+1}-b)\Big) \\ &= \frac{m_i^{t+1}}{b}\Big(R(m_i^{t+1}) - R(0) + \frac{\alpha c_l \cdot q_i^{t+1}}{q_i^{max} \cdot l_i}(m_i^{t+1}-b)\Big). \end{aligned}$$

Since $b > m_i^{t+1}$,

$$R(m_i^{t+1}) - R(0) < -\frac{\alpha \cdot c_l \cdot q_i^{t+1}}{q_i^{max}} m_i^{t+1}.$$

Then we have

$$\begin{aligned} R(m_i^{t+1}) + z\frac{R(m_i^{t+1}) - R(m_i^{t+1}-b)}{b} & \\ = R(m_i^{t+1}) - z\frac{\alpha c_l \cdot q_i^{t+1}}{q_i^{max}} & \\ < R(0) - (m_i^{t+1}+z)\frac{\alpha c_l \cdot q_i^{t+1}}{q_i^{max}} \leq A + R(m_i^{t+1}+z). & \end{aligned} \tag{5.52}$$

Hence, $R(m_i^{t+1})$ is $A-convex$ for all cases. □

Theorem 5.2. *If function J_i^t is* A-convex*, the optimal duty cycle control for IEEE 802.15.4 with Go-back-N ARQ scheme is a multi-period policy, the duty cycle control parameter $SO(r_i^t)$ is set according to its current queue length q_i^t and its threshold T_i^t: when q_i^t is smaller than the threshold T_i^t, the optimal $SO(r_i^t)^*$ is set based on (5.30), otherwise, $SO(r_i^t)^*$ equals to zero:*

$$SO(r_i^t)^* = \begin{cases} \left\lceil \log_2(\left\lceil \frac{r_i^{t*} D_p}{b} \right\rceil + \lceil \delta + D_{ACK} + D_{bcn} \rceil) \right\rceil & \text{if } q_i^t < T_i^t, \\ \lceil \log_2(\lceil D_{bcn} \rceil) \rceil & \text{if } q_i^t \geq T_i^t. \end{cases} \tag{5.53}$$

where r_i^{t*} is the optimal number of packets the device should received at each time

period [LCCL15].

5.7 Optimal Dynamic Programming based Cluster Head Control

The standard DP algorithm recursively computes the optimal solution in a backward fashion. DP is applicable only when the *principle of optimality* holds for the problem. And DP algorithm solves all the tail sub-problems by using the Bellman equation. However, the optimal control policy cannot be tractably computed in general. This is because the size of a state space typically grows exponentially in the number of state variables, which is known as the *curse of dimensionality*. This phenomenon makes DP intractable for the problems with practical scale.

The general DP algorithm is presented as follow. The cost-to-go function J is the sum of the additive utility $U(s_t, a_t)$ over time, where J is defined as

$$J = \mathbb{E}\Big\{U(s_t) + \sum_{t=0}^{T-1} U(s_t, a_t)\Big\}. \tag{5.54}$$

The policy $\pi(a_t|s_t)$ denotes the conditional probability of choosing the control a_t at the given state s_t. The MDP problem aims at of finding a policy which maximise the expected utility,

$$\pi^* = \arg\min_{q_\pi} \mathbb{E}\Big\{U(s_t) + \sum_{t=0}^{T-1} U(s_t, a_t)\Big\}, \tag{5.55}$$

where the distribution over trajectories under policy π is,

$$q_\pi(\bar{x}, \bar{u}|s_0) = \pi(u_0|s_0) \prod_{t=1}^{T} \pi(a_t|s_t) P(s_{t+1}|s_t, a_t). \tag{5.56}$$

The "tail subproblem" at s_t at time t aims to maximise the cost-to-go function J from time t to time T

$$J = \mathbb{E}\Big\{ U(s_T) + \sum_{t}^{T-1} U(s_t, \mu_t(s_t)) \Big\}, \tag{5.57}$$

where $\mu_t, \mu_{t+1}, \cdots, \mu_{T1}$ is the tail policy for the system which states with s_t.

Following the same logic, the optimal DP based duty cycle control is capable to solve the cluster head control with both Stop-and-wait and Go-Back-N. This standard DP algorithm is also called value iteration (VI) algorithm in some contexts. The specific duty cycle control applies DP algorithm is given in Algorithm 1.

5.8 Duty Cycle Control Simulation Results

In Section 5.1 and Section 5.3 the duty cycle control for IEEE 802.15.4 with Stop-and-Wait and Go-Back-N ARQ scheme are derived, respectively. In this section, the simulation results of the duty cycle control are presented.

Algorithm 1 Dynamic Programming based Duty Cycle Control

Require: cluster head $i \in \mathcal{I}_n$, total control time period T and current time period t

for each $i \in \mathcal{I}_n$ **do**
  Initialise the number of receive packets r_i^0 arbitrarilyand
  cost-to-go function $J_i^0 = 0$
  for $t = T - 1 \rightarrow 0$ **do**
    for each $r_i^t \leq q_i^{max}$ **do**
      Calculate the cost function $J(r_i^t)$
    end for
    the cost-to-go function $J_i^t \leftarrow \sum_{k=k}^{t} J(r_i^t) + J_i^{t+1}$
  end for
  for $t = 0 \rightarrow T$ **do**
    Step 1: Compute optimal transmission policy
    calculate the optimal number of receive packets r_i^{t*} for cluster head i:
    $r_i^{t*} \leftarrow \arg\min J_i^t$
    Step 2: Assign the duty cycle
    The duty cycle control with Stop-and-Wait should be:
    $SO(r_i^{t*}) \leftarrow \left\lceil \log_2(\frac{r_i^t \times P_s}{b} + D_{bcn}) \right\rceil$ or
    The duty cycle control with Go-Back-N should be:
    $SO(r_i^{t*}) = \left\lceil \log_2(\left\lceil \frac{r_i^t D_p}{b} \right\rceil + \lceil \delta + D_{ACK} + D_{bcn} \rceil) \right\rceil$.
  end for
end for

5.8.1 Duty Cycle Control for IEEE 802.15.4 with Stop-and-Wait and Go-back-N ARQ

Fig. 5.1 shows the co-relation between the duty cycle parameter SO and the number of received packets. The result of duty cycle control for Stop-and-Wait is shown in red line and that of the Go-back-N scheme is shown in blue line. From the Fig. 5.1, it can be seen that for same amount of transmitted packets the SO of duty cycle control with Go-back-N ARQ scheme is smaller than that of the Stop-and-Wait ARQ scheme. As the duty cycle is used to represent energy efficiency, with same BO setting, the smaller the SO is, the higher the energy efficiency can be achieved. Thus, the duty cycle control with Go-Back-N ARQ scheme achieves

higher energy efficiency, especially when then number of transmitted packets is small.

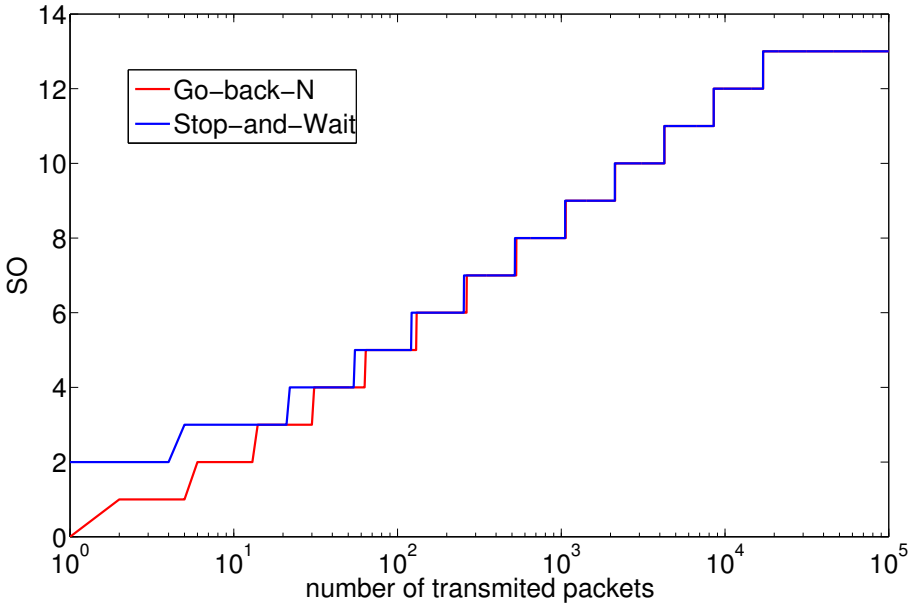

Figure 5.1: Duty cycle setting with different ARQ schemes.

The difference between the compared two schemes becomes less with the increase of the transmitted packets. This is due to the fact that the difference between the compared two schemes lies in the ACK packets transmission. With the increase of transmitted packets the portion of required ACK packets transmission become ignorable, thus the two controls behave similarly when the number of transmitted packets is large.

5.8.2 Optimal Duty Cycle Control for IEEE 802.15.4 based Hierarchical M2M Networks

In this subsection, the performance of the optimal DP transmission policy is evaluated in Matlab.

Table 5-A: Duty Cycle Control Simulation Parameters

Parameter	**Value**	**Parameter**	**Value**
frequency	2.4 GHz	traffic model	Poisson
transmit power	57.24mw	packet size	50 bytes
receive power	62mw	data rate	250 kbps
idle listen power	1.4mw	time period length	3.93 s
duty cycle	10%	T	2, 5 & 10

Focusing on the inherent properties of the proposed policy, a two hop cluster-tree network is considered in the simulation. The parameters on energy consumption are set based on the CC2420 data sheet [Ins] and MAC layer parameters are based on the IEEE 802.15.4 standard [Soc11]. Each simulation is repeated for 100 times. For cluster head i, the number of its child M2M devices $\mathcal{C}_i$ equals to 2.

The devices generate packets following Poisson distribution. The average packet arrival rate is varied in order to study the impact of traffic load. The service rate of cluster head i also follows Poisson distribution, and the mean value of packet service rate is 5 packets per active period. The maximum queue length is set to be 50 packets. The length of each time period is 3.93s ($15.36 * 2^8$ ms) according to IEEE 802.15.4 standard. In each time period, the length of the active period is decided by duty cycle. α and β are set to be 0.4 and 0.6, respectively. The simulation parameters are shown in the Table. 5-A.

First, DP algorithm is used to find the minimum threshold T_i of the optimal transmission policy. The simulation result is given in Fig. 5.2.

The threshold T_i of DP algorithm is the maximum number of packets the cluster head i can receive at each active period. Due to the convexity of the cost functions, the optimal T_i^* is obtained when the joint-cost value remains the same while the

simulated threshold increased.

In Fig. 5.2, the joint-cost value is given by the optimal solution found by DP algorithm. The joint-cost value remains similar when the simulated threshed T_i is bigger than 6, thus the optimal threshold T_i^* of the simulated scenario is 6 packets per active period. In addition, it can be seen that the converge point of the joint-cost value is same with different settings of the total control time period T.

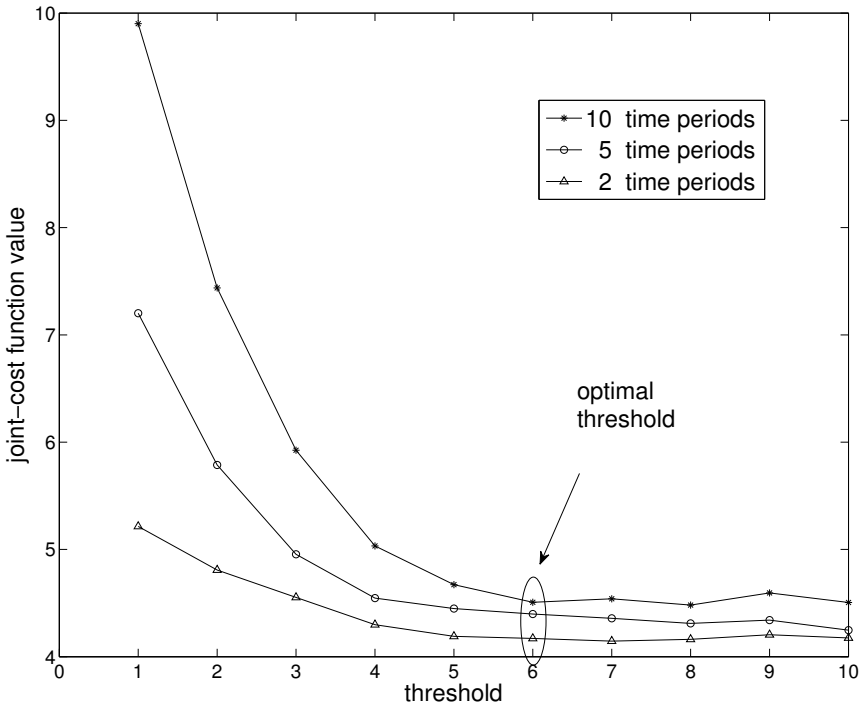

Figure 5.2: Optimal transmission threshold by applying DP.

Then, comparison between the optimal transmission policy and a random policy is given.

- *random policy*, the device receives a random number of packets in each time period based on Poisson distribution the mean value of which equals to 3;

- *DP optimal transmission policy*, the threshold T_i of the optimal transmission policy is set to be 6 packets based on the result of DP algorithm as shown in Fig. 5.2.

For the compared random policy, the duty cycle is set to be fixed 10% with the active period of 0.1s, which is long enough to transmit all generated packets under the simulation setting. The evaluated performance metrics are average energy consumption per packet and average end-to-end delay under various traffic loads:

Average energy consumption per packet: is calculated as the total energy consumption in T active periods over the total number of transmitted packets.

Average end-to-end delay: is the total delay caused by buffered packets over the total number of successfully transmitted packets.

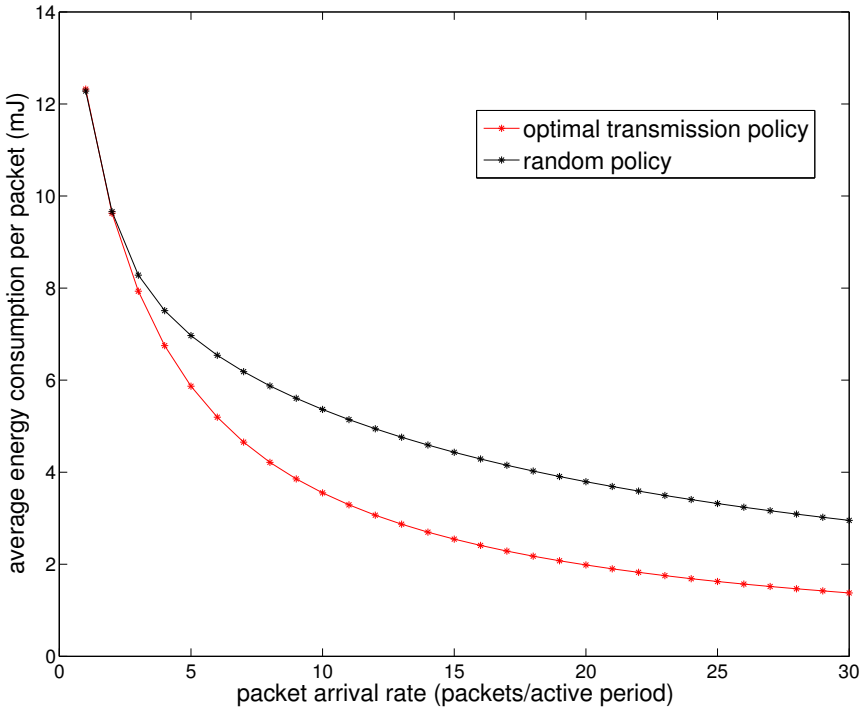

Figure 5.3: Average energy consumption of DP based duty cycle control.

Fig. 5.3 shows the result of the average energy consumption per packet under different traffic arrival rates. The energy consumption per packet decrease as the network traffic increases for both policies. This is because higher packet arrival rates provide more available packets to be transmitted, when the active period is long enough to forward all these packets. With fixed duty cycle, the increased number of transmitted packets reduce the average consumption of each packet.

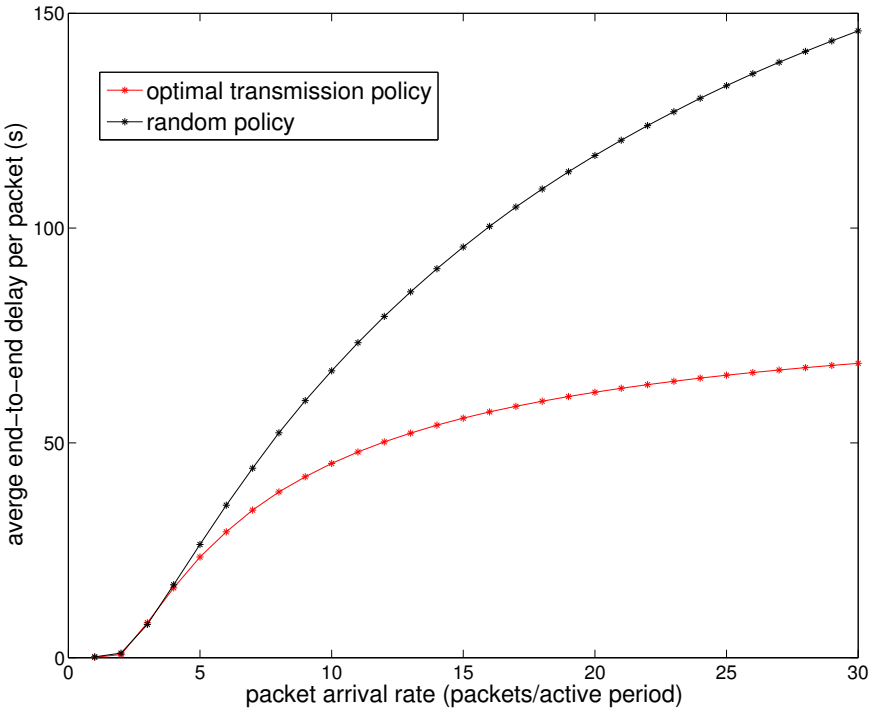

Figure 5.4: Average end-to-end delay of DP based duty cycle control.

Fig. 5.4 shows the result of average end-to-end delay under different traffic arrival rates. The average end-to-end delay increases as the increase of packet arrival rates. Due to the increased traffic loads and the limitation of the service rate, some packets are buffered in the queue. The buffered packets have to wait to next time period for transmission, which increase the average per packet end-to-end delay.

Taking traffic loads, network topology and application requirements into account, the optimal transmission policy achieved both lower energy consumption and end-to-end delay compared to the random policy, by adaptively scheduling the number of packets the device received at each active time period.

According to the simulation results, the optimal transmission policy is able to achieve about 50% saving in both energy consumption and end-to-end delay compared to that of the IEEE 802.15.4 random policy when the packet arrival rate is above 15 packets per active period.

5.9 Summary

In this chapter, the duty cycle control optimisation problem for IEEE 802.15.4 is formulated. The aim of the duty cycle control is to minimise the expected joint-cost of energy consumption and end-to-end delay. The duty cycle control for IEEE 802.15.4 with both Stop-and-Wait and Go-back-N ARQ scheme are calculated. Then the optimal duty cycle control is derived by applying DP algorithm. Furthermore, the proposed DP based duty cycle controls for both Stop-and-Wait and Go-back-N schemes require no initial control setting and is well compatible with the current IEEE 802.15.4 standard.

Simulation results show that the optimal transmission policy effectively reduced both energy consumption and end-to-end delay under various network traffics. Especially, when the traffic load is high, the reduction of energy consumption and end-to-end delay are more than 50% compared to the standard IEEE 802.15.4 standard.

Chapter 6

Cluster Head Control with Cluster Utility Maximisation

This chapter focuses on the cluster head control of the proposed control framework. The proposed cluster head controls aim to solve the formulated optimisation problem $\mathcal{P}3$ in Chapter 4. More specifically, three practical cluster head controls are proposed to fit into different practical hierarchical M2M scenarios. The cluster head controls aim at maximising the single cluster utility, which contains both empirical network performance component and economic component. For the empirical network performance component, the cluster throughput and the join-cost of energy efficiency and end-to-end delay have been taken into consideration.

6.1 Cluster Head Utility Design

Aforementioned in Chapter 4, the designed network optimisation problem $\mathcal{P}1$ is decomposed into the distributed cluster head control $\mathcal{P}3$ and the gateway control $\mathcal{P}4$. The aim of the cluster head control is to maximise the single cluster utility.

The first step of performing theoretical optimisation is to design a utility function which is able to reflect the identified network performance aimed to be im-

proved [WPL06]. The defined cluster utility function is a mathematical measurement of the QoS performance based on the provided network resource, such as bandwidth, transmission rate and resource blocks.

In this thesis, the utility of the cluster head i is designed with both empirical network performance component V_i^t and economic component R_i^t. The utility function of cluster head i is defined with a $quasi-linear$ form:

$$U_i(r_i^t) = \log(1 + V_i^t) + R_i^t, \tag{6.1}$$

where the empirical component V_i^t combines both empirical throughput and empirical cost of transmission, and the economical component R_i^t is the economic profit of the transmission. The economic profit is the return on revenue of packets transmission, which includes charges of receiving packets and costs of forwarding packets. The quasi-linear form of value function is chosen, since any equilibrium solutions to utility maximisation problems are independent of the initial economical setting of each cluster head.

In order to obtain the optimal theoretical solution, the formulation of the empirical component V_i^t, which named as value function needs to be monotonic and concave. The value function reflects the node's empirical network performance for receiving or forwarding certain amount of packets. For each cluster head $i \in \mathcal{I}_n$, the value function consists of two terms, the first term represents the throughput of receiving packets and the second term represents the joint-cost of energy and end-to-end delay.

$$V_i^t = \epsilon_1 \log(1 + \frac{f_i^t - r_i^t}{q_i^{max}}) - \epsilon_2 J(r_i^t) * \log\left(1 + J(r_i^t)\right), \tag{6.2}$$

where $J(r_i^t)$ is the joint-cost of energy and end-to-end delay defined in the last chapter.

As designed in Chapter 4, the cluster heads charge its child nodes for forwarding packets to gain some economic benefits. If $R_i^t, \forall i \in \mathcal{I}$ is expressed as the product of the corresponding price and number of transmitted packets,

$$R_i^t = p_l^t r_i^t - p_i^t f_i^t, \forall l \in \mathcal{L}_i, \tag{6.3}$$

where the per packet service price $p_l^t = p_i + 1$ of cluster head i on link $l_{i,j}$.

Cluster heads are assumed to be non-communicative as they are unable to observe the situation of the other cluster heads in many practical applications. Thus the utility function of each cluster head does not consider the impacts of 1) the set of the cluster heads that compete with the cluster head i; 2) the performance measurements on cluster head from its child device; 3) the utility function of its child devices; and 4) the price of other cluster heads. The cluster heads will make the control decision with consideration of the cluster traffic condition, its buffer capacity and the bid price it offered to the gateway.

6.2 Policy Iteration (PI) Algorithm based Cluster Head Control

According to the previous chapter, the optimal cluster head control can be found by running DP algorithm. To reduce the computational complexity of the optimal DP algorithm, the policy iteration (PI) algorithm based cluster head control is proposed in this chapter.

The cluster head control has two steps, the first step is to compute the transmission policy; The second step is to assign the duty cycle based on the computed

Algorithm 2 Policy Iteration Algorithm based Cluster Head Control

Require: number of cluster head $i \in \mathcal{I}_n$, total control time periods T and current control time period t

1: Initialise control policy π to be evaluated arbitrarily, and
2: policy-stable $\leftarrow$ false
3: **for each** $i \in \mathcal{I}_n$ **do**
4: **Step 1: Compute transmission policy**
5: *a) Policy evaluation:*
6: **for** $t = 0 \rightarrow T$ **do**
7: Find number of receive packets r_i^t according to the given control policy π
8: $r_i^t \leftarrow \pi$
9: Calculate the aggregated utility $U_\pi(r_i^t)$ with utility till time period t
10: and the estimated utility $U_i(r_i^{t+1})$ afterwards:
11: $U_\pi(r_i^t) \leftarrow \sum_{k=0}^{t} U(r_i^t) + U_i(r_i^{t+1})$
12: **end for**
13: *b) Policy improvement:*
14: **for each** $\pi \in \mathcal{D}$ **do**
15: $r_i^t \leftarrow \arg\min U_i(r_i^t)$
16: Check whether the current control r_i^t is aligned with the policy π
17: **if** $r_i^t = u_i^t \in \pi$ **then**
18: policy-stable $\leftarrow$ true
19: **end if**
20: **if** policy-stable = true **then**
21: stop
22: **else**
23: go to line 16.
24: **end if**
25: **end for**
26: **Step 2: Assign the duty cycle**
27: **for** $t = 0 \rightarrow T$ **do**
28: Calculate the number of received packets based on the policy π
29: $r_i^{t+1} \leftarrow u_i^t \in \pi$
30: Assign the Stop-and-Wait duty cycle control parameter $SO(r_i^t)$:
31: $SO(r_i^t) \leftarrow \left\lceil \log_2(\frac{r_i^t \times P_s}{b} + D_{bcn}) \right\rceil$ or
32: Assign the Go-Back-N duty cycle control parameter $SO(r_i^t)$:
33: $SO(r_i^t) = \left\lceil \log_2(\left\lceil \frac{r_i^t D_p}{b} \right\rceil + \lceil \delta + D_{ACK} \rceil + \lceil D_{bcn} \rceil) \right\rceil$.
34: **end for**
35: **end for**

optimal transmission policy. The PI algorithm is applied in the first step.

i) Policy evaluation, a policy π is evaluated by computing the aggregated utility function $U_\pi(r_i^t)$.

ii) Policy improvement, the PI algorithm looks for a policy π' that has higher utility value than the previously evaluated policy π. The heuristic based policies are applied accordingly in the policy improvement step to maximise the function $U(r_i^t)$. When the same policy is found in two consecutive iterations, the algorithm has converged.

The exact embodiment of the proposed PI based cluster head control is shown in Algorithm 2.

Due to the limitation of the buffer size, the cluster head control has finite action and state spaces as well as bounded and stationary utility function. Under these conditions PI algorithm is proven to converge to the optimal policy. What's more, it has been shown that PI converges in fewer iterations than VI in practice [Ber05].

6.3 Rollout Algorithm (RA) based Cluster Head Control

To further reduce the computational complexity of Algorithm 2, a low complexity suboptimal solution, named rollout algorithm (RA) based cluster head control is proposed. The utility lower bound, which is the theoretical worst case of RA based cluster head control is provided.

6.3.1 Low Complexity Suboptimal Solution

An effective way to reduce the computation required by DP is to truncate the time horizon and use a devision based on lookahead of a small number of states. The most straight forward way is to use a *one-step lookahead policy* whereby at state s_t, the controller chooses the control $\bar{\mu}_t(s_t)$, which gives the minimum of

$$\min_{u_t \in U_t(s_t)} \mathbb{E}\Big\{ g_t(s_t, u_t, w_t) + \tilde{J}_{t+1}(f_t(s_t, u_t, w_t)) \Big\}. \tag{6.4}$$

The approximating function $\tilde{J}_{t+1}$ is the cost-to-go $\tilde{J}^{\pi}_{t+1}$ of some known heuristic or suboptimal policy $\pi = \{\mu_1, \mu_2, \cdots, \mu_T\}$, called *base policy*. The policy thus obtained is called the *rollout policy* based on π. Thus, the rollout policy is a one-step lookahead policy, with the optimal cost-to-go approximated by the cost-to-go of the base policy.

The process of starting from some suboptimal policy and generating another policy using the one-step-look ahead process, which is known as policy improvement, and is the basis of a primary method for solving the DP problems in *policy iteration* method. The rollout algorithm can be viewed as a single policy iteration. Thus, the reduction of computational complexity of RA based policy is achieved by reducing the iteration times of the optimal PI policy.

Rollout algorithms have demonstrated excellent performance on a variety of dynamic optimisation problems. Interpreted as an approximate DP algorithm, rollout algorithm estimates the utility at each time period by estimating future utility while following a heuristic control, referred to as the base policy.

6.3.2 Rollout Algorithm based Cluster Head Control

To ensure the stable of queue length, the devices should receive no more packets than it could transmit. Thus, instead of searching the optimal solution by running DP, the most straight forward approach is to set the T_i equal to the mean value of f_i^t for each cluster head i. Based on the Theorem 5.1 and Theorem 5.2 the heuristic base cluster head control with Stop-and-Wait ARQ is designed as

$$SO(r_i^t) = \begin{cases} \left\lceil \log_2(\frac{r_i^t \times P_s}{b} + D_{bcn}) \right\rceil & \text{if } q_i^t < f_i^t, \\ \lceil \log_2(D_{bcn}) \rceil & \text{if } q_i^t \geq f_i^t. \end{cases} \tag{6.5}$$

And the heuristic base cluster head control with Go-Back-N ARQ is designed as

$$SO(r_i^t) = \begin{cases} \left\lceil \log_2(\left\lceil \frac{r_{n_i}^k D_p}{b} \right\rceil + \lceil \delta + D_{ACK} \rceil + \lceil D_{bcn} \rceil) \right\rceil & \text{if } q_i^t < f_i^t, \\ \lceil \log_2(\lceil D_{bcn} \rceil) \rceil & \text{if } q_i^t \geq f_i^t. \end{cases} \tag{6.6}$$

The proposed RA based cluster head control is the one that attains the maximum of the long-term utility function

$$U_i(r_i^t) = \max_{\pi_i \in \mathcal{S}} \left[\mathbb{E} \left\{ V(r_i^t) + \mathbb{E}\{\tilde{U}(r_i^{t+1})\} \right\} \right], \tag{6.7}$$

where $\tilde{U}_i(r_i^{t+1})$ is the approximation of $U_i(r_i^{t+1})$ based on the heuristic base control. The exact RA based cluster head control is shown in Algorithm 3.

Given the approximation $\tilde{U}_i(r_i^t)$, which is calculated based on the heuristic base control, the computational saving of RA based cluster head control is evident. This is because only one single minimisation problem has to be solved at each

Algorithm 3 Rollout Algorithm Base Cluster Head Control

Require: number of cluster heads $i \in \mathcal{I}_n$, total control time periods T and current control time period t

for each $i \in \mathcal{I}_n$ **do**
  for $t = 0 \rightarrow T$ **do**
    Step 1: Compute transmission policy
    a) Base policy estimation
    for $t = t + 1 \rightarrow T$ **do**
      Set the based policy threshold T_i^{t+1} according to service rate f_i^{t+1}
      $T_i^{t+1} \leftarrow f_i^{t+1}$
      Calculate the number of receive packets r_i^{t+1} according to the threshold base policy
      if $q_i^{t+1} < T_i^{t+1}$ **then**
        $r_i^{t+1} \leftarrow T_i^{t+1} - q_{ni}^{t+1}$
      else
        $r_i^{t+1} \leftarrow 0$
      end if
      Calculate the utility value $U_i(r_i^{t+1})$ of time period $t+1$
    end for
    The estimated aggregated utility $\tilde{U}_i(r_i^{t+1})$ from time period $t+1$ is,
    $\tilde{U}_i(r_i^{t+1}) \leftarrow \sum_{t=t+1}^{T} U_i(r_i^t)$
    b) Rollout algorithm based control
    for each $r_i^t \in \bar{\mathcal{S}}$ **do**
      Calculate the current time period utility value $U_i(r_i^t)$
      The aggregated utility $U_i(r_i^t)$ of cluster i is
      $U_i(r_i^t) \leftarrow U_i(r_i^t) + \tilde{U}_i(r_i^{t+1})$
    end for
    $r_i^t \leftarrow \arg\min U_i(r_i^t)$
    Step 2: Assign the duty cycle
    Assign the Stop-and-Wait duty cycle control parameter $SO(r_i^t)$:
    $SO(r_i^t) \leftarrow \left\lceil \log_2(\frac{r_i^t \times P_s}{b} + D_{bcn}) \right\rceil$ or
    Assign the Go-Back-N duty cycle control parameter $SO(r_i^t)$:
    $SO(r_i^t) \leftarrow \left\lceil \log_2(\left\lceil \frac{r_i^t D_p}{b} \right\rceil + \lceil \delta + D_{ACK} \rceil + \lceil D_{bcn} \rceil) \right\rceil$.
  end for
end for

time period. Noticed that even with readily available approximations $\tilde{U}_i(r_i^{t+1})$, the calculation of the minimisation over $\pi_i \in \mathcal{S}$ may involve substantial computation. To further save the computation, a subset $\bar{\mathcal{S}}$ of the promising controls is identified in the proposed RA based cluster head control. Thus, the minimisation over $\mathcal{S}$ is

replaced by a minimisation over the subset $\bar{\mathcal{S}} \subset \mathcal{S}$.

Theorem 6.1. *Let's denote $\hat{U}_i(r_i^t)$ as the estimate cost-to-go of RA based cluster head control, of which the control range is $\bar{\mathcal{S}} \subset \mathcal{S}$. $U_i(r_i^t)$ as the expected actual aggregated utility incurred by RA based cluster head control. Then $U_i(r_i^t) \leq \tilde{U}_i(r_i^t)$, which means $\tilde{U}_i(r_i^t)$ is the uitlity lower bound of RA based cluster head control.*

Proof. For $t = 0, 1, \cdots, T-1$, denote

$$\hat{U}_i(r_i^t) = \max_{\pi_i \in \bar{\mathcal{S}}} \Big[V(r_i^t) + \mathbb{E}\{\tilde{U}_i(r_i^{t+1})\} \Big]. \tag{6.8}$$

Thus for all q_i^t, we have $\hat{U}(r_i^t) \leq \tilde{U}(r_i^t)$, if the emphasis is given to the network performance component, let

$$\begin{aligned} \hat{U}(r_i^t) &= V(r_i^t) \\ &= \epsilon_1 \log(1 + \frac{f_i^t - r_i^t}{q_i^{max}}) - \epsilon_2 J(r_i^t) * \log\Big(1 + J(r_i^t)\Big). \end{aligned} \tag{6.9}$$

Applying backward induction, we have $U(r_i^t) = \hat{U}(r_i^t) = V(r_i^t)$ for all q_i^t. Assuming that $U(r_i^{t+1}) \geq \hat{U}(r_i^{t+1})$ for all q_i^{t+1}, we have

$$\begin{aligned} U(r_i^t) &= \mathbb{E}\Big\{ V(r_i^t) + U(r_i^{t+1}) \Big\} \\ &\geq \mathbb{E}\Big\{ V(r_i^t) + \hat{U}(r_i^{t+1}) \Big\} \\ &\geq \mathbb{E}\Big\{ V(r_i^t) + \tilde{U}(r_i^{t+1}) \Big\} = \hat{U}(r_i^t), \end{aligned} \tag{6.10}$$

for all q_i^t.

The first equality above follows from the definition of the utility $U_i(r_i^t)$ of RA based cluster head control, while the first inequality follows from the induction

hypothesis, and the second inequality follows from the assumption $\hat{U}_i(r_i^t) \geq \tilde{U}_i(r_i^t)$. Then, we have $U_i(r_i^t) \geq \hat{U}_i(r_i^t) \geq \tilde{U}_i(r_i^t)$ for all q_i^t. Thus, the $\tilde{U}_i(r_i^t)$ is a readily obtainable utility lower bound for the utility function $U_i(r_i^t)$. □

In addition, two remarks on computational complexity and control overhead of the proposed RA based cluster head control are provided as follows.

Remark 6.1. *The proposed RA based cluster head control has lower computation complexity as compared to the PI optimal control and VI optimal control. If S is the average search range of the devices, the computation complexity of DP algorithm is $O(TS^{N+S})$, while that of the RA based cluster head control is only $O(TNS)$.*

Remark 6.2. *The proposed suboptimal controls have lower synchronisation overhead as compared to controls in [WWXY10] and [BY13]. The proposed control does not need additional SYNC packet to ensure the devices are active at the same time as it employs the same BO as defined in IEEE 802.15.4 (2011) and all devices are activated at the beginning of each BI.*

6.4 Reinforcement Learning (RL) based Cluster Head Control

In many practical scenarios it is not reasonable to assume the cluster heads have the perfect network information. The framework of RL known as the learning procedure is applied to such scenario where no perfect network information is available to compute the DP or PI based cluster head control. By applying RL algorithm, each cluster head updates its control decision according to its experience with different decisions without explicit modelling of the network.

6.4.1 Reinforcement Learning

RL is a simulation-based technique for solving the large-scale and complex problems, which is rooted in DP. RL is useful when a model is difficult or costly to derive. When the state-space of the system is large, it combines with algorithms to approximate the utility function, thereby generating a solution. It has been shown through mathematically rigorous arguments that RL can produce optimal or near-optimal solutions.

Q-learning is a model-free RL technique, which is used to find the optimal state-action policy for any finite state DP problems. It works by learning an action-utility table that ultimately gives the expected utility of taking a given action in a given state and following the optimal policy thereafter. When such an action-utility table is learned, the optimal policy can be constructed by selecting the action with the highest utility at each state.

As one branch of ADP algorithms, Q-learning uses simulation to approximate the cost j^{π} or the Q-factor $Q(s,a)$ of the current policy μ. The optimal Q-factor of (s,a) is defined as:

$$Q^*(s_t,a_t) = \mathbb{E}\Big\{ g(s_t,a_t,w_t) + \gamma J^*(s_{t+1}) \Big\}. \tag{6.11}$$

The policy π is applied at state s_t, and the optimal is applied thereafter. Then the Bellman's equation is written as

$$J^*(s_t) = \min_{a \in A} Q^*(s_t,a_t), \quad \forall s \in S, \tag{6.12}$$

and Q_{t+1} is generated by

$$Q_{t+1}(s,a) = \mathbb{E}\Big\{ g(s,a,w) + \alpha \min_{a \in A} Q_t(s',g) \Big\}, \tag{6.13}$$

with $s' = f(s,a,w)$.

Once the optimal Q-factor $Q^*(s,a)$ are known, the model of the system is not needed, and the optimal policy can be implemented online by

$$\pi^*(s) = \min_{a \in A(s)} Q^*(s,u). \tag{6.14}$$

6.4.2 Reinforcement Learning based Cluster Head Control

The RL based cluster head control is formulated as a stochastic learning process. One challenge of the approach is that the cluster heads do not know the information of the other cluster heads due to the noncooperation among clusters. Then, the networking environment is non-stationary for all cluster heads and the convergence of learning process may not be assured. To alleviate the lack of mutual information exchange, the cluster heads form internal conjectures learn how the other cluster heads react to their present actions with only local observations form direct interactions with the network environment. Thus, learning is finished asymptotically by appropriately making use of the past experience.

In the cluster head control problem, the devices try to learn the optimal policy from its history of interaction with the network with Q-learning algorithm. In other words, the Q-learning does not require perfect information as it will try to learn the optimal solution directly by updating the state-action value (Q-value) while interacting with the network, thus it is also called model-free RL.

A history of cluster head i is a sequence of state-action-utility set $\{q_i^t, r_i^t, U_i^t\}$, which shows that the device was in state q_i^t, did action r_i^t, and received an immediate utility U_i^t. Then the cluster head transferred into the next state q_i^{t+1}. For a given policy π, a Q-value is the expected aggregated utility when executing action r_i^t at state q_i^t and then following the policy π thereafter, and it is defined as $Q_\pi(q_i^t, r_i^t) = U_i^t + \delta \min Q_\pi(q_i^{t+1}, r_i^{t+1})$, where γ is the discount factor. Then given the learning rate δ, the device will update its estimation for $Q(q_i^t, r_i^t)$ at iteration t $(0 < t < T)$ as

$$Q^t(q_i^t, r_i^t) = Q^{t-1}(q_i^t, r_i^t) + \delta\Big\{U_i^t + \min Q^t(q_i^t, r_i^t) - Q^{t-1}(q_i^t, r_i^t)\Big\}. \tag{6.15}$$

The learning rate $\delta \in (0, 1]$ specifies how far the current estimation of $Q(q_i^{t-1}, r_i^{t-1})$ is adjusted toward the update target $U_i^t + \min Q(q_i^t, r_i^t)$. The learning rate is typically time varying, decreasing with time. The expression inside the curly bracket in (6.15) is the temporal difference, which is the difference between the estimation of $Q^*(q_i^t, r_i^t)$ at two successive time period, t and $t + 1$.

One of the conditions the sequence $Q(q_i^t, r_i^t)$ provably converges to $Q^*(q_i^t, r_i^t)$ is that the device keeps trying all actions in all states with nonzero probability. This means that the device must sometime explore, i.e., perform other actions than dictated by the current policy. Thus, finding a balance between exploitation of the current knowledge, and exploration of improving current knowledge by performing information-gathering actions is crucial to the efficiency of Q-learning algorithm.

The ϵ-greedy, a variation on normal greedy selection, is applied in the proposed Q-learning based cluster head control, as shown in Algorithm 4. In ϵ-greedy, the device identifies the best action according to the state-action table. At the same time, there is a small probability ϵ that, rather than take the currently known best

action, the device will arbitrarily select an action from the remaining actions to perform the exploration.

Algorithm 4 Q-Learning based Cluster Head Control

Require: number of cluster heads $i \in \mathcal{I}_n$, maximum iteration times T and current control time period t

for each $i \in \mathcal{I}_n$ **do**
  Initialise the Q-factor table $Q^0(q_i^0, r_i^0) = 0$
  for $t = 1 \rightarrow T$ **do**
    for $k = 0 \rightarrow 16$ (as each contention free period is divided into 16 slots) **do**
      if $rand < \epsilon$ **then**
        [Exploration step]:
        Select the number of receive packets r_i^t arbitrarily
      else
        [Exploration step]:
        Update the Q-factor table $Q^t(q_i^t, r_i^t)$ according to:
        $Q^t(q_i^t, r_i^t) = V_i^t + \delta \min Q^t(q_i^{t+1}, r_i^{t+1})$
        Calculate the number of receive packets
        $r_i^t \leftarrow \arg\min Q^t(q_i^t, r_i^t)$
      end if
      Assign the Stop-and-Wait duty cycle control parameter $SO(r_i^t)$:
      $SO(r_i^t) \leftarrow \left\lceil \log_2(\frac{r_i^t \times P_s}{b} + D_{bcn}) \right\rceil$ or
      Assign the Go-Back-N duty cycle control parameter $SO(r_i^t)$:
      $SO(r_i^t) \leftarrow \left\lceil \log_2(\left\lceil \frac{r_i^t D_p}{b} \right\rceil + \lceil \delta + D_{ACK} \rceil + \lceil D_{bcn} \rceil) \right\rceil$.
    end for
    Update the Q-factor table $Q(q_i^t, r_i^t)$ according to (6.10)
  end for
end for

6.5 Simulation Results of Cluster Head Controls

In this section, the proposed PI based cluster head control, RA based cluster head control and the RL based cluster head control are evaluated in Matlab. Simulation results and analysis are provided.

6.5.1 Performance of PI Based Cluster Head Control

6.5.1.1 Simulation Setup

The MAC layer parameters used in the simulation are based on the IEEE 802.15.4 standard, as shown in Table 6-A. α and β are set to be 0.2 and 0.4, respectively. Device energy consumption parameters of M2M gateway, cluster heads and M2M devices are based on XBee® RF Module data sheet [Int], respectively.

Table 6-A: Simulation Parameters of Cluster Head Controls

Parameter	**Value**	**Parameter**	**Value**
data rate	250kbps	frequency	2.4 GHz
transmit power	396 mw	packet size	50 bytes
receive power	102.3 mw	CCA size	8 symbols
idle listen power	102.3 mw	ACK packet size	10 symbols
sleep power	0.033 mw	unit backoff period	20 symbols

In this simulation, the performance of the proposed PI cluster head control is compared with the DP optimal control and a benchmark control.

-*PI Optimal control*: the optimal r_i^{t*} follows the threshold structure based on the **Theorem 5.1** and is computed by policy iteration (PI) based control algorithm. This method is labeled as PI optimal.

-*VI Optimal control*: this optimal solution follows the basic concept of DP. At each time period t, r_i^{t*} is the one obtains the maximum utility value $U(r_i^t)$. This method is labeled as value iteration (VI) optimal.

-*Benchmark control*: the benchmark control aims at maximising the number of

received packets r_i^t to reduce the end-to-end delay. The maximum SO is bounded by the service rate f_i^t of the cluster head.

6.5.1.2 Simulation Results

The performance of the proposed PI based cluster head control is evaluated in terms of the cluster utility, energy efficiency, end-to-end delay, cluster throughput, packet drop ratio and cluster profit. The definition of all the performance metrics are given in Chapter 4.4.2.

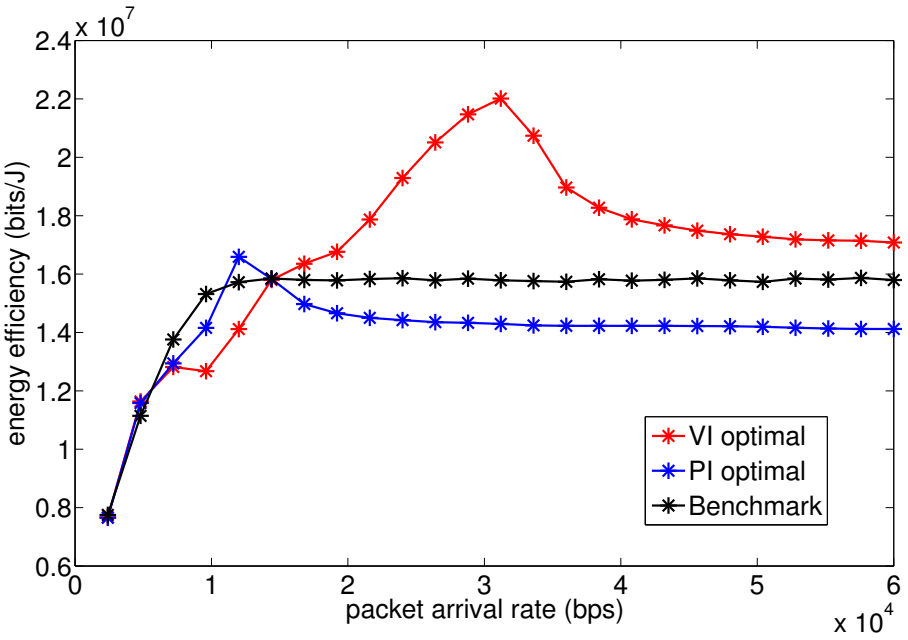

Figure 6.1: Energy efficiency of PI based cluster head control.

Fig. 6.1 shows the energy efficiency of the cluster head. Since SO can only be integer as defined by IEEE 802.15.4, the change of active period length is radical. The idle listening energy consumption caused by the change of SO leads to the non monopoly change of the energy efficiency curve of VI optimal control between 20-40 kbps.

The energy efficiency curves of benchmark control, VI optimal control and PI optimal become flat after the packet arrival rate is higher than 40 kbps. This is because the maximum number of transmitted packets is reached, which means the network is saturated. At the stable state, the energy efficiency of PI optimal control is slightly lower than that of the compared two controls.

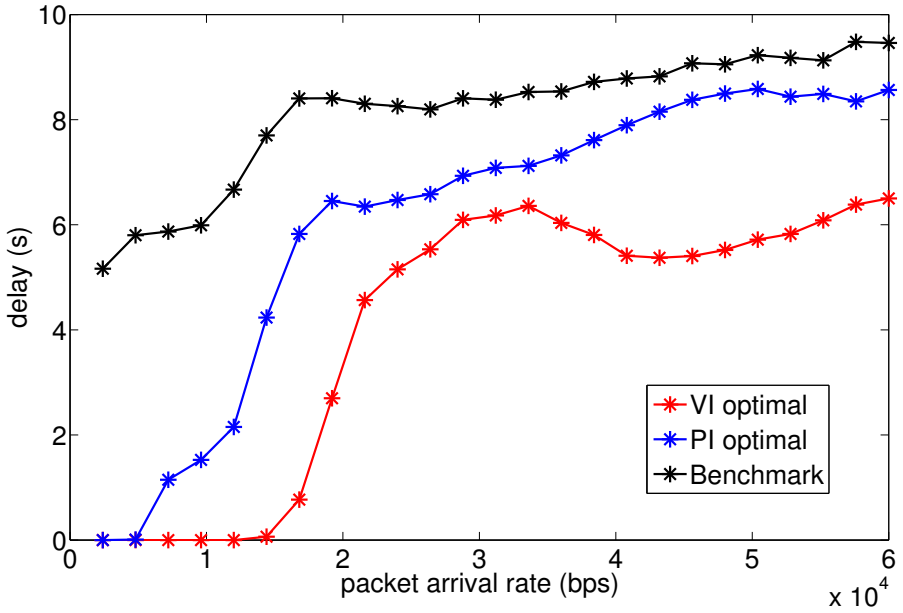

Figure 6.2: End-to-End delay of PI based cluster head control.

Fig. 6.2 shows the averaged end-to-end delay of the successfully transmitted packets. The average end-to-end delay increased with the increase of the packet arrival rates. Among the compared results of different controls, the end-to-end delay of PI based cluster head control is higher than that of the VI optimal control, but lower than that of the benchmark control. The rapid increase of the end-to-end curve of VI optimal control between 20-30 kbps is due to the same *SO* with increased traffic arrival rate. This lead to more packets need to be buffered before being transmitted. Then, the end-to-end delay of VI optimal control begin to decrease between 30-40 kbps, this is due to the radical increase of *SO* which

extend the active period lengths, which allowed more packets to be transmitted directly without any buffering.

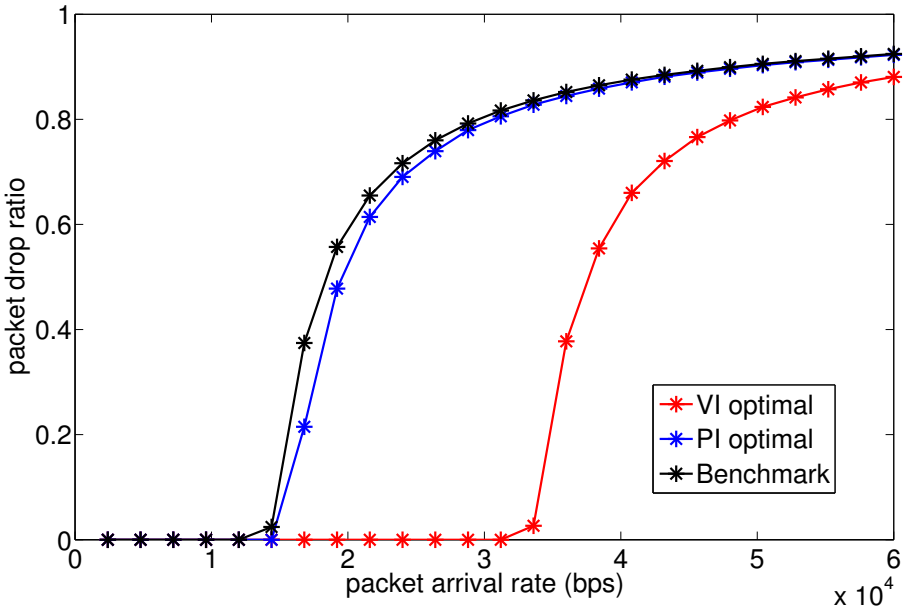

Figure 6.3: Packet drop ratio of PI based cluster head control.

Fig. 6.3 shows the packet drop ratio of the cluster head. No packet drop is observed when packet arrival rate is less than 15 kbps for both PI based optimal control and the benchmark control. The packets begin to be dropped when the packet arrival rate is larger than 35 kbps for the VI based optimal control. The packet drop ratio of PI optimal control is slightly less than that of the benchmark control.

The packet drop in this simulation happened only when the queue length reached the limited buffer size, and no transmission drop is considered. Thus, the packet drop ratios are always less than 1 for all simulated controls.

Fig. 6.4 shows the average cluster throughput. The throughput of PI based cluster head control is higher than that of the benchmark control, but lower than

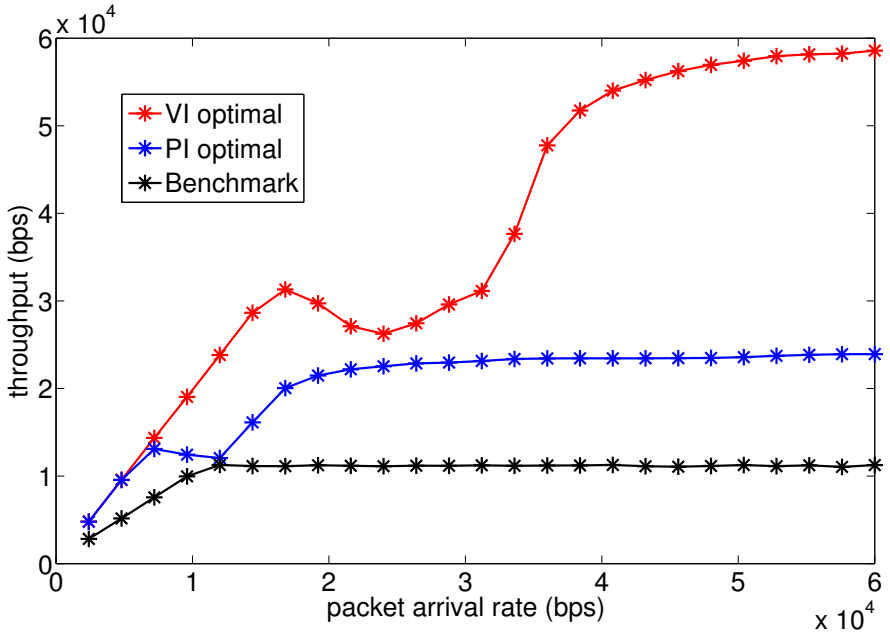

Figure 6.4: Throughput of PI based cluster head control.

that of the VI optimal cluster head control as expected. The concave change of the throughput curve of PI based cluster head control between 10-20 kbps and VI optimal cluster head control between 20 - 40 kbps is due to the radical change of SO. The throughput curves become flat when the network reached its saturation stable state.

Fig. 6.5 shows the cluster utilities of the compared controls. It can be seen that the utility value of the PI based cluster head control is higher than that of the benchmark control under all simulated packet arrival rates. Compare to that of the VI optimal control, the computational complexity reduction of PI based cluster head control is at the cost of the degradation of utility.

The utility value curves of all three compared controls have the concave shape. This also illustrated that the designed cluster utility function is a concave function. For a given cluster head service rate, there is a most suitable traffic load for the

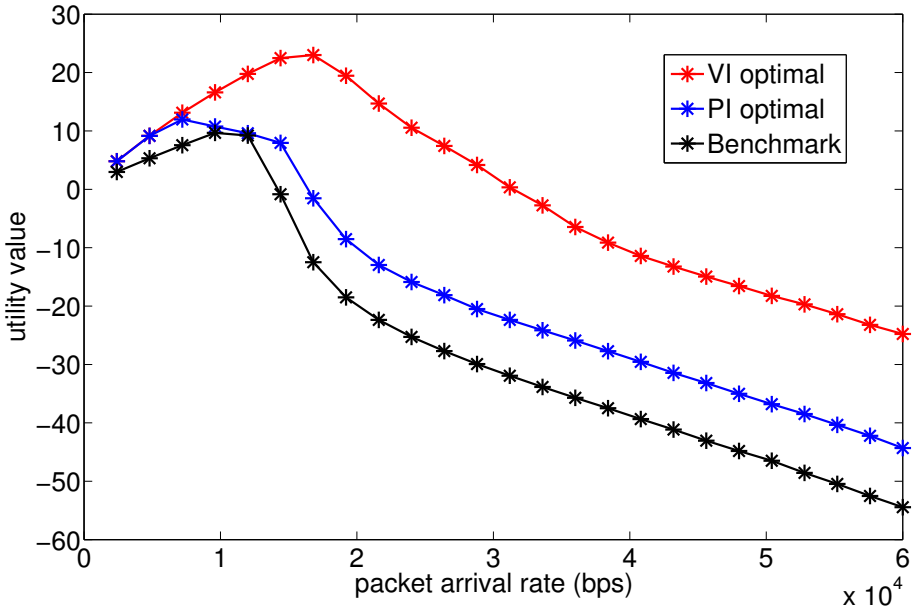

Figure 6.5: Cluster utility of PI based cluster head control.

cluster, at which the cluster head will gain the highest utility.

6.5.2 Performance of RA based Cluster Head Control

6.5.2.1 Simulation Setup

As shown in Table 6-B, the energy consumption parameters for M2M gateways, cluster heads and devices are based on Cisco 819 [Cis], XBee and XBee-Pro RF module data sheet [Int], respectively.

The performance of the proposed RA based cluster head control is compared with that of a benchmark control, the PI optimal control, and the heuristic base control of the RA based cluster head control.

Benchmark control: the benchmark control aims at maximising the number of received packets r_i^t to reduce the end-to-end delay. The maximum SO is bounded

Table 6-B: Energy Consumption and Buffer Parameters

Device	**Parameter**	**Value**
M2M Devices	Memory	32 Kb
	Device sensitivity	- 90 dBm
	Transmit power	108.9 mw
	Receiving power	92.4 mw
	Idle listen power	92.4 mw
	Sleep power	0.033 mw
Cluster Heads	Memory	32 Kb
	Device sensitivity	- 102 dBm
	Transmit power	396 mw
	Receiving power	102.3 mw
	Idle listen power	102.3 mw
	Sleep power	0.033 mw
M2M Gateway	Memory	1 GB
	Power	25 w

by the service rate f_i^t of the cluster head.

PI Optimal control: based on *Theorem 5.1* the optimal r_i^{t*} follows threshold structure. The optimal cluster head control in this section is computed by PI based control algorithm.

Base control: the heuristic base control has a fixed threshold equals to f_i^t. Thus, $r_i^t = f_i^t - q_i^t$. The maximum SO is bounded by the service rate f_i^t of the cluster head.

RA based control: Rollout based control will do one search at each time period to find the maximum utility at each time period, while the future utility is estimated by applying the heuristic based control. The maximum SO is bounded the search range $\bar{\mathcal{S}}$ at each time period.

6.5.2.2 Simulation Results

In this part, the performance of the proposed RA based cluster head control is presented for cluster heads with both limited buffer capacity and sufficient buffer capacity.

Fig. 6.6 shows energy efficiency performance of the compared cluster head controls. Fig. 6.6 a) is the performance of cluster head with limited buffer capacity and Fig. 6.6 b) is the performance of cluster head with sufficient buffer capacity. In both Fig. 6.6 a) and Fig. 6.6 b), the energy efficiency curves of RA base control and DP optimal control have the wave shape before the packet arrival rate is lower than 30kbps.

As has been pointed out earlier, the SO is integer and the duty cycle is defined as $2^{(SO-BO)}$, thus the change of duty cycle is radical. For a given duty cycle, the energy efficiency curve has a convex shape with the increase of the number of transmitted packets. This convex shape illustrated the trade-off between the idle listening and transmitting energy consumption. The decrease of the energy efficiency is due to the long idle listening energy consumption and the lack of sufficient packets to transmit.

Compared with the Fig. 6.6 a) and Fig. 6.6 b), the energy efficiency of DP optimal control, RA based cluster head control and the benchmark control performed similarly for cluster heads with limited buffer capacity and sufficient buffer capacity. However, the performance of benchmark control various a lot. This shows the cluster head buffer size has a direct impact on the performance of the benchmark control, thus a co-relation between the fixed threshold selection and the buffer capacity may exist.

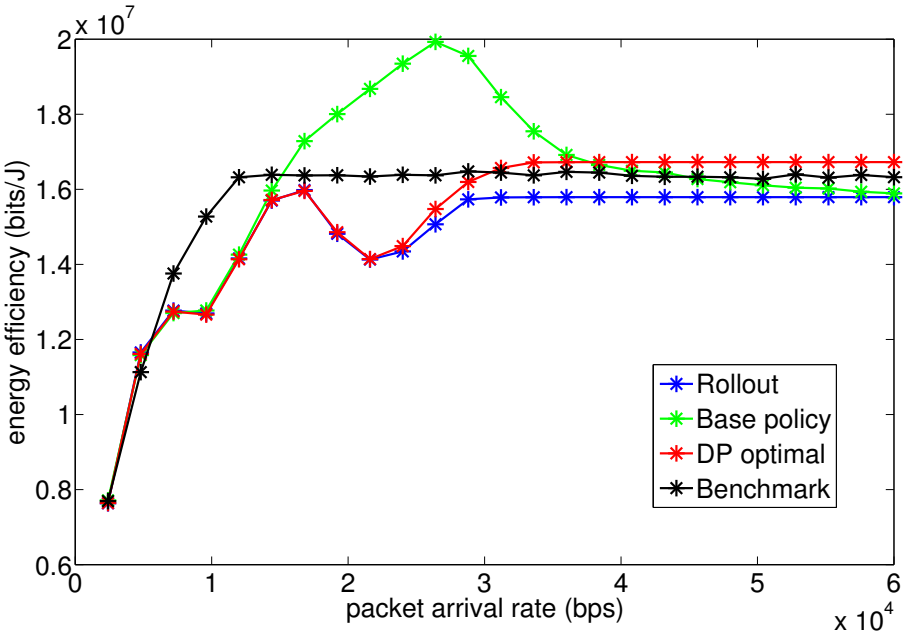

a) limited buffer capacity

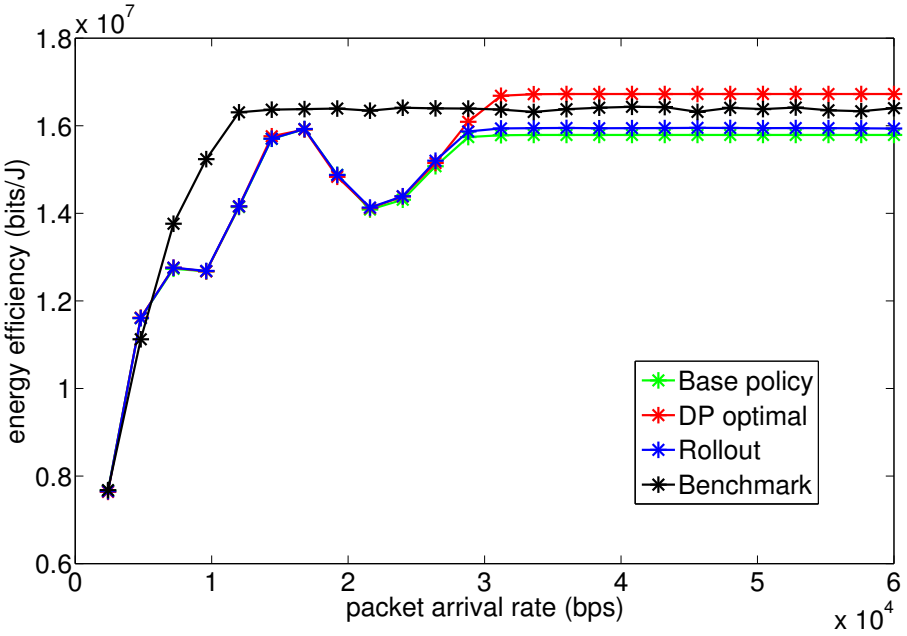

b) sufficient buffer capacity

Figure 6.6: Energy efficiency of RA based cluster head control.

Fig. 6.7 shows the end-to-end delay performance of the compared cluster head controls. For cluster heads with both limited and sufficient buffer capacity, the end-to-end delay increases with the increase of the packet arrival rates for all

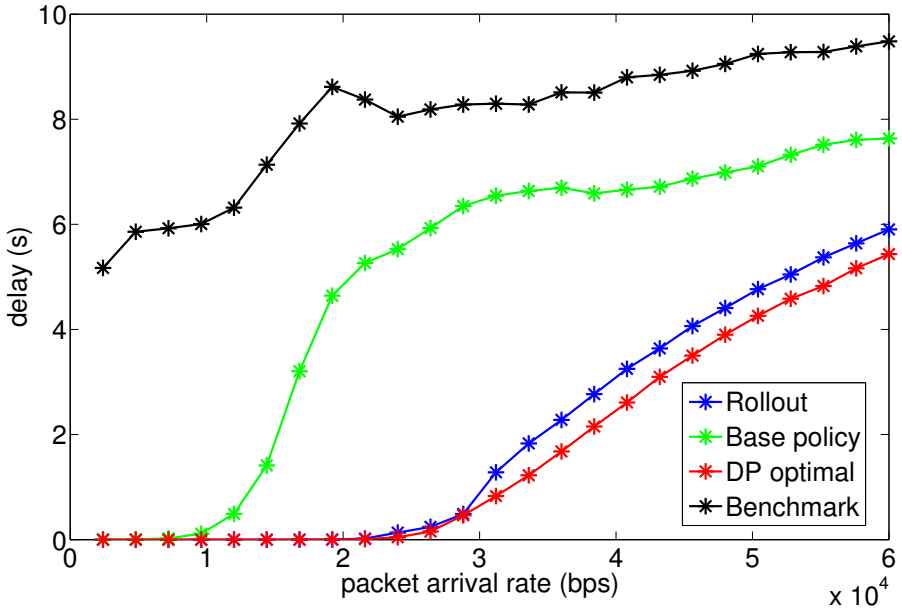

a) limited buffer

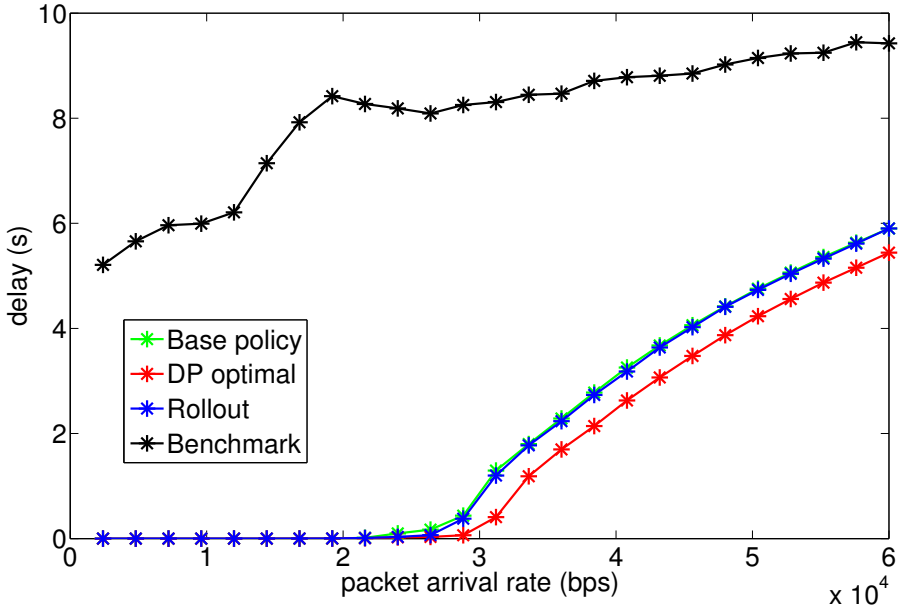

b) sufficient buffer capacity

Figure 6.7: End-to-end delay of RA based cluster head control.

compared controls. The end-to-end delay of RA based control is close to that of the DP optimal control, and on average is 4 times less than that of the benchmark control.

It can be obtained from Fig. 6.7 a) and Fig. 6.7 b) that the buffer capacity of the cluster head has a direct impact on end-to-end delay performance of the fixed threshold base policy.

Fig. 6.8 shows the cluster throughput performance. The cluster throughput increase with the increase of the packet arrival rates for all compared controls. The cluster throughputs became stable when the cluster heads reached their maximum packet transmission capabilities. The throughput of RA based cluster head control is closed to that of the DP optimal control. At the stable state, RA based cluster head control achieved 5.5 times throughput increase compared to that of the benchmark control for both cases where cluster head has limited and sufficient buffer capacity.

Comparing Fig. 6.8 a) and Fig. 6.8 b), the performance of the base policy various for cluster heads with limited buffer capacity and sufficient buffer capacity, while the other three controls performed similarly. This also shown that the DP optimal control and RA based control are able to adjust the control for devices with different capacities.

Fig. 6.9 shows the packet drop ratio performance of the compared controls. The packet drop ratio of RA based cluster head control is close to that of the DP optimal control and slightly lower than that of the base policy under all simulated packet arrival rates. For RA based cluster head control the packets begin to be dropped when the packet arrival rate is around 30 kbps, while that of the benchmark control is around 15 kbps.

Comparing Fig. 6.9 a) and Fig. 6.9 b), the packet drop ratio of the base policy shown tighter co-relation with the cluster head buffer capacity. The packet drop ratio of DP optimal control in Fig. 6.9 b) begin to increase when the packet arrival

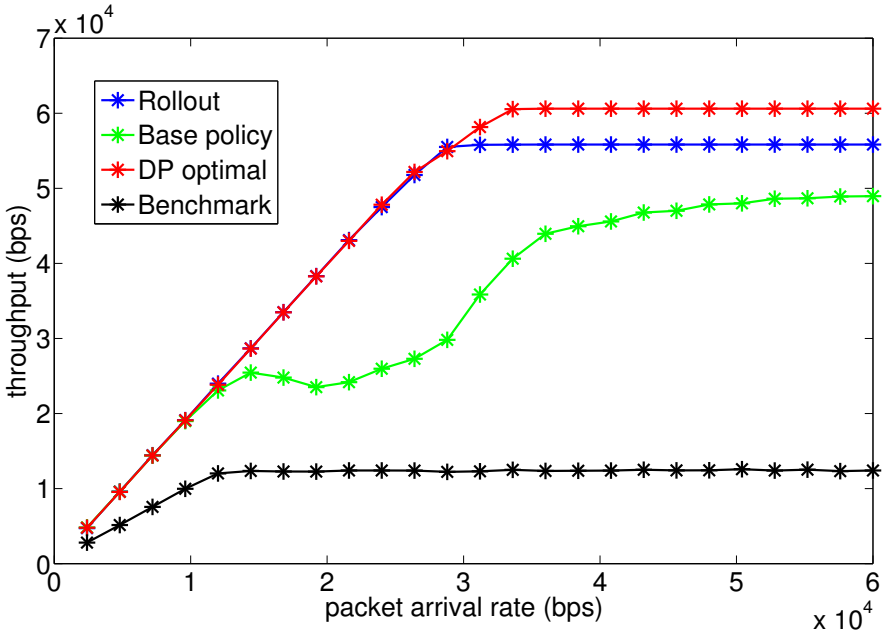

a) limited buffer capacity

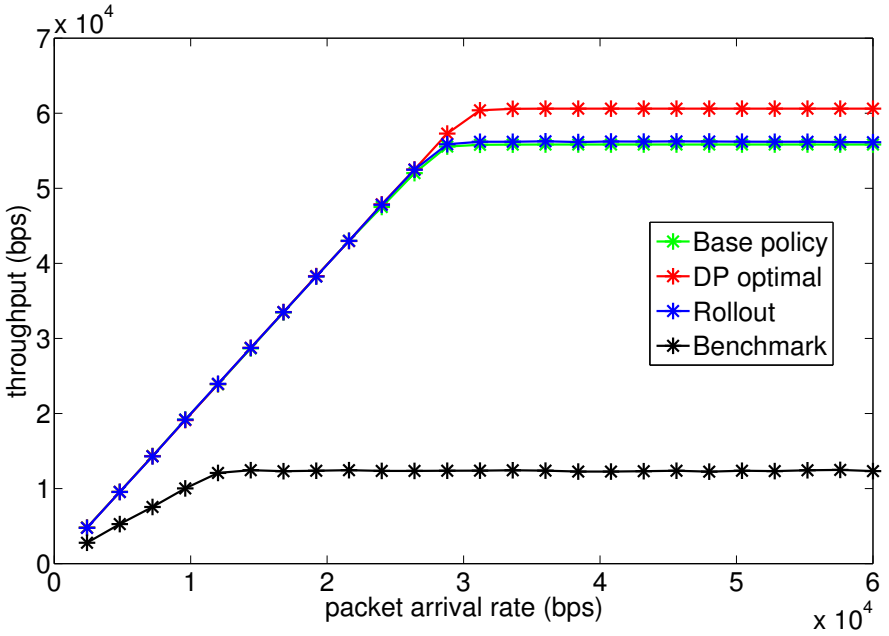

b) sufficient buffer capacity

Figure 6.8: Throughput of RA based cluster head control.

rate is larger than 30 kbps while that in Fig. 6.9 a) is around 27 kbps.

The packet drop ratio performance of RA based cluster head is similar for

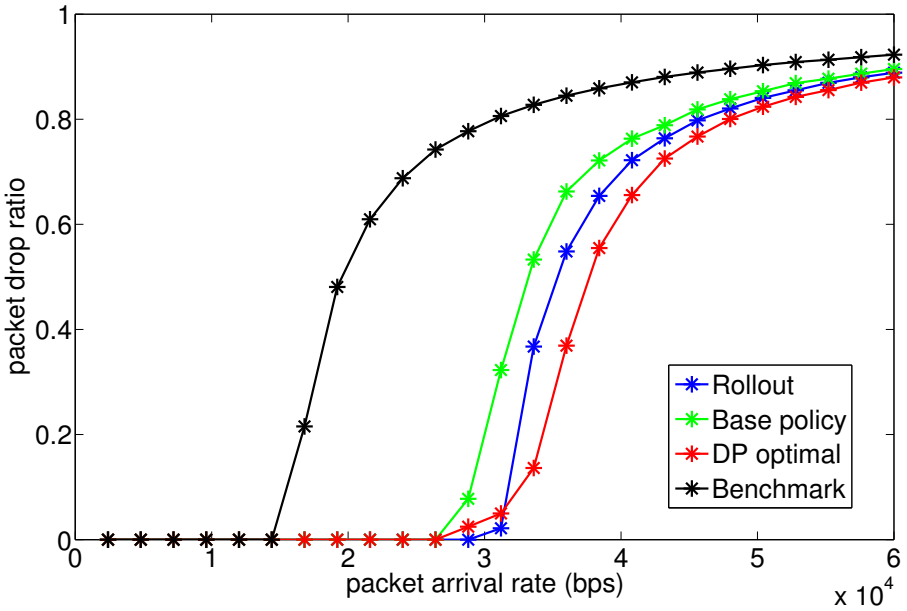

a) limited buffer

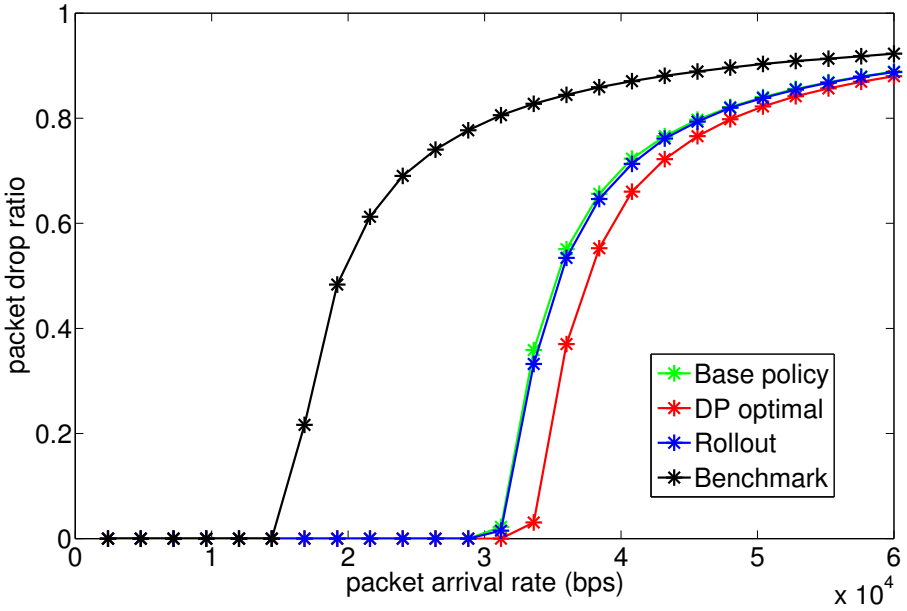

b) sufficient buffer capacity

Figure 6.9: Packet drop ratio of RA based cluster head control.

cluster head with limited and sufficient buffer capacity. This indicates that the packet drop in the simulation mainly happened at the M2M devices rather than at the cluster head.

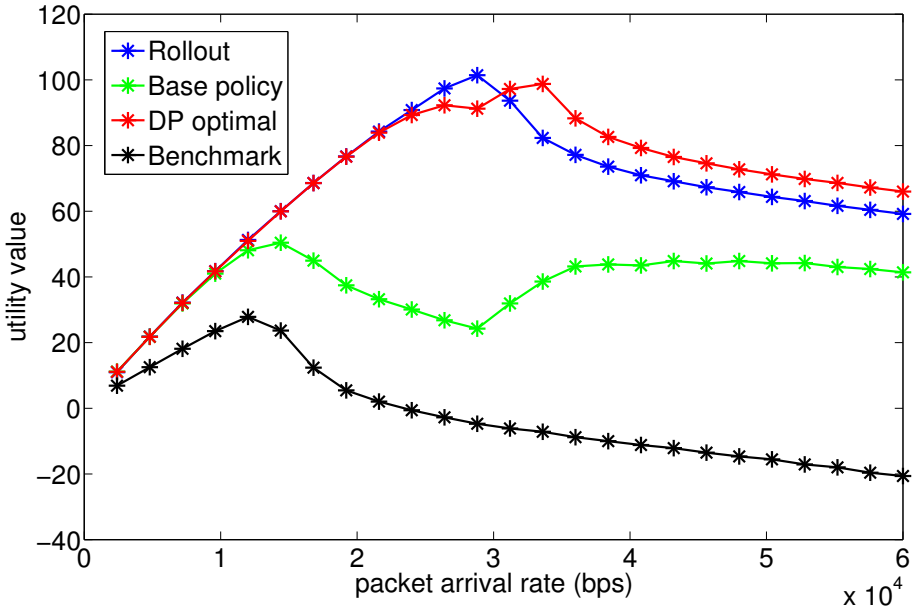

a) limited buffer capacity

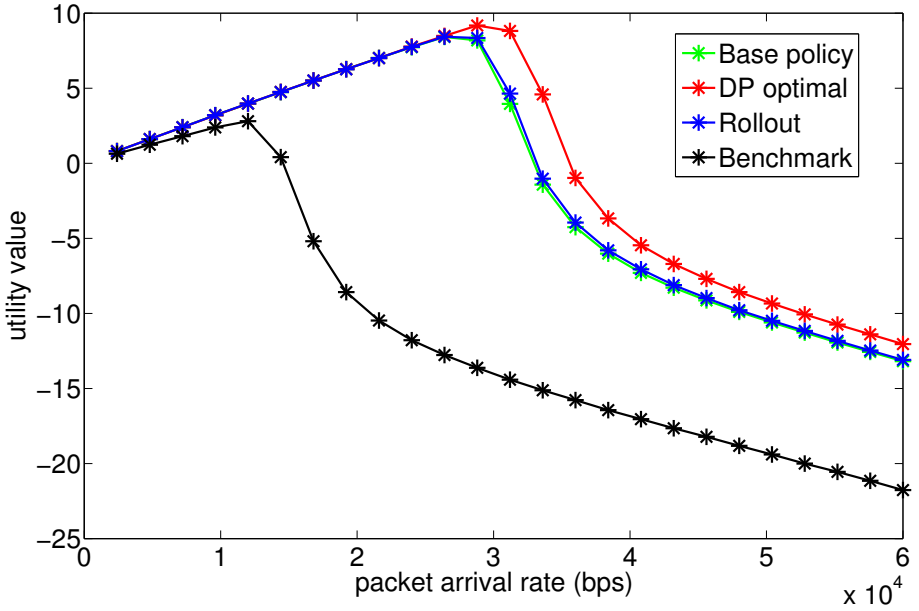

b) sufficient buffer capacity

Figure 6.10: Cluster utility of RA based cluster head control.

Fig. 6.10 shows the cluster utility performance of the compared controls. The RA based cluster head achieved close performance compared to that of the DP optimal control for both cases where cluster heads have limited and sufficient buffer

capacities. For RA based cluster head control and DP optimal control, the peak utility values are about 5 times higher than that of the benchmark control.

From the peak points of the utility curves, it can be seen that compared to the benchmark control, the proposed RA based cluster head control and DP optimal control are able to deal with heavy traffic conditions while achieving higher utility value. In addition, the performance of the base policy is highly related with the buffer capacity of the cluster heads.

6.5.3 Performance of RL based Cluster Head Control

6.5.3.1 Simulation Setup

The performance of the proposed Q-learning based control is compared with a benchmark control, DP optimal and RA based cluster head control.

The DP optimal control: processes DP exhausted search for entire observed time periods to find the optimal control.

Benchmark control: aims at minimising the end-to-end delay by maximising the number of transmitted packets r_i^t at each time period. A fixed $SO = 3$ is set, which is sufficient large to transmit all generated packets.

Optimal control: based on the **Theorem 5.1** the optimal r_i^{t*} follows threshold structure. The optimal duty cycle control in this section is computed by PI based control algorithm.

RA based control: RA based control is the rollout algorithm based control which searches the maximised utility of current time period and estimates future utility based on a heuristic control. The maximum SO is bounded the search range $\bar{\mathcal{S}}$ at

each time period.

For generosity, the action-utility Q-factor is initialised to zero. The initial bid price of each cluster head is an unit price proportional to the amount of its child devices. The choice of the learning parameters: greedy parameter ϵ, learning rate δ, discount factor γ are presented as following.

The δ is the learning rate of the action-utility Q-factor. The small δ value increases the time of the learning process. The large value introduces the oscillations of the Q elements. In this simulation, δ is chosen from the set 0.1, 0.01, 0.001. For all three parameter values, similar results are obtained. Specifically, $\delta = 0.01$ is chosen in the simulation.

The discount factor γ determines the relative importance of the short-term utility and long-term utility. For learning with focus on maximising long-term utility, this parameter is set arbitrarily near 1. In this simulation, $\gamma = 0.95$.

In ϵ-greedy method the parameter ϵ determines the probability of random action selection and must be taken from the interval (0,1]. This parameter impacts the possibility of environment exploration, which means searching for a better solution by changing the currently used policy. If the value of ϵ tends to zero, then the probability of random action selection also tends to zero. In this simulation, the greedy parameter is set to be 0.5.

6.5.3.2 Simulation Results

Fig. 6.11 shows the energy efficiency of the compared controls. Q-learning based control has the highest energy efficiency compared to the other controls, especially after the packet arrival rate is higher than 30 kbps. The energy efficiency curves

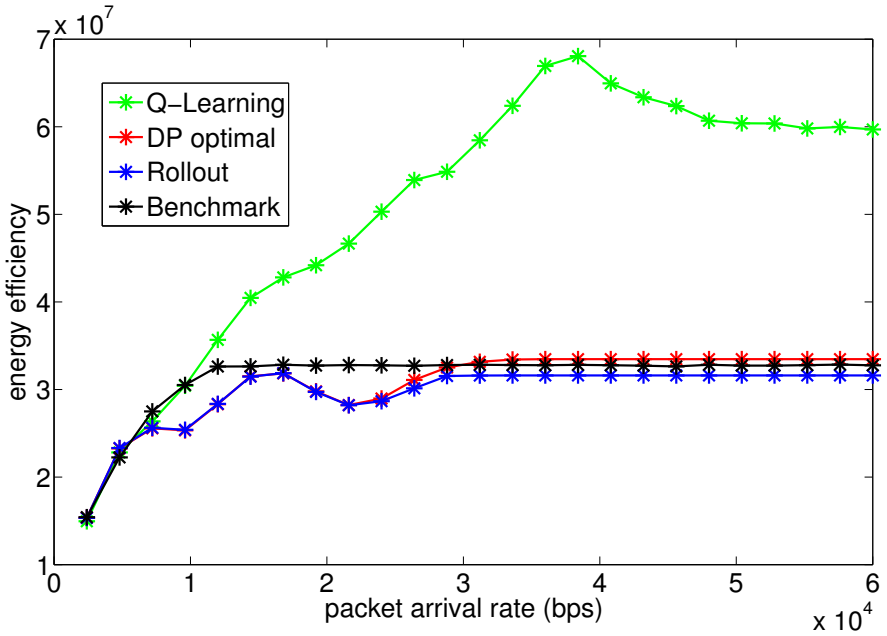

Figure 6.11: Energy efficiency of RL based cluster head control.

of the benchmark control, DP optimal control and rollout based control are flat after the packet arrival rate is higher than 30 kbps.

Since the change of duty cycle is radical, the idle listening energy consumption caused by the change of SO lead to the non monopoly change of the energy efficiency curves. The energy efficiency of Q-learning based control is doubled compared to that of the other compared controls at stable states.

Fig. 6.12 shows the delay performance of the compared controls. The proposed Q-learning based cluster head control has higher end-to-end delay compared to that of the DP optimal control and rollout based control, but lower than that of the benchmark control.

It is observed from Fig. 6.11 and Fig. 6.12 that the increase of energy efficiency is always came with the increase of end-to-end delay for all compared controls. This observation also illustrates the trade-off between energy efficiency and end-to-end

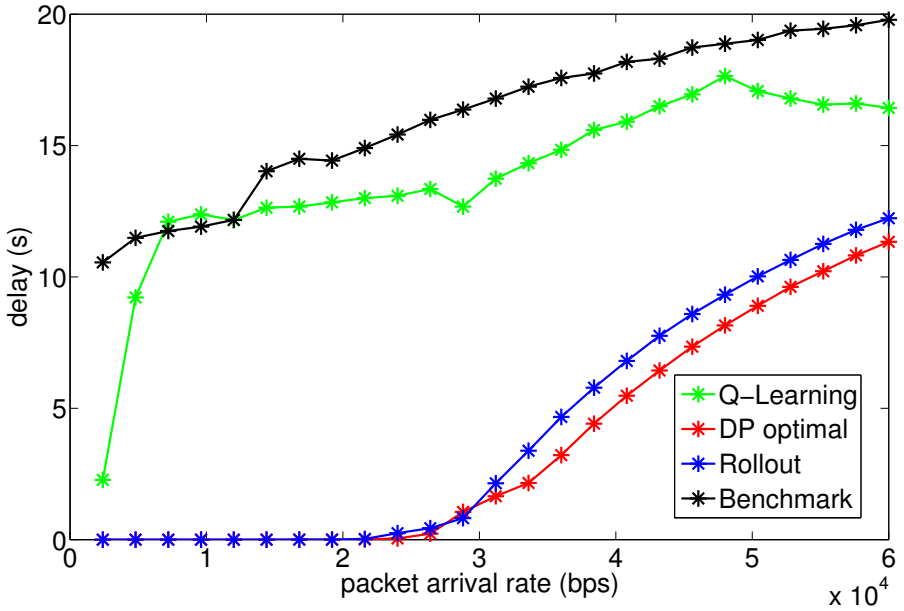

Figure 6.12: End-to-End delay of RL based cluster head control.

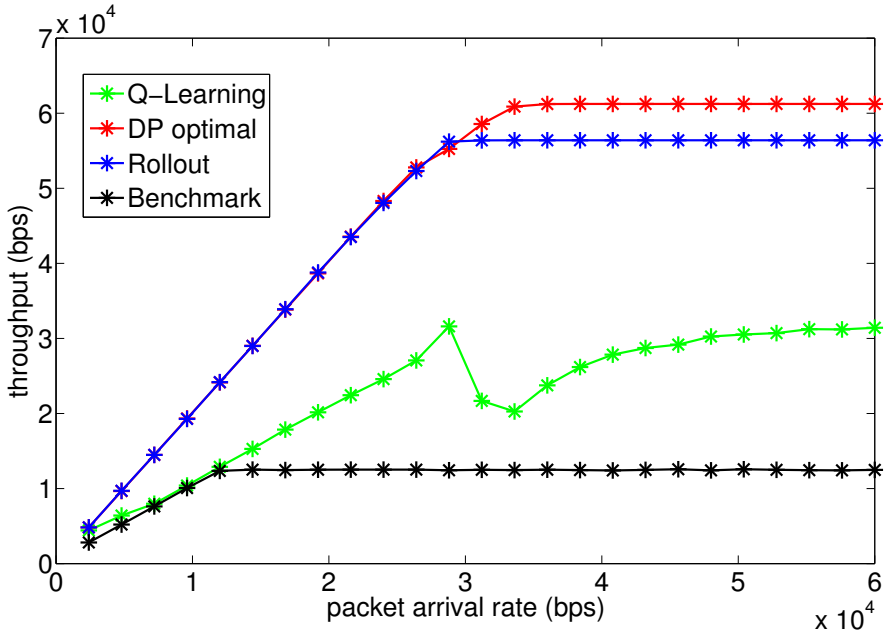

Figure 6.13: Throughput of RL based cluster head control.

delay.

Fig. 6.13 shows the cluster throughput of the compared controls. The through-

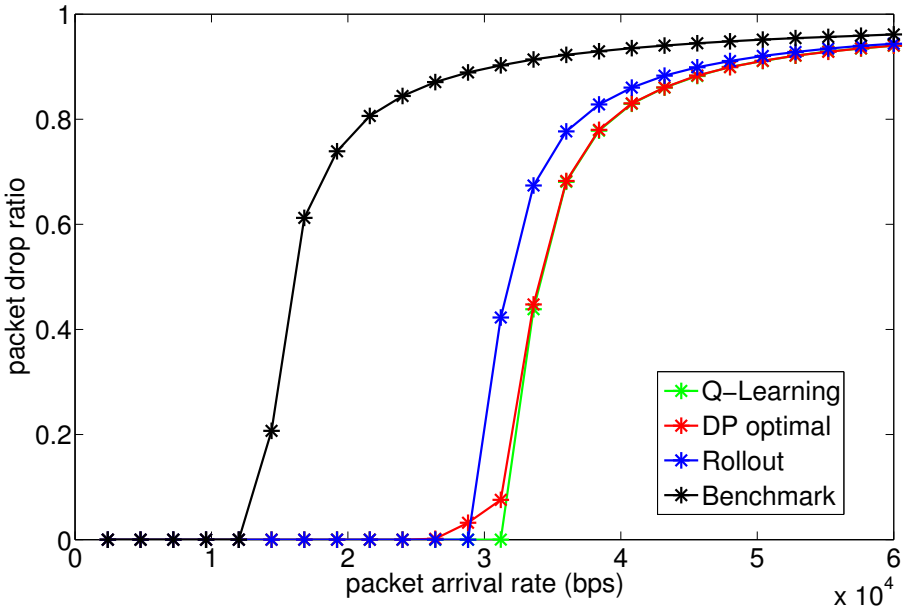

Figure 6.14: Packet drop radio of RL based cluster head control.

put of Q-learning based control is lower than that of the DP optimal control and rollout based control, but higher than that of the benchmark control. The lower throughput of Q-learning based control is due to its needs to gradually approach to the optimal solution over time.

The performance of the overall two-hop packet drop ratio is shown in Fig. 6.14. Although the packet drop is not considered in the utility function, Q-learning based control is able to reduce the packet drop ratio. The Q-learning based control has lower packet drop ratio compared to that of the DP optimal. In addition, the packet drop ratio of Q-learning based control only started to increase when the packet arrival rate is higher than 30 kbps, while that of the optimal control started around 25 kbps.

Fig. 6.15 shows the utility of the compared controls. The utility curve of the Q-learning based control is lower than that of the DP optimal control and rollout

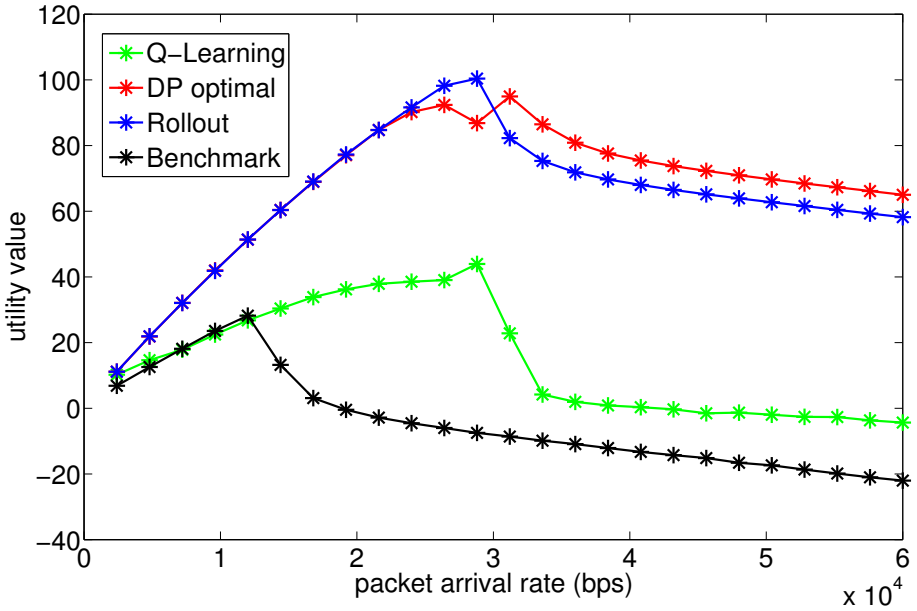

Figure 6.15: Cluster utility of RL based cluster head control.

based control, but higher than that of the benchmark control. This is because the learning process of Q-learning based control needs to gradually approach the optimal solution over time.

The utility curves have concave shape, where the peaks of the curves show the maximum utilities the cluster head can achieve under the simulated scenarios. From the peaks of the utility curves, it can be seen that the Q-learning based control is capable of dealing with the heavy traffic situations.

The proposed Q-leaning based duty cycle control achieved higher energy efficiency, similar end-to-end delay and packet drop ratio compare to the benchmark control. When compared with the DP optimal and RA based control, the proposed Q-leaning based control striked a balance between optimality and algorithm stability.

6.6 Summary

This chapter focuses on the cluster utility maximisation problem for IEEE 802.15.4 based hierarchical M2M networks. The cluster utility function is designed with both empirical component and economic component. The PI based optimal cluster head control is proposed to reduce the computational complexity of the DP optimal control. Then, a suboptimal RA based cluster head control is proposed to further reduce the computational complexity of the PI based cluster head control. In the end, a Q-learning based cluster head control is developed for the situation where priori network information is not available.

Simulation results shown that the proposed PI based cluster head control has close performance to the optimal control while achieving exponential complexity reduction. The RA based cluster head control reached a balanced trade-off between the computational complexity and optimality. Compared to the optimal and the other cluster head controls, the Q-learning based cluster head control achieved the best balance between optimality and stability.

Chapter 7

Gateway Control with Network Utility Optimisation

This chapter focuses on the gateway control of the proposed control framework. The proposed gateway controls aim to solve the formulated optimisation problem $\mathcal{P}4$ in Chapter 4.

As has been discussed in Section 3.3, the applications running in the hierarchical M2M networks are classified into four classes. In this chapter, the utility functions are formulated for the four classes applications. The gateway control with network utility optimisation is proposed. To allocate resources to clusters while addressing their different application requirements, the gateway control is solved with the aim of maximising the network utility. Novel distributed gateway control algorithms for multi-application hierarchical M2M networks are proposed.

7.1 Gateway Utility Function Design

Given the nature of the devices and topoligy, the hierarchical M2M networks may have different types of applications [ZHW+12, JSKP10]. Based on the modelled hierarchical M2M system in Chapter 3, the application runs within each cluster may

be different. As has pointed out by [ZHW+12], the applications that run in the hierarchical M2M networks are classified into four classes: traditional elastic application, hard-real time application, delay adaptive application and rate adaptive applications.

According to the designed control framework in Chapter 4, the M2M gateway control aims at maximising the long-term network utility while satisfying different application requirements. The first task for gateway control optimisation is to design the utility functions for different applications.

The traditional logarithmic utility functions can only capture the QoS requirement for elastic applications, where a non-zero utility is presented as long as it has a non-zero resource block allocated to it. However, it is not suitable to use logarithmic utility functions for real-time traffics, such as audio and video surveillance, real-time traffic monitoring and real-time seismic activity monitoring. These real-time traffics are generally generated by inelastic applications. The key feature of inelastic applications is that they will keep present nearly zero-utility unless a minimum amount of resource blocks have been allocated.

According to [She95, JSKP10], for the inelastic applications (hard-real time applications, delay adaptive applications and rate adaptive applications), the utility function $U_n(f_i^t, \theta_i^t)$ can be presented by a sigmoid function, while for the elastic applications the utility function $U_n(f_i^t, \theta_i^t)$ can be presented by a logarithmic function. Specifically, the application indictor θ_i^t specifies the application type of cluster head. If the application of cluster head i falls into the elastic applications, then the utility function of cluster head i is given as,

$$U_n(f_i^t) = \log(1 + f_i^t), \tag{7.1}$$

where f_i^t is offset by $+1$ to ensure the positiveness of the utility.

If the application of cluster head i falls into the inelastic applications, the utility function of cluster head i is given as,

$$U_n(f_i^t) = \begin{cases} 0 & \text{if} \quad f_i^t < 0 \\ \frac{1}{1+e^{-a(f_i^t - b)}} & \text{if} \quad 0 \leq f_i^t \leq C_{i,n} \\ 1 & \text{if} \quad f_i^t > C_{i,n} \end{cases}, \tag{7.2}$$

where the utility parameter set (a, b) controls the slope of the sigmoid. Fig. 7.1 shows an example of the modelled utility functions for the four application classes.

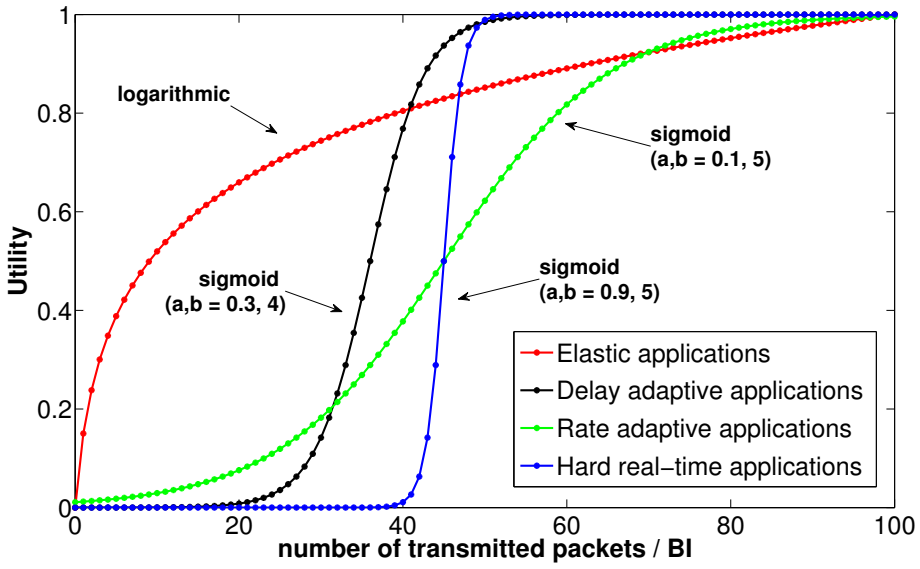

Figure 7.1: Utility function for different application classes.

Recall the gateway control optimisation problem $\mathcal{P}4$ which has been defined in Chapter 4. The gateway control optimisation is formulated by applying the "pseudo utility" optimisation problem to accommodate the mixed applications

running within the network, which is expressed as,

$$\mathcal{P}4 : \max \sum_{t=0}^{T} \sum_{l \in \mathcal{I}_n} \mathcal{U}_n(f_i^t, p_i^t, \theta_i^t) \tag{7.3a}$$

$$s.t. \qquad \sum_{i \in \mathcal{I}_n} f_i^t \leq C_{n,b}^t, \tag{7.3b}$$

$$0 \leq f_i^t \leq C_{i,n}^t. \tag{7.3c}$$

where p_i^t is the bid price provided by the cluster head i. θ_i^t is the application indicator which indicates the utility function of the cluster head i is in logarithmic form as defined in (7.1) or in sigmoid form as defined in (7.2).

As discussed previously in Chapter 4, the classic NUM framework provides not only an efficient congestion control mechanism for the network, but also gives an easy way to provide a fair resource allocation among competing clusters. In addition, the utility-fair control is proposed for CSMA based wireless networks in [JSKP10] with a queue back-pressure-based algorithm.

The objective of the gateway control optimisation problem $\mathcal{P}4$ is to optimise its overall network utility subject to different link capacity constraints, while satisfying different application requirements among clusters.

7.2 Lagrangian based Gateway Control

According to [JSKP10], by applying the Lagrangian approach, the control result of $\mathcal{P}4$ is utility proportional fair. By associating dual variables $\omega_i^t \geq 0$ to the second

constraint, a partial Lagrangian of $\mathcal{P}4$ is

$$\begin{aligned}
&\mathcal{L}(f_i^t, p_i^t, \theta_i^t; \omega_i^t) \qquad (7.4)\\
&= \sum_{i\in\mathcal{I}_n} \mathcal{U}_n(f_i^t, p_i^t, \theta_i^t) + \sum_{k=1}^{t} \omega_i^t \Big(\sum_{i\in\mathcal{I}_n} f_i^t - \sum_{i\in\mathcal{I}_n} q_i^t - \sum_{i\in\mathcal{I}_n} r_i^t \Big)\\
&= \sum_{i\in\mathcal{I}_n} \mathcal{U}_n(f_i^t, p_i^t, \theta_i^t) - \sum_{i\in\mathcal{I}_n} \omega_i^t (q_i^t + r_i^t) + \sum_{i\in\mathcal{I}_n} \sum_{k=1}^{t} \omega_i^t f_i^t.
\end{aligned}$$

Since the vectors q_i^t and r_i^t are provided with fixed values at time period t, f_i^t is solved in the below sub-problem,

$$\max_{p_l^t} \sum_{i\in\mathcal{I}_n} \sum_{k=1}^{t} \omega_i^t f_i^t \qquad (7.5a)$$

$$s.t. \quad \sum_{i\in\mathcal{I}_n} f_i^t \le C_{n,b} \qquad (7.5b)$$

$$f_i^t \le q_i^t + r_i^t. \qquad (7.5c)$$

The solution of the above problem is quite straightforward: at each time period t which has 16 slots, the gateway schedules the transmission to the cluster head with maximum service index $\omega_i^t = p_i^t \cdot q_i^t / q_i^{max}$.

Substitute the solution of (7.5) into (7.4), we have

$$\mathcal{L}(f_i^t, p_i^t, \theta_i^t; \omega_i^t) = \sum_{i\in\mathcal{I}_n} p_i^t f_i^t + \sum_{i\in\mathcal{I}_n} \mathcal{U}_n(f_i^t, p_i^t, \theta_i^t) - \sum_{i\in\mathcal{I}_n} p_i^t q_i^t. \qquad (7.6)$$

Then, the distributed gateway control algorithm is given in Algorithm 5.

The number of packets each cluster head can transmit at time period t is de-

Algorithm 5 Proposed Network Utility Optimisation Gateway Control (P-UPF)

Require: cluster heads $i \in \mathcal{I}$, total control time periods T and current time period t

Initialise the number of forward packets $f_i^0 = 0$
for $t = 0 \rightarrow T$ **do**
  for each $i \in \mathcal{I}_n$ **do**
    Calculate the service index $\omega_i^t = \frac{q_i^t}{q_i^{max}} \cdot p_i^t$
    Update the utility $U_n(f_i^t, p_i^t, \theta_i^t)$ if slot k is allocated to i
    $U_n(f_i^t, p_i^t, \theta_i^t) \leftarrow U_n(f_i^t, p_i^t, \theta_i^t) + U_n(f_i^{t-1}, p_i^t, \theta_i^t)$
  end for
  Schedule the cluster head $i \in \mathcal{I}$ which has the maximum increase of utility.
  The optimal number of transmit packets of cluster head i is,
  $f_i^{t*} = \max U_n^t(\frac{1}{U_i(f_i^t, p_i^t, \theta_i^t)})$
  Allocate cluster i with f_i^t.
  Calculate the gateway utility at time period t
  $\mathcal{U}_n = \sum_{l \in \mathcal{I}_n} \mathcal{U}_n(f_i^t, p_i^t, \theta_i^t)$
end for

termined by

$$f_i^{t*} = \arg\max(\sum_{i \in \mathcal{I}_n} \mathcal{U}_n(f_i^t, p_i^t) - \sum_{i \in \mathcal{I}_n} p_i^t(q_i^t + r_i^t)) = U_n^{-1}(\frac{1}{p_i^t}), \tag{7.7}$$

where the bid price p_i^t is updated by

$$p_i^t \leftarrow \left[p_i^t - \alpha(\sum_{i \in \mathcal{I}_n} f_i^t - \sum_{i \in \mathcal{I}_n} q_i^t - \sum_{i \in \mathcal{I}_n} r_i^t) \right]^+. \tag{7.8}$$

7.3 Mixed Integer Programming based Gateway Control

According to the IEEE 802.15.4 standard, there are 16 slots in each CAP. It should be noted that standard Lagrangian-based duality technique cannot guarantee the maximum utilisation of all 16 slots, as the whole 16 slots can only be allocated to

one cluster for each time period t.

To increase the slot utilisation by allowing different clusters to transmit in the same time period but different slots, the optimisation problem $\mathcal{P}5$ is transfered into a mixed integer programming (MIP) problem. The MIP problem defines a slot allocation matrix [WOM09] which ensures the adjacency of allocated slots for each cluster head.

The size of the slots allocation matrix is $K \times A$, where each row correspond to the slot index and each column corresponds to a feasible (meeting adjacency restriction) slot allocation pattern, and A denotes the total number of feasible allocation patterns given by $A = 0.5 \times (K^2 + K)$. In each allocation pattern, 1 means the slot is allocated to a cluster, 0 means no cluster head is allocated to this slot. The idea of this slot allocation matrix is illustrated by (K=3):

$$\boldsymbol{M}^K = \begin{bmatrix} 1 & 0 & 0 & 1 & 0 & 1 \\ 0 & 1 & 0 & 1 & 1 & 1 \\ 0 & 0 & 1 & 0 & 1 & 1 \end{bmatrix}. \tag{7.9}$$

A slot indicator vector $\boldsymbol{x} \triangleq [\boldsymbol{x}_i]_{K\times 1}$, where $\boldsymbol{x}_i = [\boldsymbol{x}_{i,a}]_{A\times 1}$ is defined, such that each entry $\boldsymbol{x}_{i,a}$ indicates whether the slot allocation pattern a is allocated to the cluster head i or not. In this way, the gateway control problem $\mathcal{P}5$ is rewritten as

a MIP problem as follows,

$$\mathcal{P}5 : \max \sum_{i \in \mathcal{I}_n} \mathcal{U}_i \Big(f_i^t(x_i^a), p_i^t, \theta_i^t \Big) \tag{7.10a}$$

$$s.t. \qquad \sum_{i \in \mathcal{I}_n} f_i^t \leq C_{n,b} \tag{7.10b}$$

$$f_i^t \leq q_i^{t-1} + r_i^{t-1} \tag{7.10c}$$

$$\sum_{a=1}^{A} x_i^a = 1 \tag{7.10d}$$

$$\sum_{i \in \mathcal{I}_n} \sum_{a=1}^{A} x_i^a M_{k,a}^i = 1, \quad 0 < k \leq 16, \tag{7.10e}$$

where $f_i^t(x_i^a) = \min(\sum_{a=1}^{A} x_i^a R, q_i^{t-1} + r_i^{t-1})$, and R is the maximum number of packers each time slot $k \leq 16$ could support. The constraints 7.10b) and 7.10c) gives the search space of f_i^t. The constraint 7.10d) ensures that at most one allocation pattern is chosen for each user. The constraint 7.10e), where $M_{k,a}^i$

Algorithm 6 MIP based Gateway Control

Require: the set of cluster head $\mathcal{I}$, control time period T

Initialise $f_i^0 = 0$
for $t = 0 \rightarrow T$ **do**
  for each slot number $k \leq 16$ **do**
    for each $i \in \mathcal{I}_n$ **do**
      Calculate the service index $\omega_i^t = \frac{q_i^t}{q_i^{max}} \cdot p_i^t$
      Calculate $U_n(f_i^k, p_i^t, \theta_i^t)$ if slot k is allocated to i
      $U_n(f_i^t, p_i^t, \theta_i^t) \leftarrow U_n(f_i^t, p_i^t, \theta_i^t) + U_n(f_i^k, p_i^t, \theta_i^t))$
    end for
    Schedule packets transmission at time slot k:
    $f_i^{k*} = \max \Delta \mathcal{U}_n^t(\frac{1}{U_i(f_i^t, \theta_i^t)})$
    Allocate current slot k to cluster i,
    $f_i^t \leftarrow f_i^t + f_i^{k*}$
  end for
  Calculate the gateway utility at time period t
  $\mathcal{U}_n = \sum_{l \in \mathcal{I}_n} \mathcal{U}_n(f_i^t, p_i^t, \theta_i^t)$
end for

denotes the k^{th} row and a^{th} column of the matrix $\boldsymbol{M}^K$, ensures the exclusivity of allocated slots.

The optimisation problem $\mathcal{P}5$ is an MIP equivalent of the problem $\mathcal{P}4$. The MIP based gateway control algorithm is given in Algorithm 6.

7.4 Gateway Control Simulation Results

Table 7-A shows the MAC layer simulation parameters in the simulation. Energy consumption parameters for the M2M gateways, cluster heads and M2M devices are based on Cisco 819 [Cis], XBee and XBee-Pro RF Module data sheet [Int], as shown in Table 7-B, respectively.

Table 7-A: Gateway Control Simulation Parameters

Parameter	**Value**	**Parameter**	**Value**
data rate	250kbps	frequency	2.4 GHz
transmit power	36.5 mw	packet size	100 bytes
receive power	41.4 mw	CCA size	8 symbols
idle listen power	41.4 mw	ACK packet size	10 symbols
sleep power	0.042 mw	unit backoff period	20 symbols
learning rate	0.9	discount factor	0.5

To show the overall network performance of the proposed joint scheduling and duty cycle control framework, all the gateway control, cluster head control and the duty cycle control for IEEE 802.15.4 are implemented in the simulation.

With the purpose of demonstrating the proposed gateway control algorithms, the implemented cluster head control and the duty cycle control are chosen as Q-

Table 7-B: Gateway Control Energy and Buffer Parameters

Device Type	**Parameter**	**Value**
M2M Devices	Memory	32 Kb
	Device sensitivity	- 90 dBm
	Transmit power	108.9 mw
	Receiving power	92.4 mw
	Idle listen power	92.4 mw
	Sleep power	0.033 mw
Cluster Heads	Memory	32 Kb
	Device sensitivity	- 102 dBm
	Transmit power	396 mw
	Receiving power	102.3 mw
	Idle listen power	102.3 mw
	Sleep power	0.033 mw
M2M Gateway	Memory	1 GB
	Power	25 w

learning based cluster head control and duty cycle control with Go-back-N ARQ, respectively.

The gateway control simulation results are presented with two scenarios: i) the cluster heads run same class application, but different priorities. In our simulation, suppose that all applications are elastic applications; ii) the cluster heads run applications that fall into different classes. As an example, the simulation results of the M2M network with mixed elastic applications and the rate adaptive applications are presented. The simulation results of the other traffic combinations are omitted due to the space limitation.

The network setting for the simulation is given in Table. 7-C. The low traffic load means that the traffic range of the cluster is between 0 to 120kbps and the high traffic load means the traffic range of the cluster is between 0 to 180kbps.

Table 7-C: Gateway Control Network Setting

Cluster	**Traffic load**	**Scenario 1 Priority**	**Scenario 2 Application**
1	Low (0-120kbps)	High	Inelastic
2	Low (0-120kbps)	High	Inelastic
3	High (0-180kbps)	High	Inelastic
4	Low (0-120kbps)	Low	Elastic
5	Low (0-120kbps)	Low	Elastic

The performance of different gateway control algorithms are compared, legend as No PF control, UPF control, P-UPF control and MIP control. The details of the compared gateway control algorithms are,

-*No PF control*: no secluding algorithm is implemented for the gateway control. The number of forwarded packets to the gateway of cluster head i f_i^t is a random value.

-*UPF control*: the classic utility proportional fair scheduling algorithm is implemented on the gateway. No application differentiation has been taken into account for different clusters.

-*P-UPF control*: The proposed gateway control algorithm is based on the classic UPF control. The application differentiation is achieved by taking the QoS indicator θ_i^t of cluster head i into account. The P-UPF is shown in Algorithm 5.

-*MIP control*: MIP control is the proposed gateway control algorithm in Algo-

rithm 6. The main advantage of MIP control is reducing the transmission switch by ensuring the adjacency of allocated slots for each cluster head.

7.4.1 Same Class Applications with Different Priorities

The network setting of this scenario is shown in Table. 7-C as scenario 1, where all cluster heads run same class applications (elastic application) but with different priorities.

In this scenario, five clusters are randomly deployed. Among these 5 clusters, cluster 1, 2 and 3 run high QoS priority applications with a large θ_i, while 4 and 5 have low QoS priority applications with a small θ_i.

For the purpose of illustration, Fig 7.2 a) and Fig 7.2 b) show an snapshot of the averaged throughput and the throughput cumulative density function (CDF) of each cluster head. It shows that the proposed P-UPF and MIP based gateway controls is able to provide priority differentiation. For both P-UPF and MIP based gateway controls, the throughput of the high priority clusters (cluster 1, 2 and 3) are higher than that of the low priority clusters (cluster 4 and 5), while the classic UPF and random gateway controls share similar throughputs among 5 clusters. In addition, for the clusters with same priority, the throughput of cluster with heavy traffic load (cluster 3) is higher than that of cluster with light traffic load (cluster 1 and 2). The smooth trend of the CDF function also shown that the simulation iteration is large enough to get the representative averaged results.

Fig. 7.3 a) shows the normalised network total throughput. For all simulated gateway controls, the throughput increased with the increase of packet arrival rate, then the network got saturated when the normalised throughput reached around

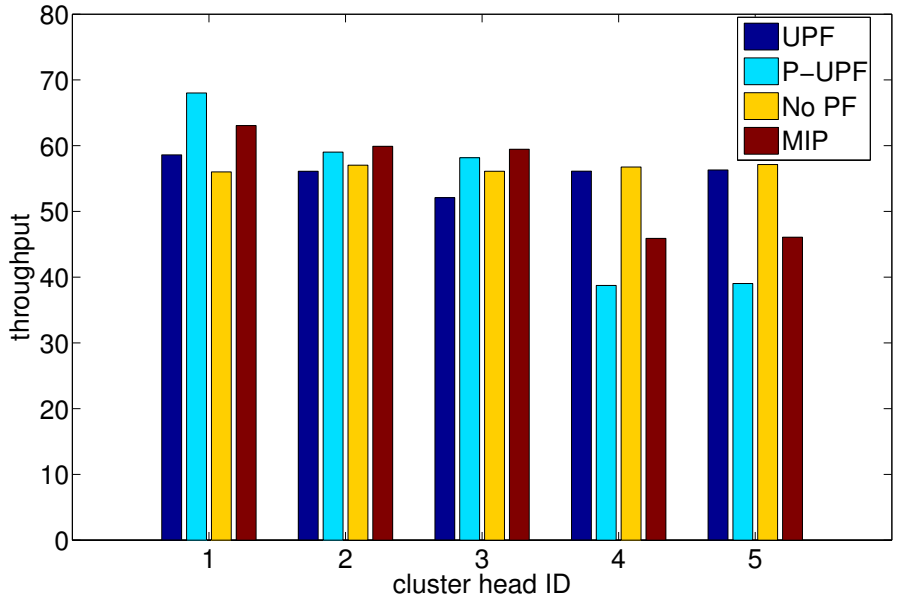

a) averaged throughput

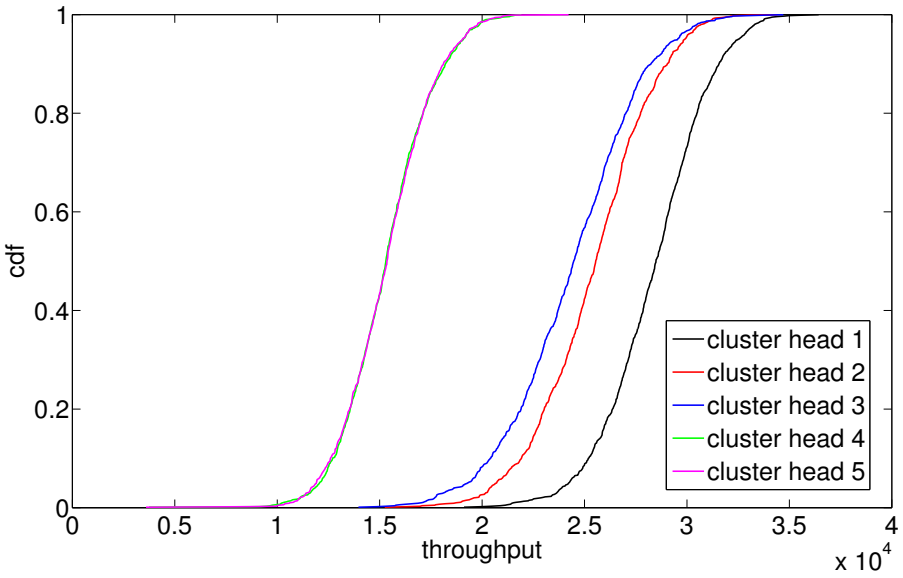

b) throughput cdf

Figure 7.2: Throughput of clusters run different priority applications.

90%. The saturated normalised throughput is less than 1 due to the contention of CSMA/CA. For UPF and MIP based gateway controls, the network became saturated when the network packet arrival rate is around 300kbps, and for P-

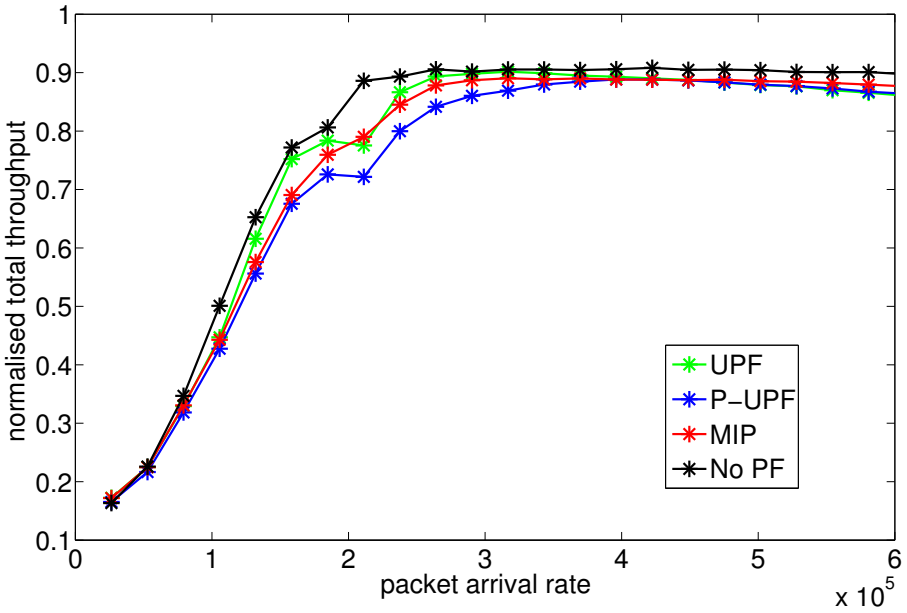

a) Total throughput

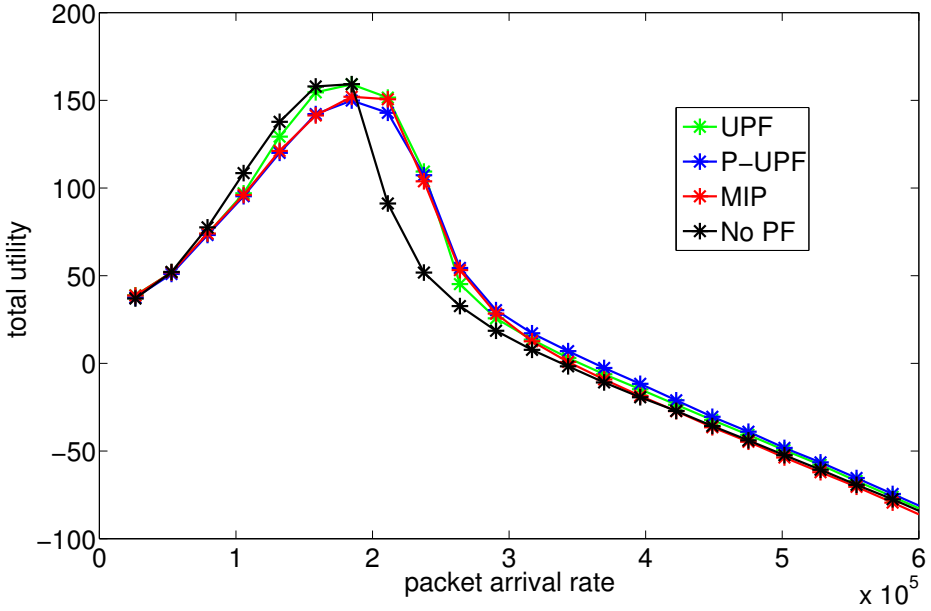

b) Total utility

Figure 7.3: Network performance with different priorities.

UPF it is around 350kbps. Compared to that of the random gateway control, the network got saturated much earlier, which is around 200 kbps.

Fig. 7.3 b) shows that the network total utility. It can be seen that the utility of the random gateway control decreased dramatically after the packet arrival rate is 200kbps. The network utility of UPF, P-UPF and MIP based controls are very tight. The utility of the proposed P-UPF and MIP based controls are slightly lower than that of UPF. This is due to the aim of UPF is to maximise the network throughput, while P-UPF and MIP based gateway controls have also taking the priority of cluster heads into consideration.

The following results presented in Fig 7.4 - Fig 7.5 are the performance of example cluster 1, cluster 3 and cluster 5. The performance are presented in terms of throughput, utility, energy efficiency, end-to-end delay, packet drop ratio and profit.

The throughput of each example cluster head (cluster 1, 3 and 5) in Fig. 7.4 a) Fig. 7.5 a) and Fig. 7.6 a) shown the proposed P-UPF and MIP based controls with higher priority cluster heads are higher than that of the UPF and random controls.

For the MIP based control, the throughput of the cluster with high priority and higher traffic load is similar to that of the cluster with high priority and lower traffic load, while that of P-UPF based control has decreased. On the other hand, with MIP based control, the throughput of the cluster with lower priority is lower than that of P-UPF after network saturation. This implies that, MIP improved the throughput for clusters with higher traffic load at the cost of degrading the performance of lower priority clusters compared to P-UPF.

The energy efficiency of each example cluster head (cluster 1,3 and 5) in Fig. 7.4 c), Fig. 7.5 c) and Fig. 7.6 c) shown that the energy efficiency of UPF, P-UPF and MIP based gateway controls are higher than that of the random control under

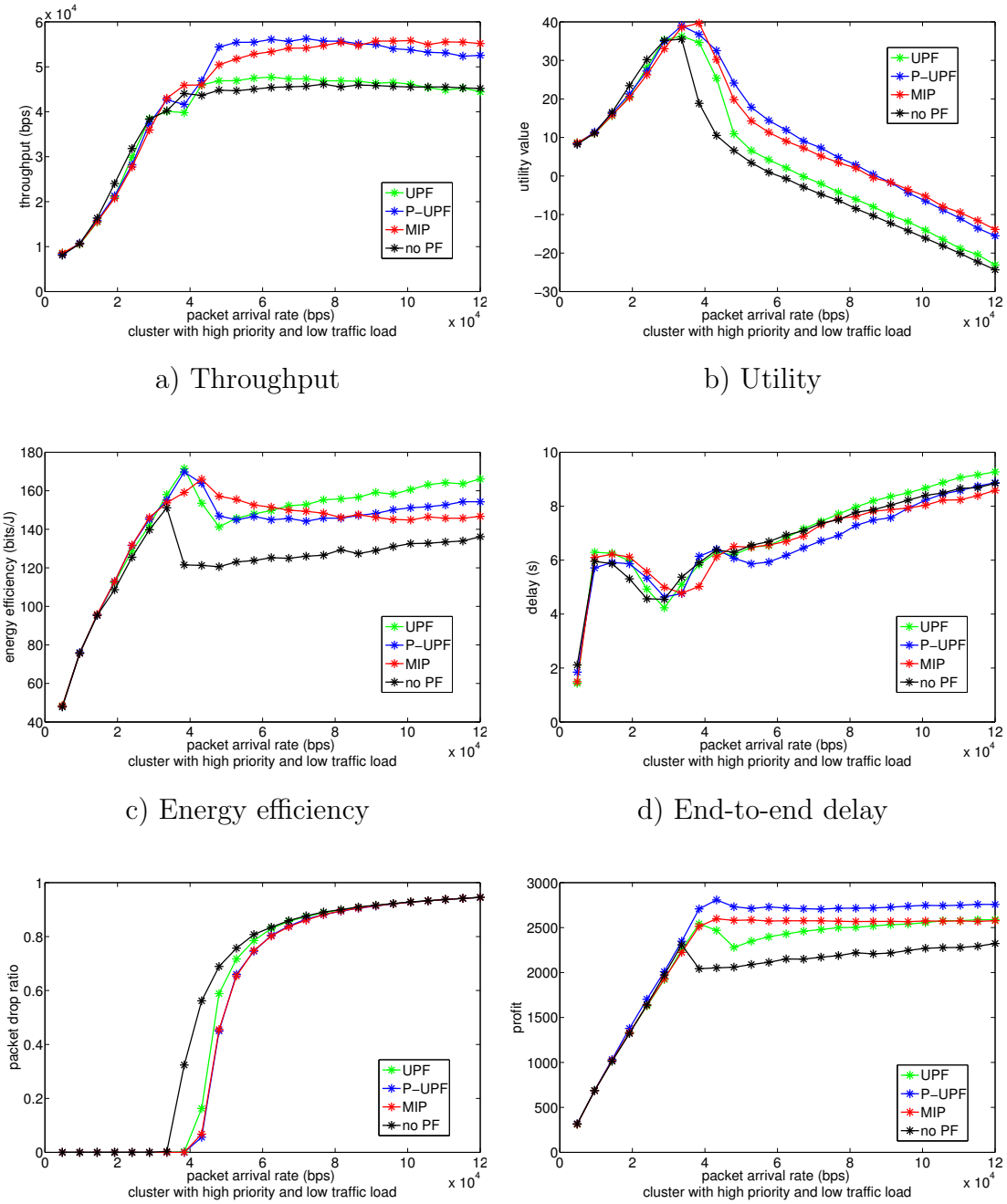

a) Throughput b) Utility

c) Energy efficiency d) End-to-end delay

e) Packet drop ratio f) Profit

Figure 7.4: Performance of cluster with high priority and low traffic load: a) throughput, b) utility, c) energy efficiency, d) end-to-end delay, e) packet drop ratio, and f) profit.

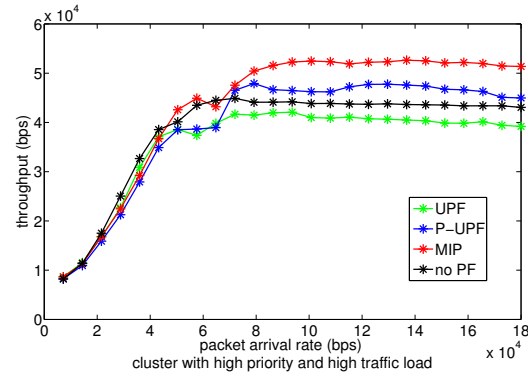

a) Throughput

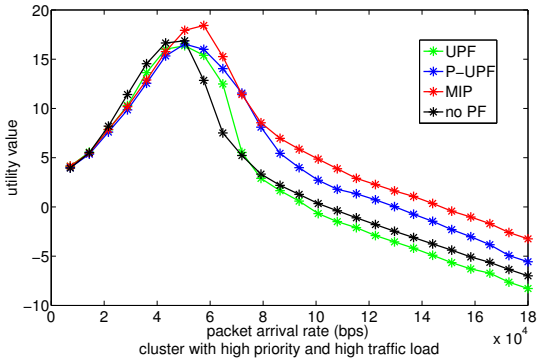

b) Utility

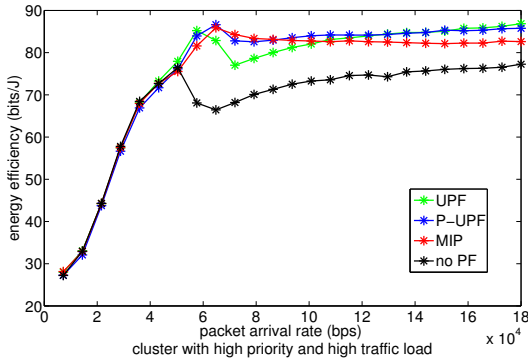

c) Energy efficiency

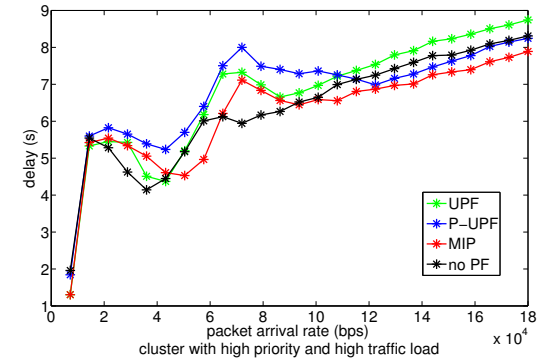

d) End-to-end delay

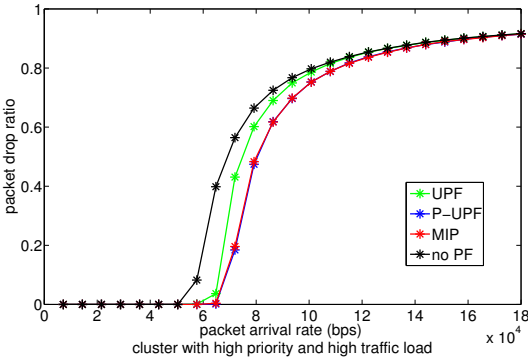

e) Packet drop ratio

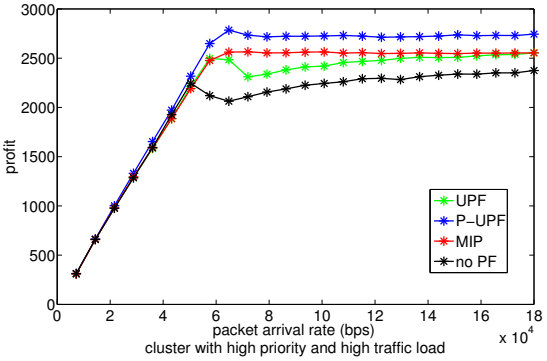

f) Profit

Figure 7.5: Performance of cluster with high priority and high traffic load: a) throughput, b) utility, c) energy efficiency, d) end-to-end delay, e) packet drop ratio, and f) profit.

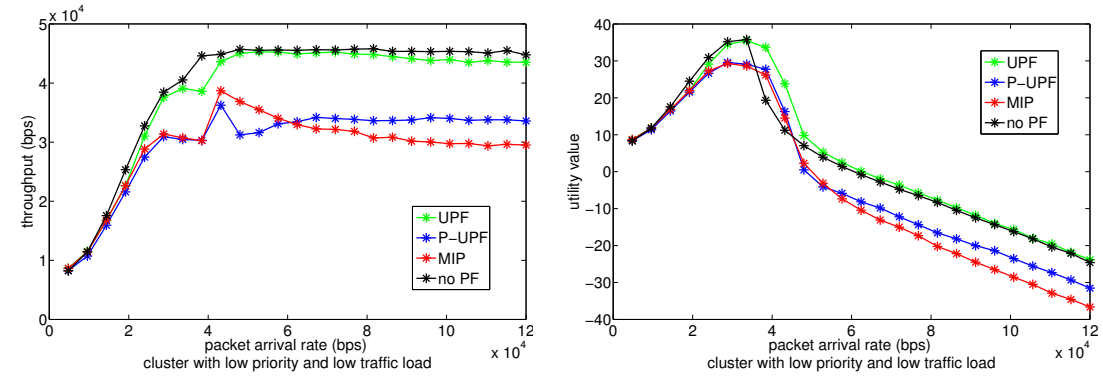

a) Throughput

b) Utility

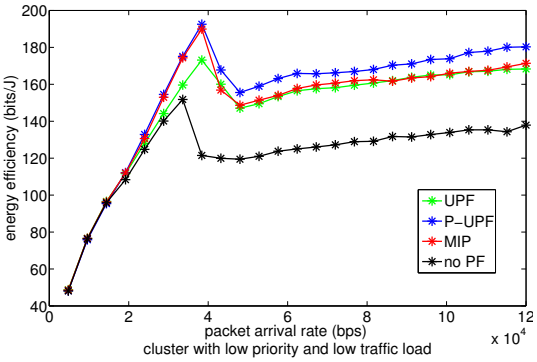

c) Energy efficiency

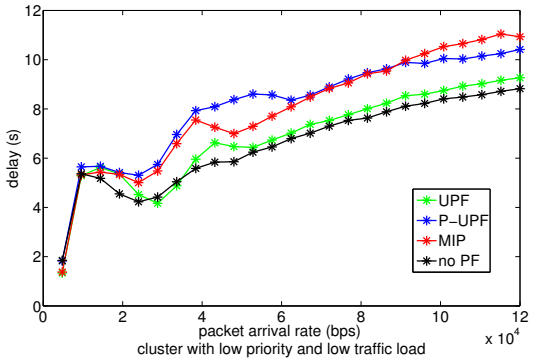

d) End-to-end delay

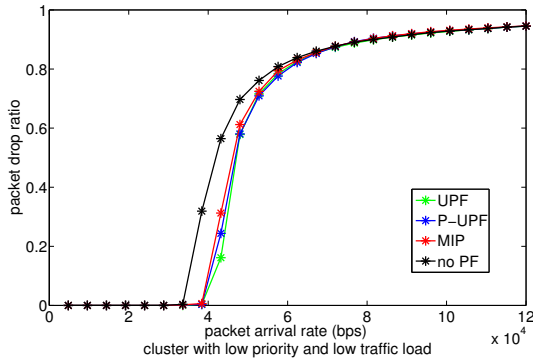

e) Packet drop ratio

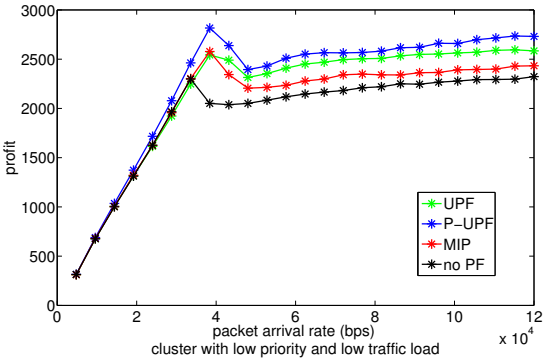

f) Profit

Figure 7.6: Performance of cluster with low priority and low traffic load: a) throughput, b) utility, c) energy efficiency, d) end-to-end delay, e) packet drop ratio, and f) profit.

all packet arrival rates. The saturated energy efficiency of cluster with lower traffic load is around double of that of the cluster head with higher traffic load. This is due to the radical increase of IEEE 802.15.4 duty cycle is based on 2. Thus, the duty cycle of cluster head with heavy traffic load could be doubled of the cluster with light traffic load with slightly increase of throughput.

For the end-to-end delays of each example cluster head (cluster 1,3 and 5) are shown in Fig. 7.4 d) Fig. 7.5 d) and Fig. 7.6 d). It can be seen that while the end-to-end delay of random and UPF based controls are similar to all three cluster heads, that of the P-UPF and MIP based gateway controls increased with the increase of traffic load (cluster head 1 vs. 3) and decrease of the priority (cluster head 1 vs. 5). For cluster heads with same priority, the end-to-end delay due to the increase of traffic load with MIP based control is less than with P-UPF based control.

The packet drop ratios of each example cluster head (1,3 and 5) are shown in Fig 7.4 e) Fig 7.5 e) and Fig 7.6 e). For cluster with high priority, the proposed P-UPF and MIP based controls always have the lowest packet drop ratio. The packet drop ratio of UPF is slightly higher than that of the P-UPF and MIP based controls, but lower than that of the random control. For the cluster head with low priority, the UPF, P-UPF and MIP based controls have lower packet drop ratio than that of the random control.

7.4.2 Heterogeneous Applications

In this scenario, the simulation results for scenario where the clusters run different class applications. More specifically, the elastic applications and rate adaptive applications are chosen as example. The simulation setting is shown in Table. 7-C

as scenario 2.

The network total throughput and utility analysis are omitted due to the limit of space. The network performance in terms of network total throughput and total utility of all 5 clusters in this scenario is similar with those of the above scenario 1. This shown that the network has achieved similar total throughput and utility regardless of application type of each cluster head. The scheduling results of the proposed P-UPF and MIP based control various under the scenario where clusters run different applications, as shown in Fig. 7.7.

Fig. 7.7 a) and Fig. 7.7 b) shown a snapshot of the averaged throughput and averaged utility of each example cluster head when the data arrival rate is 80kbps. It is clear that the proposed P-UPF and MIP based control achieved the differentiation for clusters with different applications, while no differentiation can be found in the results of UPF and random controls. In addition, the P-UPF and MIP have different preference when doing the schedule. For the presented scenario, P-UPF is capable of dealing with the elastic application while MIP is capable of dealing with the rate adaptive application, especially in terms of the utility.

To further explore the difference of P-UPF and MIP based controls, Fig. 7.8 shows the cumulative density function (CDF) of end-to-end delay of each example cluster 1, cluster 3 and cluster 5. It can be seen that the end-to-end delay CDF of the cluster heads with inelastic application are similar. The range of the end-to-end delay are all within 5s to 12s for both P-UPF and MIP based control. However, for the cluster with elastic application the range of end-to-end delay distribution is wider, and the mean value of the MIP based control is smaller than that of the P-UPF based control.

The performance of example cluster 1, cluster 3 and cluster 5 are presented in

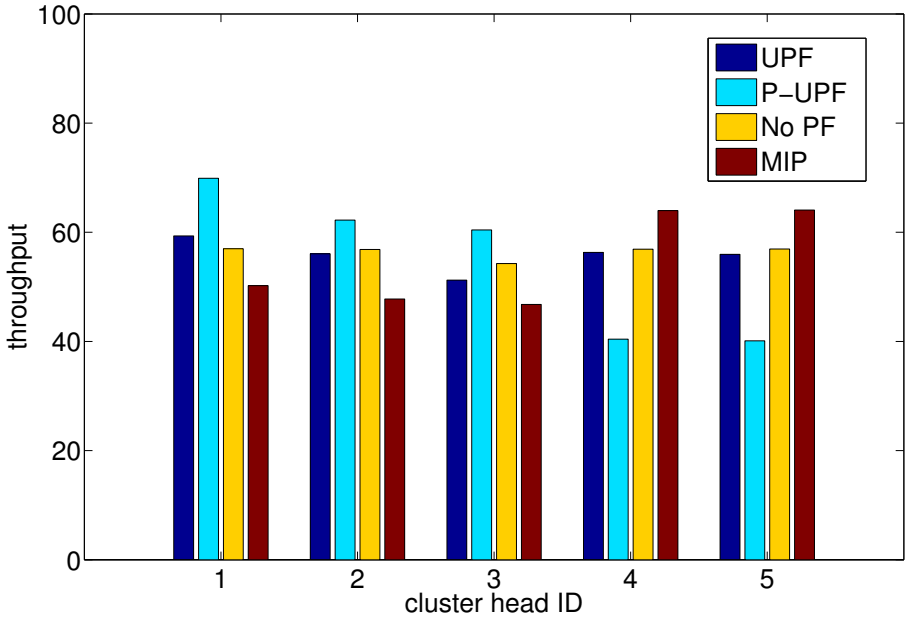

a) Averaged throughput

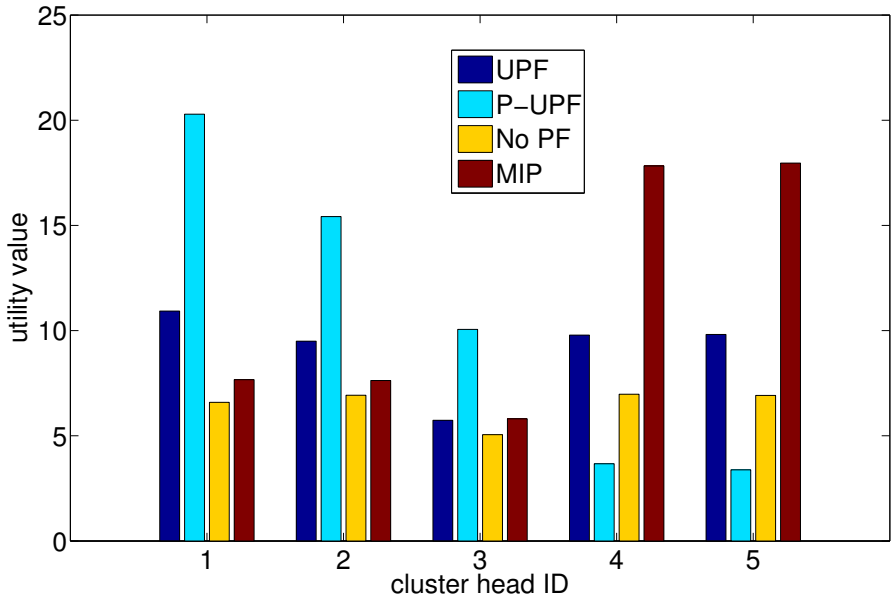

b) Averaged utility

Figure 7.7: Network performance with heterogeneous applications.

Fig. 7.4.2 - Fig. 7.4.2.

The average throughput performance of each example cluster is shown in Fig.

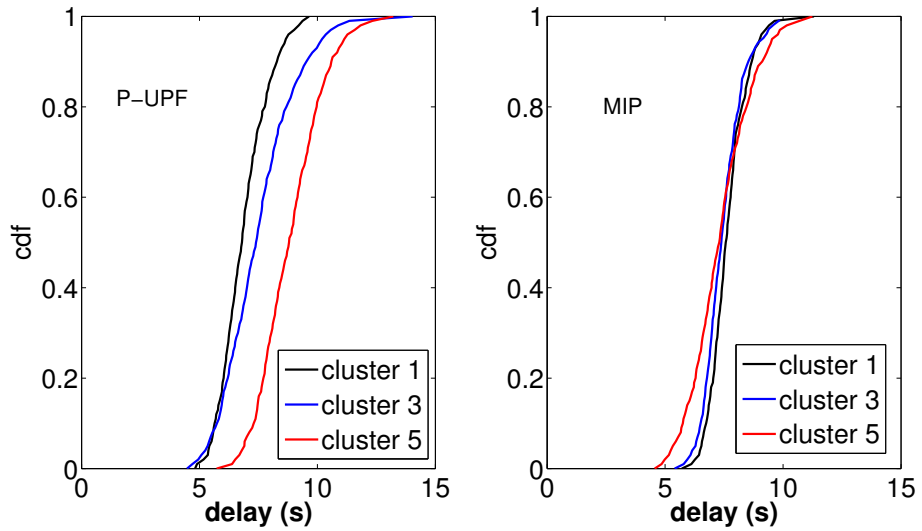

Figure 7.8: CDF of end-to-end delay with heterogeneous applications.

7.9 a), Fig. 7.10 a) and Fig. 7.11 a). The UPF based control and the random based control have similar throughput. The throughput of cluster with inelastic application is higher when applying P-UPF based control and the throughput of cluster with elastic application is higher when applying MIP based control.

The energy efficiency performance of each example cluster is shown in Fig. 7.9 c), Fig. 7.10 c) and Fig. 7.11 c). UPF, P-UPF and MIP based controls have higher energy efficiency compared to that of random based control. The energy efficiency of MIP based control is similar to that of UPF based control. The energy efficiency with P-UPF based control is higher than that of the other compared controls for cluster with elastic application. However, for cluster with inelastic application, the energy efficiency is slightly lower than that of MIP and UPF based controls when the arrival rate is larger than 60kbps. Similar to scenario 1, the energy efficiency of cluster head with light traffic load is doubled that of the cluster with heavy traffic load. This is due to the radical increment of the IEEE 802.15.4 duty cycle.

The end-to-end delay performance of each example cluster is shown in Fig.

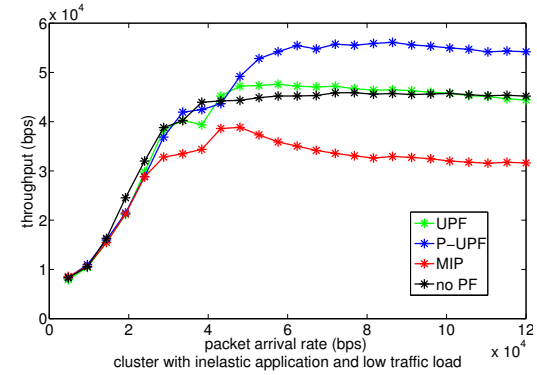

a) Throughput

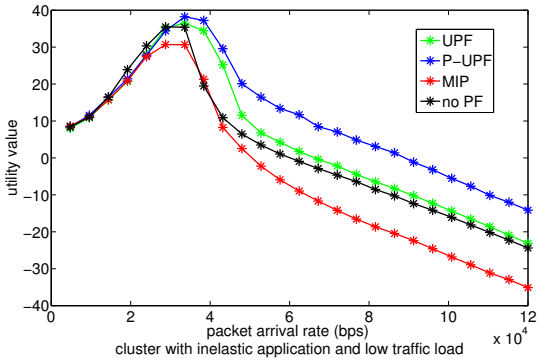

b) Utility

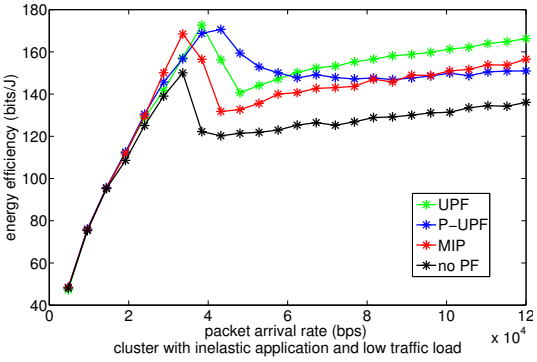

c) Energy efficiency

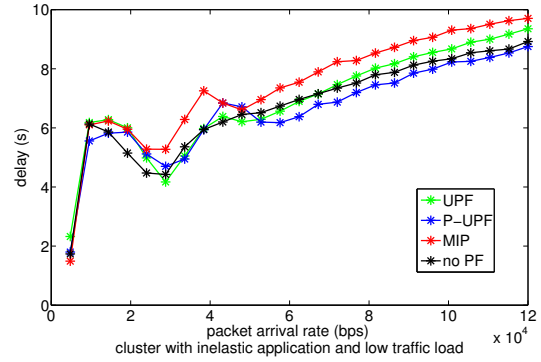

d) End-to-end delay

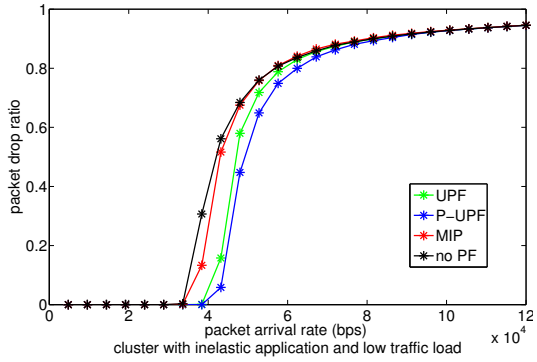

e) Packet drop ratio

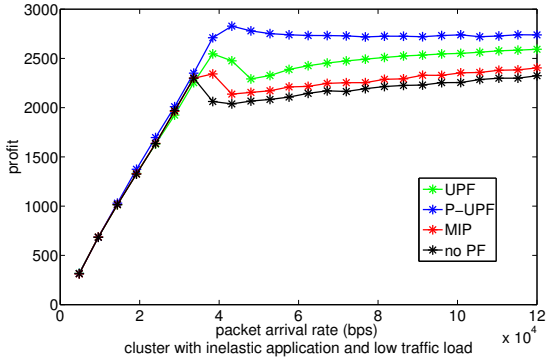

f) Profit

Figure 7.9: Performance of cluster with inelastic application and low traffic load (cluster head 1)

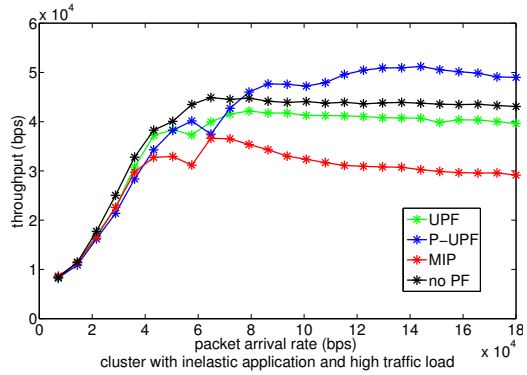

a) Throughput

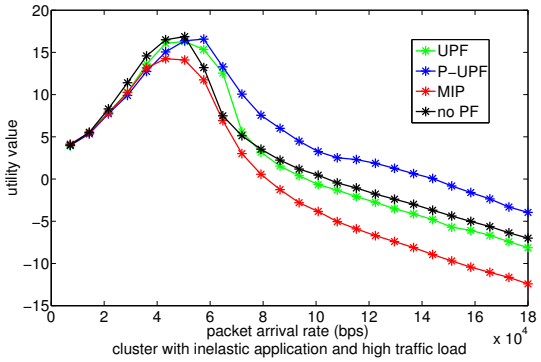

b) Utility

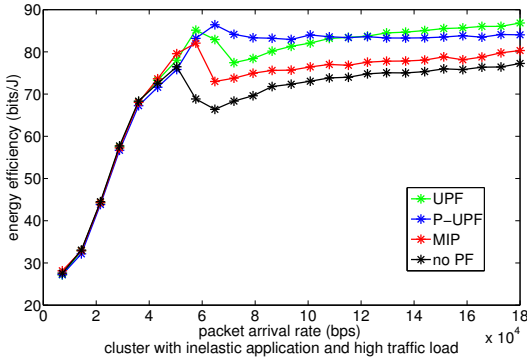

c) Energy efficiency

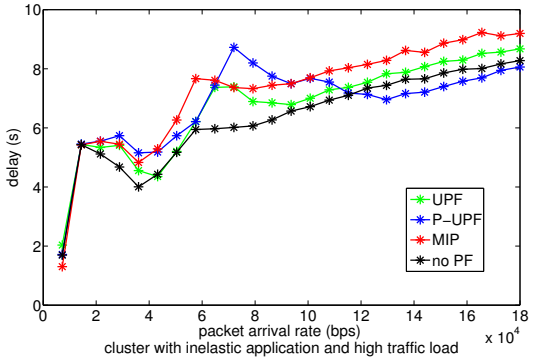

d) End-to-end delay

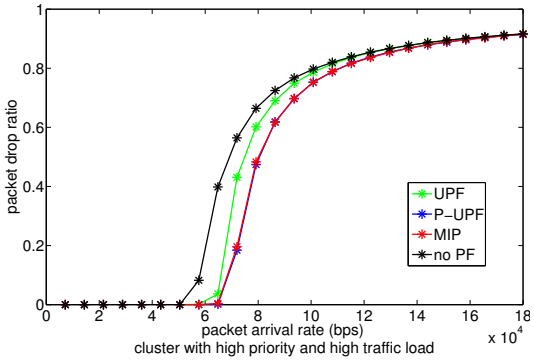

e) Packet drop ratio

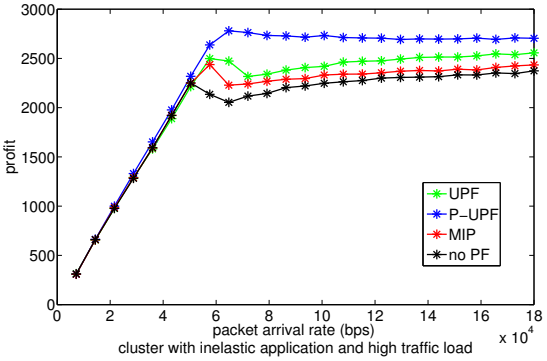

f) Profit

Figure 7.10: Performance of cluster with inelastic application and high traffic load (cluster head 3)

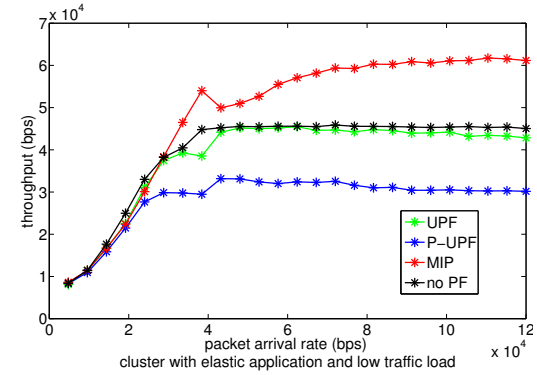

a) Throughput

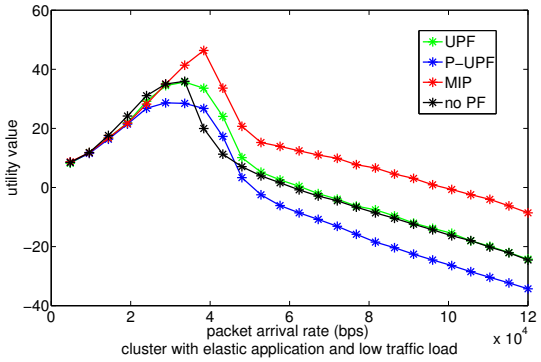

b) Utility

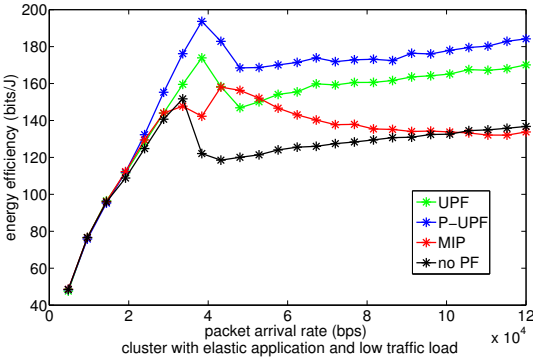

c) Energy efficiency

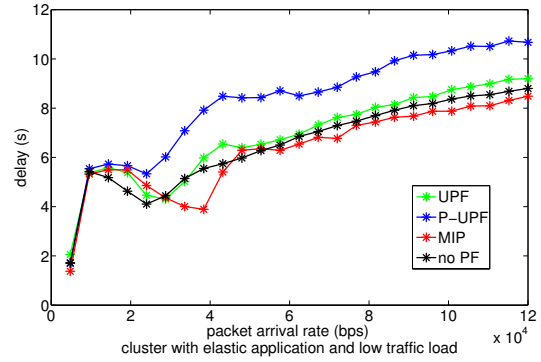

d) End-to-end delay

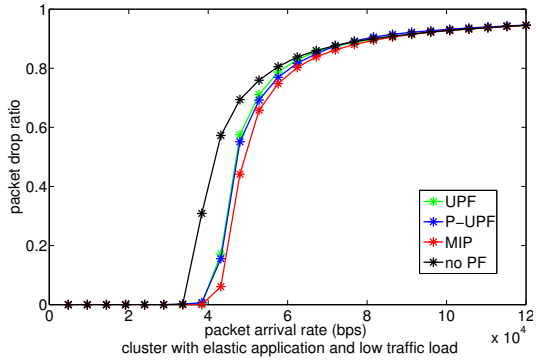

e) Packet drop ratio

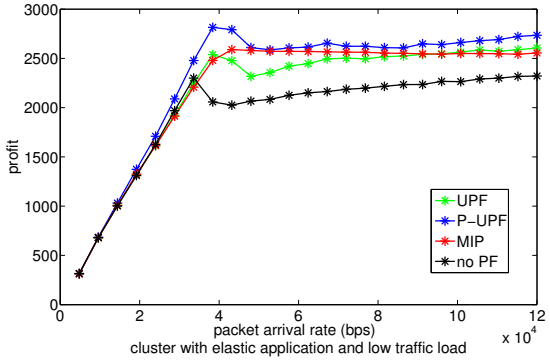

f) Profit

Figure 7.11: Performance of cluster with elastic application and low traffic load (cluster head 5)

7.9 d), Fig. 7.10 d) and Fig. 7.11 d). The end-to-end delay of UPF, MIP and random controls are similar for cluster with different application and same traffic load. However, with P-UPF based control, the end-to-end delay of cluster with elastic application is on average 2s higher than that of the other controls. And the end-to-end delay of the cluster with inelastic application is similar than that of the other controls. The end-to-end delay of cluster with heavy traffic load is slightly higher than that of cluster with light traffic load, if they are running same application.

The packet drop ratio performance of each example cluster is shown in Fig. 7.9 e), Fig. 7. 10 e) and Fig. 7.11 e). The UPF, P-UPF and MIP based controls have lower packet drop ratio compared to that of the random control. The P-UPF based control has the lowest packet drop ratio for clusters with inelastic application, while MIP based control has the lowest packet drop ratio for cluster with elastic application. For cluster with light traffic load, packets started to be dropped when the packet arrival rate is between 35kbps to 40kbps. For cluster with heavy traffic load, packets started to be dropped when the packet arrival rate is between 50kbps to 65kbps.

Due to the fact that the MIP based control takes the adjacent resource allocation constraint into account, MIP based control uses accumulated utility increase of multiple time slots as scheduling criteria while P-UPF takes the utility increase of each time period as scheduling criteria. The utility increase of elastic applications is much higher than that of inelastic application due to their different utility features. Thus, the P-UPF is capable of dealing with elastic applications while achieving higher energy efficiency. The MIP based control is capable of dealing with inelastic applications.

7.5 Summary

In this chapter, the gateway control optimisation problem is formulated and derived by applying Lagrangian-based duality techniques. The optimal gateway control P-UPF is proposed to achieve the long-term network utility maximisation and to achieve application differentiation among clusters. In addition, MIP based gateway control is proposed to ensure the adjacent resource allocation.

Through the simulation results and simulation analysis, it can be concluded that the proposed control framework outperforms the existing solutions and is capable of achieving long-term network utility maximisation with different applications under various scenarios.

Chapter 8

Conclusions and Future Works

This thesis proposed joint scheduling and duty cycle control framework for the IEEE 802.15.4 based hierarchical M2M networks. The proposed control framework aims to improve overall network performance, including energy efficiency, end-to-end delay, throughput and packet drop ratio for networks with heterogeneous applications.

i) The duty cycle control with Stop-and-Wait ARQ and Go-back-N ARQ. The aim of the duty cycle control is to address the trade-off between energy efficiency and end-to-end delay for IEEE 802.15.4 based networks. Simulation results shown that the optimal transmission policy can effectively reduce both energy consumption and end-to-end delay under various network traffics.

ii) The cluster head control aims to optimise the cluster utility which contains both empirical and economic components. The DP optimal cluster head control, PI based cluster head control, RA based cluster head control and Q-learning based cluster head control are proposed to address the trade-off between performance optimal and computational complexity. Simulation

results shown that the proposed cluster head control algorithms effectively addressed the challenges in terms of algorithm optimality, computational complexity, network dynamics and non-available network information, respectively.

iii) The gateway control aims to achieve the transmission schedule which optimise the long-term network utility while satisfying different application requirements among clusters. The proposed P-UPF based gateway control and MIP based gateway control for the M2M networks with heterogeneous applications. Simulation results and thorough simulation analysis shown that the proposed gateway controls outperformed the existing solutions, achieved long-term network utility maximisation, while providing application differentiate and utility provision under various scenarios.

The potential areas for future works include:

i) In this thesis, special attention is given to IEEE 802.15.4 based hierarchical M2M networks. Potential work can be explored on the network optimisation for hierarchical M2M networks which is supported by other short-range wireless technologies, such as low power Wi-Fi.

ii) The network optimisation in this thesis is based on cluster-tree networks. Taking the random deployment nature of the M2M networks into consideration, network optimisation for ad-hoc or mesh based networks is another open issue worth to be addressed.

References

[3GP11a] TR 23.888. 3GPP. System improvements for machine-type communications. Technical Report v.1.6.0 (release 11), November 2011.

[3GP11b] TR 37.868. 3GPP. Study on ran improvements for machine-type communications. Technical Report v.11.0.0 (release 11), September 2011.

[3GP11c] TS 22.368. 3GPP. Service requirements for machine-type communications (mtc). Technical Report v.11.3.0 (release 11), September 2011.

[ACF09] Giuseppe Anastasi, Marco Conti, and Mario Di Francesco. The mac unreliability problem in ieee 802.15.4 wireless sensor networks. In *in Proc. of the 12th ACM international conference on Modeling, analysis and simulation of wireless and mobile systems*, MSWiM '09, pages 196–203, October 2009.

[Aok76] Masahiko Aoki. Stochastic control in economic theory and economic systems. *Automatic Control, IEEE Transactions on*, 21(2):213 – 220, 1976.

[AP12] Rodolfo Alberola and Dirk Pesch. Duty cycle learning algorithm (dcla) for ieee 802.15.4 beacon-enabled wireless sensor networks. *Ad Hoc Networks*, 10(4):664 – 679, June 2012.

[Ast70] Karl J Astrom, editor. *Introduction to Stochastic Control Theory.* Academic Press, New York, 1970.

[ATN+14] Adnan Aijaz, Mati Tshangini, Mohammad Reza Nakhai, Xiaoli Chu, and Abdol-Hamid Aghvami. Energy efficient uplink resource allocation in lte networks with m2m/h2h co-existence under statistical qos guarantees. *Communications, IEEE Transactions on*,

–(–):–, Jun. 2014.

[Azi12] Vida Azimi. Accommodating machine-to-machine traffic in ieee 802.15.4: the prioritized wait time approach. Master's thesis, Ryerson University, Toronto, Ontario, Canada, Jan. 2012.

[BDWL10] Abdelmalik Bachir, Mischa Dohler, Thomas Watteyne, and Kin K. Leung. Mac essentials for wireless sensor networks. *Communications Surveys & Tutorials, IEEE*, 12(2):222 – 248, April 2010.

[Ber05] Dimitri Bertsekas, editor. *Dynamic Programming and Optimal Control, 3rd Edition*. Athena Scientific, 2005.

[BJL+14] Federico Boccardi, Robert W. Heath Jr., Angel Lozano, Thomas L. Marzetta, and Petar Popovski. Five disruptive technology directions for 5g. *Communications Magazine, IEEE*, 52(2):74 – 80, 2014.

[BSLG74] Y. Bar-Shalom, R. Larson, and M. Grossberg. Application of stochastic control theory to resource allocation under uncertainty. *Automatic Control, IEEE Transactions on*, 19(1):1–7, 1974.

[BY13] Heejung Byun and Junglok Yu. Adaptive duty cycle control with queue management in wireless sensor networks. *Mobile Computing, IEEE Transactions on*, 12(6):1214–1224, June 2013.

[CCC+10] Jiming Chen, Xianghui Cao, Peng Cheng, Yang Xiao, and Youxian Sun. Distributed collaborative control for industrial automation with wireless sensor and actuator networks. *Industrial Electronics, IEEE Transactions on*, 57(12):4219 – 4230, 2010.

[CCZS08] Xianghui Cao, Jiming Chen, Yan Zhang, and Youxian Sun. Development of an integrated wireless sensor network micro-environmental monitoring system. *Elsevier ISA Transactions*, 47(3):247 – 255, 2008.

[CFH14] Woon Hau Chin, Zhong Fan, and Russell J. Haines. Emerging technologies and research challenges for 5g wireless networks. *Wireless Communications, IEEE*, 21(2):106–112, 2014.

[Cis] Cisco. Cisco 819 4g lte m2m gateway integrated service routers data sheet. Technical report.

[CWGD10] Feng Chen, Nan Wang, Reinhard German, and Falko Dressler. Simulation study of ieee 802.15.4 lr-wpan for industrial applications. *Wireless Communication and Mobile Computing*, 10(5):609621, May 2010.

[CZ99] Zhiruo Cao and Ellen W. Zegura. Utility max-min: an application-oriented bandwidth allocation scheme. In *in Proc. IEEE Eighteenth Annual Joint Conference of the IEEE Computer and Communications Societies*, INFOCOM'99, pages 793 – 801, March 1999.

[DHVV14] Harpreet S. Dhillon, Howard Huang, Harish Viswanathan, and Reinaldo A. Valenzuela. Fundamentals of throughput maximization with random arrivals for m2m communications. *Communications, IEEE Transactions on*, 62(11):4094 – 4109, Nov. 2014.

[DL03] Tijs Van Dam and Koen Langendoen. An adaptive energy-efficient mac protocol for wireless sensor networks. In *in Proc. 1st International Conference on Embedded Networked Sensor Systems*, SenSys '03, pages 171–180, May 2003.

[DSJ07] Shu Du, Amit Kumar Saha, and David B. Johnson. Rmac: A routing-enhanced duty-cycle mac protocol for wireless sensor networks. In *in Proc. 26th IEEE International Conference on Computer Communications. IEEE*, INFOCOM' 07., pages 1478 – 1486, May 2007.

[ETS] ETSI. Etsi tr 102 935: Machine-to-machine communications (m2m);

applicability of m2m architecture to smart grid networks; impact of smart grids on m2m platform. Technical report.

[EXA] EXALTED. Description of baseline reference systems, scenarios, technical requirements and evaluation methodology. Technical Report EXALTED Deliverable 2-1.(2011).

[FMM04] Nan Feng, Siun-Chuon Mau, and Narayan B. Mandayam. Pricing and power control for joint network-centric and user-centric radio resource management. *Communications, IEEE transaction on*, 52(9):1547–1557, Septmeber 2004.

[GC13] Rung-Hung Gau and Ching-Pei Cheng. Optimal tree pruning for location update in machine-to-machine communications. *Wireless Communications, IEEE Transactions on*, 12(6):2620–2632, 2013.

[GC15] Fayezeh Ghavimi and Hsiao-Hwa Chen. M2m communications in 3gpp lte/lte-a networks: Architectures, service requirements, challenges, and applications. *Communications Surveys & Tutorials, IEEE*, 17(2):525 – 549, May 2015.

[GLA12] Antonis G. Gotsis, Athanasios S. Lioumpas, and Angeliki Alexiou. M2m scheduling over lte: Challenges and new perspectives. *Vehicular Technology Magazine, IEEE*, 7(3):34–39, 2012.

[GM00] David Goodman and Narayan Mandayam. Power control for wireless data. *Wireless Communication, IEEE transaction on*, 7(2):48–54, April 2000.

[HH12] Chieh Yuan Ho and Ching-Yao Huang. Energy-saving massive access control and resource allocation schemes for m2m communications in ofdma cellular networks. *Wireless Communications Letters, IEEE*, 1(3):209 – 212, Jun. 2012.

[HVY+09] Tian He, Pascal Vicaire, Ting Yan, Qing Cao, Gang Zhou, Lin

Gu, Liqian Luo, Radu Stoleru, John A. Stankovic, and Tarek F. Abdelzaher. Achieving long-term surveillance in vigilnet. *Sensor Networks, ACM Transactions on*, 5:9:19:39, Feb. 2009.

[Ins] Texas Instruments. Cc2420 2.4 ghz ieee 802.15.4 compliant and zigbee ready rf transceiver. Technical report.

[Int] Digi International. Xbee - rf family comparison. Technical report.

[ITA14] Mohammad Tauhidul Islam, Abd-Elhamid M. Taha, and Selim Akl. A survey of access management techniques in machine type communications. *Communications Magazine, IEEE*, 52(4):74 – 81, 2014.

[JLHK07] Joseph Jeon, Jong Wook Lee, Jae Yeol Ha, and Wook Hyun Kwon. Dca: Duty-cycle adaptation algorithm for ieee 802.15.4 beacon-enabled networks. In *in Proc. IEEE 65th Vehicular Technology Conference, 2007. VTC2007-Spring*, pages 110 – 113, April 2007.

[JSKP10] Jiong Jin, Avinash Sridharan, Bhaskar Krishnamachari, and Marimuthu Palaniswami. Handling inelastic traffic in wireless sensor networks. *Selected Areas in Communications, IEEE Journal on*, 28(7):1105 – 1115, September 2010.

[KGM14] Mounib Khanafer, Mouhcine Guennoun, and Hussein T. Mouftah. A survey of beacon-enabled ieee 802.15.4 mac protocols in wireless sensor networks. *Communications Surveys & Tutorials, IEEE*, 16(2):856 – 876, 2014.

[KKB+12] Kab Seok Ko, Min Jeong Kim, Kuk Yeol Bae, Dan Keun Sung, Jae Heung Kim, and Jae Young Ahn. A novel random access for fixed-location machine-to-machine communications in ofdma based systems. *Wireless Communications Letters, IEEE*, 16(9):1428 – 1431, September 2012.

[KMT98] FP Kelly, AK Maulloo, and DKH Tan. Rate control for communication networks: Shadow prices, proportional fairness and stability. *Journal of the Operations Research Society*, 49(3):237–252, March 1998.

[KS98] Ioannis Karatzas and Steven Shreve, editors. *Methods of Mathematical Finance*. Springer-Verlag, 1998.

[Kur12] Rebecca L. Kurrle. Resource allocation for smart phones in 4g lte-advanced carrier aggregation. Master's thesis, Virginia Polytechnic Institute and State University, Arlington, VA, September 2012.

[LA11] Athanasios S. Lioumpas and Angeliki Alexiou. Uplink scheduling for machine-to-machine communications in lte-based cellular systems. In *in Proc. IEEE GLOBECOM Workshops (GC Wkshps)*, page 353357, 2011.

[LC11] Shao-Yu Lien and Kwang-Cheng Chen. Massive access management for qos guarantees in 3gpp machine-to-machine communications. *Communications Letters, IEEE*, 15(3):311 – 313, March 2011.

[LCCL15] Yun Li, Kok Keong Chai, Yue Chen, and Jonathan Loo. Smart duty cycle control with reinforcement learning for machine to machine communications. In *in Proc. IEEE International Conference on Communications Workshops*, ICC workshop, June 2015.

[LCCZ13] Xiaolong Li, Jun Cai, Hongbin Chen, and Hong Zhang. Tldtca: A distributed approach to meeting heterogenous connectivity requirements to sink in m2m networks. In *in Proc. Global Communications Conference (GLOBECOM), 2013 IEEE*, pages 4459 – 4464, Dec. 2013.

[LCL11] Shao-Yu Lien, Kwang-Cheng Chen, and Yonghua Lin. Toward

ubiquitous massive accesses in 3gpp machine-to-machine communications. *Communications Magazine, IEEE*, 49(4):66 – 74, April 2011.

[LHJ+07] Jongwook Lee, Jae Yeol Ha, Joseph Jeon, Dong Sung Kim, and Wook Hyun Kwon. Ecap: A bursty traffic adaptation algorithm for ieee 802.15.4 beacon- enabled networks. In *in Proc. 65th IEEE Vehicular Technology Conference*, page 203207, 2007.

[LJ08] Jae-Han Lim and Byung Tae Jang. Dynamic duty cycle adaptation to real- time data in ieee 802.15.4 based wsn. In *in Proc. 5th IEEE Consumer Communications and Networking Conference*, page 353357, 2008.

[LL99] Steven H. Low and David E. Lapsley. Optimization flow control. i. basic algorithm and convergence. *Networking, IEEE/ACM Transactions on*, 7(6):861 – 874, 1999.

[LL09] Mo Li and Yunhao Liu. Underground coal mine monitoring with wireless sensor networks. *Sensor Networks, ACM Transactions on.*, 5:10:110:29, Apr 2009.

[LL15] Yang Liu and Mingyan Liu. To stay or to switch: Multiuser multichannel dynamic access. *Mobile Computing, IEEE Transactions on*, 14(4):858 – 871, April 2015.

[LLKC12] Shao-Yu Lien, Tzu-Huan Liau, Ching-Yueh Kao, and Kwang-Cheng Chen. Cooperative access class barring for machine-to-machine communications. *Wireless Communications, IEEE Transactions on*, 11(1):27–32, 2012.

[LMS05] Jang-Won Lee, Ravi R. Mazumdar, and Ness B. Shroff. Non-convex optimization and rate control for multi-class services in the internet. *Networking, IEEE/ACM Transactions on*, 13(4):827 –

840, August 2005.

[LMWCFC12] Francisco Rafael Marques Lima, Tarcisio Ferreira Maciel, Jr. Walter Cruz Freitas, and Francisco Rodrigo Porto Cavalcanti. Resource assignment for rate maximization with qos guarantees in multi-service wireless systems. *Vehicular Technology, IEEE Transactions on*, 61(3):1318 – 1332, March 2012.

[LQW04] Peng Lin, Chunming Qiao, and Xin Wang. Medium access control with a dynamic duty cycle for sensor networks. In *in Proc. of the IEEE Wireless Communications and Networking Conference*, volume 3 of *WCNC '04*, pages 1534–1539, March 2004.

[LYC+14] Yi Liu, Chau Yuen, Xianghui Cao, Naveed Ul Hassan, and Jiming Chen. Design of a scalable hybrid mac protocol for heterogeneous m2m networks. *Internet of Things Journal, IEEE*, 1(1):99 – 111, May 2014.

[LYH05] Yuan Li, Wei Ye, and John Heidemann. Energy and latency control in low duty cycle mac protocols. In *in Proc. IEEE Wireless Communications and Networking Conference*, WCNC'05, pages 676 – 682, March 2005.

[MAH13] Javier Matamoros and Carles Anton-Haro. Traffic aggregation techniques for environmental monitoring in m2m capillary networks. In *in Proc. IEEE 77th Vehicular Technology Conference (VTC Spring), 2013*, VTC Spring, pages 1–5, June 2013.

[MET] METIS. Mobile and wireless communications enablers for the twenty-twenty information society, eu 7th framework programme project. Technical report.

[MMLN12] Vojislav B. Mii, Jelena Mii, Xiaodong Lin, and Dragan Nerandzic. Capillary machine-to-machine communications: The road ahead.

In *in Proc. 11th International Conference on Ad-hoc, Mobile, and Wireless Networks*, ADHOC-NOW'12, pages 413 – 423, 2012.

[MPSM05] Farhad Meshkati, H. Vincent Poor, Stuart C. Schwartz, and Narayan B. Mandayam. An energy-efficient approach to power control and receiver design in wireless data networks. *Wireless Communications, IEEE Transactions on*, 53(11):1885 – 1894, Novermber 2005.

[NIS11] NIST. Nist priority action plan 2 guidelines for assessing wireless standards for smart grid applications. Technical report, 2011.

[NK11] Navid Nikaein and Srdjan Krco. Latency for real-time machine-to-machine communications in lte-based system architecture. In *in Proc. 11th European Wireless Conference*, volume 11, pages 1 – 6, April 2011.

[NPK] Mario Neugebauer, Jom Plonnigs, and Klaus Kabitzsch.

[OHL15] Chang-Yeong Oh, Duckdong Hwang, and Tae-Jin Lee. Joint access control and resource allocation for concurrent and massive access of m2m devices. *Wireless Communications, IEEE Transactions on*, March 2015.

[OKM12] Eng Hwee Ong, Jamil Y. Khan, and Kaushik Mahata. Radio resource management of composite wireless networks: Predictive and reactive approaches. *Mobile Computing, IEEE Transactions on*, 11(5):807 – 820, May 2012.

[PCLW14] Yuan-Chi Pang, Shih-Lung Chao, Guan-Yu Lin, and Hung-Yu Wei. Network access for m2m/h2h hybrid systems: a game theoretic approach. *Communications Letters, IEEE*, 18(5):845 – 848, June 2014.

[PKC+05] T.R. Park, T.H. Kim, J.Y. Choi, S. Choi, and W.H. Kwon. Throughput and energy consumption analysis of ieee 802.15.4 slotted csma/ca.

Electronics Letters, IEEE Transactions on, 41(18):1017 – 1019, September 2005.

[PKH14] Ieryung Park, Dohyun Kim, and Dongsoo Har. Fmac achieving low latency and energy efficiency in hierarchical m2m networks with clustered nodes. *Sensors Journal, IEEE*, 15(3):1657 – 1661, Jan. 2014.

[Pow11] Warren B. Powell, editor. *Approximate Dynamic Programming: Solving the Curses of Dimensionality, 2nd Edition*. Wiley, 2011.

[Sca60] Herbert Scarf. The optimality of (s,s) policies for the dynamic inventory problem. In *1st Stanford Symposium on Mathematical Methods in the Social Sciences*, 1960.

[SDGJ08] Yanjun Sun, Shu Du, Omer Gurewitz, and David B. Johnson. Dw-mac: A low latency, energy efficient demand-wakeup mac protocol for wireless sensor networks. In *in Proc. 9th ACM International Symposium on Mobile Ad Hoc Networking and Computing*, MobiHoc '08, pages 53–62, May 2008.

[She95] Scott Shenker. Fundamental design issues for the future internet. *Selected Areas in CommunicationsIEEE Journal on*, 13(7):1176–1188, September 1995.

[SJL+13] M. Zubair Shafiq, Lusheng Ji, Alex X. Liu, Jeffrey Pang, and Jia Wang. Large-scale measurement and characterization of cellular machine-to-machine traffic. *Networking, IEEE/ACM Transactions on*, 21(6):1960 – 1973, Dec. 2013.

[Soc11] IEEE Computer Society. Ieee std. 802.15.4, part.15.4: Wireless medium access control (mac) and physical layer (phy) specifications for low-rate wireless personal area networks (lr-wpans). Technical report, IEEE Std., 2011.

[Soc12] IEEE Computer Society. Ieee standard for air interface for broadband wireless access systems. Technical report, 2012.

[SRS12] Petcharat Suriyachai, Utz Roedig, and Andrew Scott. A survey of mac protocols for mission-critical applications in wireless sensor networks. *Communications Surveys & Tutorials, IEEE*, 14(2):240–264, Second Quarter 2012.

[SS14] Manuj Sharma and Anirudha Sahoo. Stochastic model based opportunistic channel access in dynamic spectrum access networks. *Mobile Computing, IEEE Transactions on*, 13(7):1625 – 1639, July 2014.

[SYCX15] Peng Si, Jian Yang, Shuangwu Chen, and Hongsheng Xi. Adaptive massive access management for qos guarantees in m2m communications. *Vehicular Technology, IEEE Transactions on*, 64(7):3152 – 3166, July 2015.

[SZ94] Suresh P. Sethi and Qing Zhang, editors. *Hierarchical Decision Making in Stochastic Manufacturing Systems*. Birkhuser Engineering, 1994.

[THH11] Chih-Yuan Tu, Chieh-Yuan Ho, and Ching-Yao Huang. Energy-efficient algorithms and evaluations for massive access management in cellular based machine to machine communications. In *in Proc. IEEE Vehicular Technology Conference (VTC Fall)*, pages 1 – 5, 2011.

[TLS+13] Tuomas Tirronen, Anna Larmo, Joachim Sachs, Bengt Lindoff, and Niclas Wiberg. Machine-to-machine communication with long-term evolution with reduced device energy consumption. *Transactions on Emerging Telecommunications Technologies*, 24(4):413–426, 2013.

[TPS+05] Gilman Tolle, Joseph Polastre, Robert Szewczyk, David Culler, Neil Turner, Kevin Tu, Stephen Burgess, Todd Dawson, Phil Buonadonna, David Gay, and Wei Hong. A macroscope in the redwoods. In *in Proc. 3rd ACM SenSys,*, SenSys, page 5163, 2005.

[WALJ+07] Geoff Werner-Allen, Konrad Lorincz, Jeff Johnson, Jonathan Lees, and Matt Welsh. Fidelity and yield in a volcano monitoring sensor network. In *in Proc. 3rd ACM SenSys,*, 7th OSDI, page 381396, 2007.

[WC15] Dimas Tribudi Wiriaatmadja and Kae Won Choi. Hybrid random access and data transmission protocol for machine-to-machine communications in cellular networks. *Wireless Communications, IEEE Transactions on*, 14(1):33 – 46, January 2015.

[WOM09] Ian C. Wong, Oghenekome Oteri, and Wes McCoy. Optimal resource allocation in uplink sc-fdma systems. *Wireless CommunicationsIEEE Transactions on*, 8(5):2161 – 2165, May 2009.

[WPL06] Wei-Hua Wang, Marimuthu Palaniswami, and Steven H. Low. Application-oriented flow control: Fundamentals, algorithms and fairness. *Networking, IEEE/ACM Transactions on*, 14(6):1063–6692, December 2006.

[WWXY10] Xiaodong Wang, Xiaorui Wang, Guoliang Xing, and Yanjun Yao. Dynamic duty cycle control for end-to-end delay guarantees in wireless sensor networks. In *in Proc. IEEE International Workshop on Quality of Service*, IWQoS'10, pages 1–9, June 2010.

[WZJ+13] Huasen Wu, Chenxi Zhu, Richard J.La, Xin Liu, and Youguang Zhang. Fasa: Accelerated s-aloha using access history for event-driven m2m communications. *Networking, IEEE/ACM Transactions on*, 21(6):1904 – 1917, Dec. 2013.

[XRC+04] Ning Xu, Sumit Rangwala, Krishna Kant Chintalapudi, Deepak Ganesan, Alan Broad, Ramesh Govindan, and Deborah Estrin. A wireless sensor network for structural monitoring. In *2nd ACM SenSys*, 7th OSDI, pages 13–24, 2004.

[XYWV12] Feng Xia, Laurence T. Yang, Lizhe Wang, and Alexey Vine. Internet of things. *International Journal of Communication Systems*, 25(9):1101–1102, 2012.

[YHE02] Wei Ye, John Heidemann, and Deborah Estrin. An energy-efficient mac protocol for wireless sensor networks. In *Twenty-First Annual Joint Conference of the IEEE Computer and Communications Societies. Proceedings. IEEE*, volume 3 of *INFOCOM 2002*, pages 1567 – 1576, June 2002.

[YTW+05] Shih-Hsien Yang, Hung-Wei Tseng, Eric Hsiao-Kuang Wu, , and Gen-Huey Chen. Utilization based duty cycle tuning mac protocol for wireless sensor networks. In *in Proc. IEEE Global Telecommunications Conference*, GLOBECOM'05, pages 3258–3262, November 2005.

[YZ99] Jiongmin Yong and XunYu Zhou, editors. *Stochastic Controls: Hamiltonian Systems and HJB Equations*. Springer, 1999.

[YZG+13] Rong Yu, Yan Zhang, Stein Gjessing, Wenlong Xia, and Yang Kun. Toward cloud-based vehicular networks with efficient resource management. *Networking Magazine, IEEE*, 27(5):48 – 55, 2013.

[YZWG14] Bo Yang, Guangxi Zhu, Weimin Wu, and Youjun Gao. M2m access performance in lte-a system. *Transactions on Emerging Telecommunications Technologies*, 25(1):3–10, 2014.

[ZHW+12] Kan Zheng, Fanglong Hu, Wenbo Wang, Wei Xiang, and Mischa Dohler. Radio resource allocation in lte-advanced cellular networks

with m2m communications. *Communications Magazine, IEEE*, 50(7):184–192, 2012.

[ZYX+11] Yan Zhang, Rong Yu, Shengli Xie, Wenqing Yao, Yang Xiao, and Mohsen Guizani. Home m2m networks: architecture, standards and qos improvements. *Communications Magazine, IEEE*, 49(4):44 – 52, 2011.